2016

Edge-Of-Field Water And Phosphorus Losses In Surface And Subsurface Agricultural Runoff

Laura B. Klaiber
University of Vermont

EDGE-OF-FIELD WATER AND PHOSPHORUS LOSSES IN SURFACE AND SUBSURFACE AGRICULTURAL RUNOFF

A Thesis Presented

by

Laura Klaiber

to

The Faculty of the Graduate College

of

The University of Vermont

In Partial Fulfillment of the Requirements
for the Degree of Master of Science
Specializing in Plant and Soil Science

May, 2016

Defense Date: December 8, 2015
Thesis Examination Committee:

Donald S. Ross, Ph.D., Advisor
Beverley C. Wemple, Ph.D., Chairperson
Eric O. Young, Ph.D.
Cynthia J. Forehand, Ph.D., Dean of the Graduate College

ABSTRACT

Quantifying effectiveness of soil management practices on surface and subsurface water quality at the field scale is becoming increasingly important in the Lake Champlain Basin and other agricultural watersheds. During 2012 and 2013, field plots (22.9 x 45.7 m) were established at the Lake Alice Wildlife Area in Chazy, NY to begin a long-term water quality monitoring study. Plots were established in a cool season grass field (1 ha) leased and managed by the William H. Miner Agricultural Research Institute in Chazy, NY. The soil type transitions from an excessively drained outwash soil on the upslope to a very poorly drained silty clay series at the toeslope. Tile drainage lines were installed in each plot and drained to concrete manholes at the corner of each plot where water was sampled and measured. Plots were randomly assigned to a tile-drained (TD) or naturally-drained treatment (UD). Tile outlets were plugged in the UD treatment to enable natural drainage conditions. Surface runoff water was collected at the lower boundary of each plot by shallow PVC-lined trenches that outlet to the manholes. Continuous water flow from each hydrologic pathway was measured in 5-gallon buckets with v-notch weirs and pressure transducers. Total phosphorus (TP), soluble reactive phosphorus SRP), unreactive phosphorus (UP) and sediment (TSS) loads were estimated by multiplying the mean hourly runoff volume by the respective sample concentration for each hydrologic pathway.

Data were collected April 21, 2014 through June 30, 2015. Loading rates were unable to be calculated from February 22, 2015 through April 9, 2015 due to freeze/thaw cycles preventing accurate water flow data collection. Event-based loading for TP, SRP, UP, TSS, and water yield were calculated in addition to cumulative losses over the study duration. No significant differences in cumulative TP exports were found between treatments (UD = 230.9 g ha^{-1}; TD = 233.9 g ha^{-1}). Approximately 55% more SRP and 158% more TSS was exported by UD (130.8 g ha^{-1}; 168.8 kg ha^{-1}) than TD (84.2 g ha^{-1}; 65.5 kg ha^{-1}). Unreactive P exports from TD (149.7 g ha^{-1}) were 50% greater than UD (100.1 g ha^{-1}). Two runoff events dominated the treatment response. An intense rain storm on May 16, 2014 generated the greatest sediment losses in both treatments during an individual event, contributing 65 and 67% of the cumulative losses from TD and UD, respectively. This event was also responsible for 40% of UP losses from TD. A 3 d rain/snowmelt event beginning on December 24, 2014 resulted in 61 and 84% of all SRP losses for TD and UD, respectively. The results of this study indicate that tile drainage may not have a negative impact on water quality relative to a naturally drained field. However, additional years of data are needed to develop more robust conclusions as different management strategies and weather conditions could result in different outcomes.

ACKNOWLEDGEMENTS

I would like to thank the University of Vermont's Department of Plant and Soil Science and my graduate committee members, Dr. Donald Ross, Dr. Beverley Wemple, and Dr. Eric Young. Each provided me with the support, expertise, and inspiration to complete my research as well as enjoy the experience. I would like to especially thank Dr. Eric Young for his guidance, encouragement, and enthusiasm every step of the way.

Thank you to the William H. Miner Agricultural Research Institute for the funding to establish this research project as well as the Northern New York Agricultural Development Program for the funding to continue our monitoring efforts. I would also like to thank everyone at Miner Institute for their help, guidance, and friendship. I was first introduced to, and developed a love for research working at Miner Institute and will always be grateful for the opportunities I have been afforded. A special thank you as well to Stephen Kramer and Keegan Griffith for their assistance in the field and lab.

Finally, I would like to thank my friends and family for their support and encouragement.

TABLE OF CONTENTS

Page

ACKNOWLEDGEMENTS ii

LIST OF TABLES v

LIST OF FIGURES vi

CHAPTER 1: COMPREHENSIVE LITERATURE REVIEW 1

1.1. Agriculture and Eutrophication 1

1.1.1. Nonpoint Source Pollution 1

1.1.2. Freshwater Eutrophication 2

1.1.3. Eutrophication in Lake Champlain 4

1.1.4. Risk Management 4

1.2. Phosphorus in Soils 6

1.2.1. Phosphorus Cycle 6

1.2.2. Phosphorus Solubility 11

1.3 Hydrologic Processes 16

1.3.1. Soil Water Budget 16

1.3.2. Runoff Processes 18

1.4. Agricultural Drainage 24

1.4.1. History and Status of Agricultural Drainage 24

1.4.3. Benefits of Agricultural Drainage 26

1.4.3. Effects of Drainage on P Forms and Losses 28

1.5. Research Objectives 33

CHAPTER 2: MATERIALS AND METHODS 35

2.1. Site Description and Timeline of Field Activities 35

2.2. Experimental Design 36

2.3. Water Flow Measurements 39

2.4. Water Sampling 40

2.5. Water Yield and Load Calculations 41

2.6. Statistical Analysis 43

CHAPTER 3: RESULTS AND DISCUSSION 45

3.1. Hydrology of Surface Runoff and Tile Discharge 45

3.1.1. Total Runoff Water Yield 45

3.1.2. Runoff Events 48

3.1.3. Water Table Monitoring 56

3.2. Soil Analysis 63

3.3. Phosphorus and Sediment Loads in Runoff 64

3.3.1. Cumulative Phosphorus and Sediment Loads 64

3.3.2. Phosphorus and Sediment Loads in Runoff Events 70

3.4. Flow-Weighted Mean Concentrations 75

3.5. Implications for Water Quality and Field Management 78

3.6. Study Limitations 80

3.6. Conclusions 83

BIBLIOGRAPHY 84

APPENDICES 96

LIST OF TABLES

Table Page

Table 1.1: Elements used in respiration. 14
Table 1.2: Crop yield increases following installation of tile drainage 28

Table 2.1: Rating curve equations for each runoff collection location 42

Table 3.1: Mean water yield by treatment for events and the study total 46
Table 3.2: Mean water yield by treatment pathways for events and the study total 46
Table 3.3: Timeframes of the seven intensively sampled runoff events 49
Table 3.4: Event and cumulative mean losses of SRP, UP, TP, and TSS by treatment ... 65
Table 3.5: Event and cumulative mean losses of SRP, UP, TP, and TSS by hydrologic pathway 66
Table 3.6: FWM concentrations for SRP, UP, TP, and TSS by treatment 77
Table 3.7: FWM concentrations for SRP, UP, TP, and TSS by hydrologic pathway 77

Table 4:1: Nitrate-N loads exported from each treatment during four runoff events. 96
Table 4:2: Daily rainfall totals for 5/31/15-6/30/15 105
Table 4:3: Water table elevation (m) at each well in plots 1 (UD) and 2 (TD). 106
Table 4:4: Water table elevation (m) at each well in plots 3 (UD) and 4 (TD) 107

LIST OF FIGURES

Figure Page

Figure 1.1: The soil phosphorus cycle. 6
Figure 1.2: Effects of extent of soil development on soil P forms. 9
Figure 1.3: Stratification of STP (Mehlich-3) by depth in the soil profile. 30

Figure 2.1: Schematic of plot layout at the Lake Alice Wildlife Area, Chazy, NY 37
Figure 2.2: Locations of shallow groundwater wells..... 38
Figure 2.3: Field rating curves for Plot 1 surface flows and Plot 2 tile flows 39

Figure 3.1: Monthly rainfall and mean water yield for UD and TD. 48
Figure 3.2: Water yield from the 5/16/14 rain event 51
Figure 3.3: Water yield from the 6/11/14 rain event 51
Figure 3.4: Water yield from the 6/3/14 rain event. 52
Figure 3.5: Water yield from the 12/25/14 snowmelt event 52
Figure 3.6: Water table contour map for plots 1 and 2 on 6/4/15. 58
Figure 3.7: Water table contour map for plots 1 and 2 on 6/22/15 (10:00) 59
Figure 3.8: Water table contour map for plots 3 and 4 on 6/4/15..... 60
Figure 3.9: Water table contour map for plots 3 and 4 on 6/22/15 (17:00) 61
Figure 3.10: Box plot of water table elevations in groundwater wells across the boundary between plots 1 and 2..... 62
Figure 3.11: Box plot of water table elevations in groundwater wells across the boundary between plots 3 and 4..... 62
Figure 3.12: Soil test results..... 63
Figure 3.13: Monthly SRP and TP loads for each treatment.. 67
Figure 3.16: Monthly TSS loads for each treatment. 67
Figure 3.17: TP loads by hydrologic pathway for each treatment from the 12/25/14 event. 71
Figure 3.18: TSS loads by hydrologic pathway for each treatment from the 5/16/14 event. 74

Figure 4.1: Rating curve developed in the field for Plot 2 surface flow bucket 97
Figure 4.2: Rating curve developed in the field for Plot 3 surface flow bucket 98
Figure 4.3: Rating curve developed in the field for Plot 4 surface flow bucket 99
Figure 4.4: Rating curve developed in the field for Plot 4 tile flow bucket 100
Figure 4.5: Total water yield by plot for the 5/16/14 rain event..... 101
Figure 4.6: Total water yield by plot for the 6/3/14 rain event..... 101
Figure 4.7: Total water yield by plot for the 6/11/14 rain event..... 102
Figure 4.8: Total water yield by plot for the 6/24/14 rain event..... 102
Figure 4.9: Total water yield by plot for the 8/13/14 rain event..... 103
Figure 4.10: Total water yield by plot for the 12/25/14 snowmelt event 103

Figure 4.11: Total water yield by plot for the 5/31/15 rain event 104
Figure 4.12: Water table contour map for plots 1 and 2 on 6/2/15 (09:00). 108
Figure 4.13: Water table contour map for plots 1 and 2 on 6/2/15 (17:00). 109
Figure 4.14: Water table contour map for plots 1 and 2 on 6/8/15. 110
Figure 4.15: Water table contour map for plots 1 and 2 on 6/9/15. 111
Figure 4.16: Water table contour map for plots 1 and 2 on 6/10/15 (07:45). 112
Figure 4.17: Water table contour map for plots 1 and 2 on 6/10/15 (16:00). 113
Figure 4.18: Water table contour map for plots 1 and 2 on 6/11/15. 114
Figure 4.19: Water table contour map for plots 1 and 2 on 6/12/15. 115
Figure 4.20: Water table contour map for plots 1 and 2 on 6/13/15. 116
Figure 4.21: Water table contour map for plots 1 and 2 on 6/15/15 117
Figure 4.22: Water table contour map for plots 1 and 2 on 6/17/15 118
Figure 4.23: Water table contour map for plots 1 and 2 on 6/19/15 119
Figure 4.24: Water table contour map for plots 1 and 2 on 6/22/15 (17:00) 120
Figure 4.25: Water table contour map for plots 1 and 2 on 6/23/15 121
Figure 4.26: Water table contour map for plots 1 and 2 on 6/24/15 122
Figure 4.27: Water table contour map for plots 1 and 2 on 6/29/15 123
Figure 4.28 Water table contour map for plots 3 and 4 on 6/2/15 (09:00) 124
Figure 4.29: Water table contour map for plots 3 and 4 on 6/2/15 (17:00) 125
Figure 4.30: Water table contour map for plots 3 and 4 on 6/8/15 126
Figure 4.31: Water table contour map for plots 3 and 4 on 6/9/15 127
Figure 4.32: Water table contour map for plots 3 and 4 on 6/10/15 (07:45) 128
Figure 4.33: Water table contour map for plots 3 and 4 on 6/10/15 (16:00) 129
Figure 4.34: Water table contour map for plots 3 and 4 on 6/11/15 130
Figure 4.35: Water table contour map for plots 3 and 4 on 6/12/15 131
Figure 4.36: Water table contour map for plots 3 and 4 on 6/13/15 132
Figure 4.37: Water table contour map for plots 3 and 4 on 6/15/15 133
Figure 4.38: Water table contour map for plots 3 and 4 on 6/17/15 134
Figure 4.39: Water table contour map for plots 3 and 4 on 6/19/15 135
Figure 4.40: Water table contour map for plots 3 and 4 on 6/22/15 (10:00) 136
Figure 4.41: Water table contour map for plots 3 and 4 on 6/23/15 137
Figure 4.42: Water table contour map for plots 3 and 4 on 6/24/15 138
Figure 4.43: Water table contour map for plots 3 and 4 on 6/29/15 139
Figure 4.44: USDA-NRCS Web Soil Survey map of Lake Alice Experimental Site and surrounding area 140

CHAPTER 1: COMPREHENSIVE LITERATURE REVIEW

1.1. Agriculture and Eutrophication

1.1.1. Nonpoint Source Pollution

With the passage of the Clean Water Act in 1972, the regulation of point sources of pollution (e.g., wastewater treatment effluent) reduced their contribution to the pollutant loads entering surface waters to acceptable levels. As these easily identifiable sources have invested in infrastructure improvements and come into compliance, the focus has shifted to the more difficult problem of identifying and managing non-point source pollution (Sharpley, 1994). Agricultural pollutants in runoff are considered nonpoint sources due to their spatial and temporal variability and are more difficult to mitigate than point sources because of their abundance (Myers et al., 1985). Approximately 64% of surveyed lakes and 36% of surveyed rivers in the US are considered impaired with excessive nutrients cited as the cause of impairment 19% and 16% of the time, respectively. Agricultural runoff was listed as the main nonpoint pollutant source in 16% of impaired lakes and 38% of impaired streams (U.S. EPA, 2009).

Nonpoint source pollution is a major contributor to the eutrophication and degradation of natural aquatic ecosystems (Chapman et al., 1998; Sharpley et al., 2001; Sims et al., 1998; Withers et al., 2011). These sources include urban runoff from impermeable surfaces (e.g., roads, parking lots), septic tank failures, and construction activities, among others (Smith et al., 1999). Although eutrophication is a natural process in the aging of ecosystems, Brady and Weil (2008) differentiate this natural

accumulation of nutrients over centuries (natural eutrophication), from cultural eutrophication, the excessive input of nutrients due to human activities. In freshwater systems, phosphorus (P) often limits the elevated rates of primary production associated with eutrophic environments (Foy, 2005).

1.1.2. Freshwater Eutrophication

Following 37 years of experimentation on a small lake in Ontario, Canada, Schindler et al. (2008) observed that algal biomass and P inputs remained proportional, regardless of nitrogen (N) concentrations. Although nitrogen and carbon are also essential to freshwater ecosystems, their chemical properties allow for transfer from the atmosphere, which makes them more difficult to control relative to P (Daniel et al., 1998). Nitrogen can be a limiting nutrient for some algae, but many forms are able to fix nitrogen from the atmosphere and are not limited by concentrations in the water. Schindler (1977) found that if nitrogen is limiting, the algal populations can shift to those that can fix atmospheric nitrogen. Conversely, P additions from the atmosphere are relatively small and account for approximately 0.05 to 0.5 kg ha^{-1} yr^{-1}. Therefore, land use and management factors are largely responsible for P imports to aquatic systems (Brady and Weil, 2008; Correll, 1998).

When systems become eutrophic, increased nutrient concentrations allow for an increase in the biomass that can be supported. This increase in biomass is largely due to an increase in phytoplankton populations. Upon death, phytoplankton sink to the lake bottom, decompose and create biological oxygen demand that can cause hypoxia (Foy, 2005). Hypoxic conditions occur when dissolved oxygen concentrations decline

below levels which can sustain the biota in an ecosystem. In healthy systems, the level of dissolved oxygen is 10-12 mg L^{-1}, whereas most effects associated with hypoxia can be observed when levels are < 2 mg L^{-1} (Pierzynski et al., 2005a). When the water overlying the lake bed becomes anaerobic, P can be released from redox-sensitive lake sediments (e.g., Fe, Mn oxides), which leads to further enrichment (Smith et al., 2011).

Hypoxia can result in fish kills and shifts in the biodiversity and species composition at all trophic levels (Correll, 1998). A major consequence of the disruption of the food web in freshwater lakes is the development of cyanobacteria (blue-green algae) or other harmful and nuisance algae blooms (HNABs). HNABs can thrive in these affected lakes in which there are few natural predators to limit population growth (Smith et al., 1999). In addition to being undesirable for recreation, these blooms can also produce powerful toxins (e.g., microcystins, anatoxin-a, saxitoxins) that are not only harmful to aquatic biota but also to humans and other animals that may come into contact with or ingest the contaminated water (Codd, 2000). This is of particular concern when the water body is an important source of drinking water as in the case of Lake Champlain, from which 20 million gallons are pumped daily to provide 180,000 people with public drinking water (Smeltzer and Quinn, 1996). There are no documented cases in Vermont of human illness related to these toxins, though the deaths of two dogs in 1999 and 2000 were attributed to consumption of contaminated lake water (VT Department of Health, 2015).

1.1.3. Eutrophication in Lake Champlain

Eutrophication in Lake Champlain has been a concern since 1979 with P concentrations identified as the major cause (Beaman, 1983). Despite continuous efforts in the intervening years to control non-point source pollution, conditions in the lake have continued to deteriorate. Since wide-scale monitoring of the lake began in 1990, P concentrations have not decreased significantly in any portion of the lake, with some areas continuing to increase. These increases have occurred even as the P loads of tributaries entering the lake have decreased (Smeltzer et al., 2009). The most affected areas of the lake have been in shallow, warm bays. A number of these shallow bays have tributaries that flow through agricultural landscapes and are therefore vulnerable to agricultural pollutants (Smeltzer et al., 2012). Of the total P entering Lake Champlain, 38% is estimated to be from agricultural runoff (LCBP, 2015). Further complicating the recovery efforts is the ratio of Lake Champlain's watershed to the total surface area of the lake. Whereas the Great Lakes have ratios between 1.5:1 and 3.4:1, the ratio for Lake Champlain is 18:1 (LCBP, 2015). Therefore, the impacts of land use and management are even greater due to the larger land base and greater number of nonpoint pollution sources.

1.1.4. Risk Management

Elevated nutrient concentrations in agricultural runoff are a result of the application of animal manure and/or commercial fertilizers to agricultural fields and the hydrologic connectivity of fields to surface waters (Sims et al., 1998). Managing P losses from crop fields remains a challenge because reported concentrations critical for

the control of freshwater eutrophication are just 20-30 µg P L^{-1} (measured as soluble reactive P, i.e., orthophosphate), while soil solution P concentrations of 200-300 µg P L^{-1} are required for crop growth (Heathwaite and Dils, 2000). Additionally, P is tightly bound to soil particles and insoluble under most conditions. Therefore, when farmers apply P (manure or inorganic fertilizers) to fields, only about 10-15% may be available for crop uptake after fixation by the soil, depending on soil pH and P concentration (Brady and Weil, 2008).

Many farms import grains to supplement rations that can lead to greater quantities of P remaining on the farm. Sharpley et al. (2001) estimated that more than two-thirds of the grain produced in the U.S. is exported off of the farm. Anderson and Magdoff (2000) estimated that feed sources account for 65% of P imported onto dairy farms in Vermont and 57% of total P imported remains on the farm. Approximately 40% of dietary P is utilized by dairy cattle (Arriaga et al., 2009) with the remainder excreted. Repeated manure applications can result in high soil P concentrations as more P is applied than removed by cropping. These factors often result in the over-application of P year after year, until inputs finally exceed the soil fixation capacity (Sharpley et al., 2013).

Applying P in excess of crop requirements promotes the buildup of plant-available P, which can then be exported to surface waters during rain and/or snowmelt events (Sims et al., 2000). As a result, even when additional inputs are limited, substantial export of nutrients from these excessively fertilized soils can still occur (Sharpley et al., 2013; Liu et al., 2015). However, there are many interrelated factors

involved in the fate of these applied resources, such as the location, timing, rate, and method of application that ultimately determine whether they will remain in the field or lost in runoff (Sharpley et al., 1994; King et al., 2015a). The risks of P transfer from crop fields to waterways must be negotiated due to its role in animal and crop production (Sharpley, 1994). With modern agriculture's reliance on input-intensive cropping systems and under increasingly extreme climatic conditions, maintaining the integrity of our freshwater ecosystems is a challenge that requires combining best nutrient management practices with a comprehensive understanding of the interactions among soil properties and hydrologic factors.

1.2. Phosphorus in Soils

1.2.1. Phosphorus Cycle

Phosphorus is an essential element for life and only nitrogen has a greater impact on the productivity and health of ecosystems (Brady and Weil, 2008). Phosphorus is an essential component of deoxyribonucleic acid (DNA) and ribonucleic acid (RNA). It is also necessary for most biochemical processes as it is a critical component of adenosine triphosphate (ATP), the molecule responsible for many cellular processes including energy transfer in respiration and photosynthesis. Despite this critical role in the biosphere, P is relatively scarce. On a mass basis, it is only the eleventh and thirteenth most abundant element in terrestrial and aquatic ecosystems, respectively (Smil, 2000).

The amount and forms of P naturally present in soils is the result of complex interactions dependent on parent material, texture, weathering, and biological processes (Tiessen et al., 1984; Young et al., 2012). Total P (TP) concentrations range from 50-3000 mg kg^{-1}, often with less than 1% available for biological uptake. The remainder of the soil P is insoluble and unavailable for uptake (Pierzynski, 2005; Frossard et al., 2005). The chasm between soil total P (TP) concentrations and plant-available P has promoted the development of agronomic soil tests for P (STP). These tests are intended to reflect the bioavailable P in the soil and account for regional soil differences. This relative scarcity of plant-available soil P in the natural environment is reflected in the necessity for fertilization in order to maximize economic returns for crop production, for which greater nutrient inputs are required to offset crop removal rates than native forests or grasslands (Tilman et al., 2002; Brady and Weil, 2008).

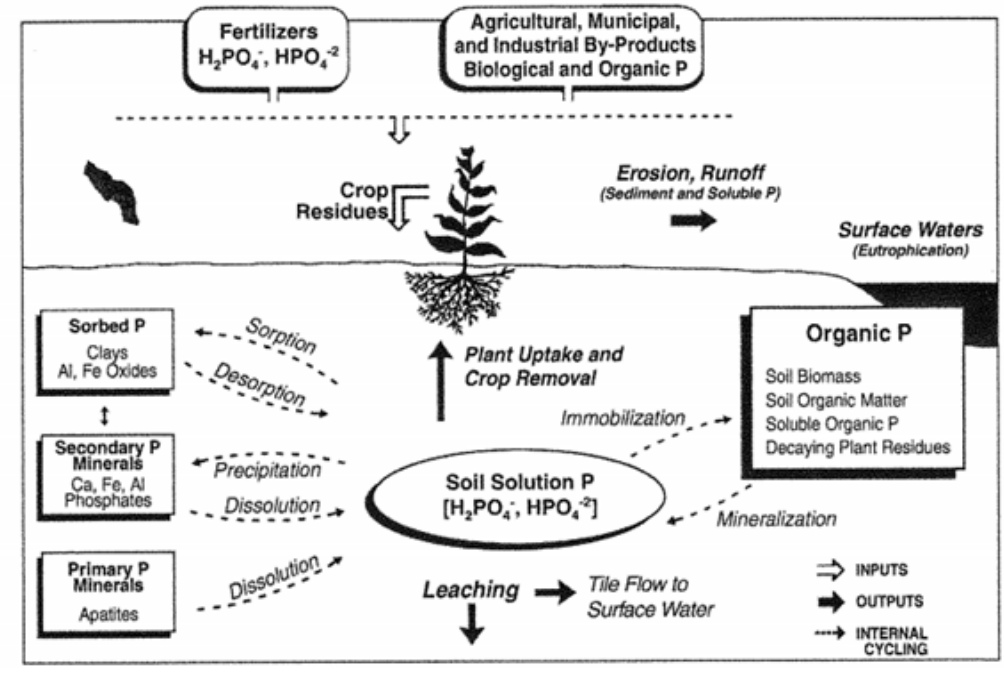

Figure 1.1: The soil phosphorus cycle. Physical, chemical and biological factors involved in P transport and availability (Pierzynski et al., 2005b).

The different fractions of soil P can broadly be categorized into organic and inorganic forms and by their solubility. Soluble reactive P (SRP) in the soil solution is bioavailable and is mainly orthophosphate. Unreactive dissolved P is primarily organic P (DOP) and unavailable until mineralized to orthophosphate via bacterial oxidation and/or hydrolyzed to orthophosphate by phosphatases (Wang et al., 2007). Total dissolved P (TDP) is a combination of inorganic and organic P available after filtration (<0.45 μm) and digestion. Particulate P (PP) can be organic or inorganic and represents the fraction that is insoluble and bound to solid particles. Total P represents the combined quantities of each of these fractions (Haygarth and Sharpley, 2000). The relative amount in soils can vary greatly, with organic forms typically representing 30-65% of total P in mineral soils depending on native soil fertility, climate, and land use and management factors (Condron et al., 2005). Organic soils (>20-30% organic matter by weight) may contain up to 90% organic P (Sims and Pierzynski, 2005). However, if drained for production, soil P can rapidly mineralize and be lost via leaching processes due to the absence of a sufficient mineral substrate to bind and retain the newly available P (McDowell and Monaghan, 2015). McDowell and Monaghan (2015) observed P movement in an organic soil converted to pasture with a mixture of swede and kale. Eighty-nine percent of applied P (87 kg P ha^{-1}) leached to 35 cm depth in the soil profile with evidence of leaching observed in soil samples taken at a depth of 100 cm. Total P content, soil pH, organic C content, and sampling depth were identified as the most important soil characteristics for predicting organic P content in a review of the literature by Harrison (1987).

Pierzynski et al. (2005a) define organic P as P bonded in some way with carbon (C). Organic P is derived from the biological accumulation of inorganic P. Plants and microorganisms in the soil take up orthophosphate which is then bonded to C via phosphorylation. Plants consist of about 0.2-0.6% P on a dry matter basis (Pierzynski and Logan, 1993). The microbial biomass can account for 2-5% of organic P in arable soils and up to 25% of organic P in grassland soils (Sims and Pierzynski, 2005). The residues of these biological organisms are the source of soil organic P. As microorganisms decompose these residues and the microorganisms themselves undergo decomposition, organic P compounds re-enter the soil P cycle with varying resistance to further transformations (Condron et al., 2005). Mineralization rates of organic P in temperate regions range from 5-20 kg ha^{-1} yr^{-1} (Brady and Weil, 2008; Frossard et al., 2000). When compared with crop removal rates of 39 and 34 kg P ha^{-1} for corn silage (assuming a wet yield of 67.2 Mg ha^{-1}) and alfalfa (13.4 Mg ha^{-1}) respectively, the need for supplemental P becomes apparent (Pierzynski and Logan, 1993).

Soil organic P can be split into two broad groups defined by their susceptibility to decomposition, rendering them biologically available or unavailable (Sims and Pierzynski, 2005). The humic acid fraction is highly stable and resistant to microbial activity. The biologically active fraction can be further broken down to three major forms of organic P: inositol phosphates, nucleic acids, and phospholipids (Pierzynski et al., 2005a). The inositol phosphates comprise the largest fraction of organic P in most soils, with estimates as high as 80% of the total organic P (Sims and Pierzynski, 2005). Their abundance is likely due to their ability to form strong associations with the

recalcitrant humic and fulvic acid fractions of organic matter (Turner et al., 2002). Nucleic acids and phospholipids can also be adsorbed by humic compounds and silicate clays. However, these fractions combined likely make up only 1-2% of organic P (Brady and Weil, 2008). Historically, organic P forms have received less attention in soil science and agronomic research than inorganic P, but recent advances in analytical techniques, such as nuclear magnetic resonance (NMR) spectroscopy, is improving our understanding of the nature and transformations of organic P in soils (Cade-Menun, 2005).

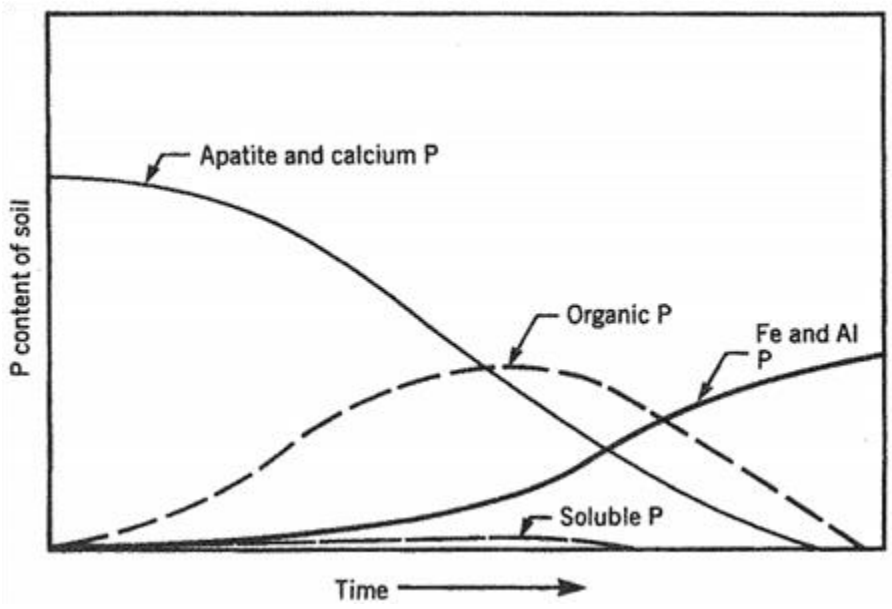

Figure 1.2: Effects of extent of soil development on soil P forms. From Sims and Pierzynski, 2005.

Inorganic P can be classified into two groups; those bonded with calcium (Ca) and those bonded with iron (Fe) and aluminum (Al). In mineral soils, the inorganic P fraction generally represents approximately 50-70% of the total P in the soil (Pierzynski et al., 2005b). In most soils, P is derived from the weathering of primary minerals,

predominantly apatite ($Ca_{10}(X)(PO_4)_6$, with X representing F^-, Cl^-, OH^-, or CO_3^{2-}. As soil genesis proceeds over time, Fe and Al phosphates (e.g., strengite, variscite) and P adsorbed to amorphous Fe and Al oxides become the dominant forms of P as illustrated in Figure 1.2 (Sims and Pierzynski, 2005). Phosphorus originating from minerals and colloids is present in the soil solution as primary orthophosphate (PO_4^{3-}) and as secondary orthophosphates (HPO_4^{2-} and $H_2PO_4^-$), depending on pH (Pierzynski et al., 2005a). These different forms are often collectively referred to as orthophosphate and will be for the remainder herein. The factors controlling the availability and movement of these compounds, namely how moisture status and pH influence the forms and mobility of P, will be discussed in the following section.

1.2.2. Phosphorus Solubility

In order to be available for biological uptake, P must be present as orthophosphate (Sharpley et al., 2003). As previously mentioned, often 1% or less of total P in the soil will be available in the soil solution for biological consumption (Pierzynski, 1991). Therefore, it is essential in agronomic systems to understand the factors influencing P solubility to ensure adequate soil fertility, or in the case of excessively fertilized soils, to understand how practices may promote P retention. The three dominant environmental controls on the solubility of P in soils are weathering, pH, and oxidation-reduction (redox) status (Frossard et al., 2000). As Figure 1.2 illustrates, soils in both early and late stages of pedogenesis have relatively small amounts of soluble P. This is due to the resistance to weathering of apatite in primary minerals and the high affinity for the Fe and Al minerals or oxides in later stages to

react with orthophosphate. Over time, these secondary reactions become increasingly stable as weathering processes remove Ca, Fe and Al minerals become dominant, and pH decreases, furthering the stability of Fe and Al complexes (Chacon, 2006; Olander, 2005; Sims and Pierzynski, 2005). The presence of organic matter can also increase P immobilization as Fe and Al are complexed within organic matter and provide a reactive surface for orthophosphate adsorption (Syers et al., 1973; Wang, 2007).

The primary reactions that immobilize P in order of increasing stability and decreasing P availability are outer-sphere anion exchange, inner sphere surface reactions, binuclear bridge complexes, and precipitation. Outer-sphere anion exchange reactions are charge dependent, weakly held by electrostatic forces, and tend to reflect the overall concentration of ions in solution. These bonds will continue to react and penetrate the mineral surface (e.g., Fe or Al oxides) to form single and binuclear bridges, the latter of which is extremely stable (Frossard et al., 2000; Sollins et al., 1988). Precipitation reactions result in slightly soluble P-containing compounds as a result of the large amount of exposed surface area (Brady and Weil, 2008).

As soils weather and Fe and Al complexes predominate, the forms and availability of P are strongly influenced by pH. Most agricultural soils have a pH between 4 and 9. At circumneutral pH values, HPO_4^{2-} and $H_2PO_4^-$ are present in roughly equal concentrations, with the former increasing as pH rises and the latter as pH decreases (Pierzynski et al., 2005b). Plant-available soil P is maximized as pH approaches 7. As acidity increases in soils, the reactive surfaces become less negative as hydrogen ions (H^+) accumulate. The negatively charged orthophosphate ions in

solution form electrostatic bonds with the positively charged surfaces and if low pH conditions persist, progression to the stronger inner-sphere reactions will further limit P availability (Essington, 2004).

University of Vermont soil fertility guidelines account for reactive aluminum on plant-available P in field crop recommendations (Jokela et al., 2004). For example, a soil with a concentration of 2.5 mg Modified Morgan-P kg^{-1} (medium range of soil test P), will result in a nutrient application recommendation of 17 lb ac^{-1} when reactive Al measures 10 mg kg^{-1}. However, when reactive Al is 100 mg kg^{-1} and at the same soil test P level, the P recommendation increases to 30 lb/ac. The reactivity of Al is strongly pH dependent and will not limit P availability when soils are limed within the optimum range of soil pH. However, when soils drop below pH 5.5, the elevated concentrations of reactive Al available to complex with soil solution P can rapidly result in P deficiencies that cannot be overcome, even by supplying large quantities of additional P (Goldberg et al., 1996).

The final important factor governing P solubility and availability is the redox status of the soil. Redox reactions refer to the coupled reactions of oxidation and reduction in which the valence state of reacting elements are altered. Oxidation reactions result in the loss of an electron from an element. Reduction reactions are the complementary reaction in which an element or molecule gains an electron from the oxidized element (Essington, 2004). Redox reactions are constantly occurring in soils because the completion of both pathways of biological respiration requires a terminal electron acceptor. In aerobic respiration, the terminal electron acceptor is always

oxygen gas (O_2). When O_2 levels are depleted and the soil becomes anaerobic, a new electron acceptor must be used. Reducing conditions are established once the oxygen supply in the soil is consumed during saturated soil conditions and the slow diffusion of atmospheric O_2 precludes aerobic respiration. These conditions stimulate anaerobic microorganisms to begin respiring utilizing additional electron acceptors (Reddy et al., 2005). Table 1.1 lists the elements in the relative order in which they become reduced and the ionic charge on the oxidized and reduced forms of each element.

Table 1.1: Elements used in respiration. Elements are listed in order used as the environment changes from oxidized to reducing conditions. From Brady and Weil 2008.

Element	*Oxidized form*	*Charge on oxidized element*	*Reduced form*	*Charge on reduced element*	*E_h at which change of form occurs, V*
Oxygen	O_2	0	H_2O	−2	0.38 to 0.32
Nitrogen	NO_3^-	+5	N_2	0	0.28 to 0.22
Manganese	Mn^{4+}	+4	Mn^{2+}	+2	0.22 to 0.18
Iron	Fe^{3+}	+3	Fe^{2+}	+2	0.11 to 0.08
Sulfur	SO_4^{2-}	+6	H_2S	−2	−0.14 to −0.17
Carbon	CO_2	+4	CH_4	−4	−0.20 to −0.28

E_h values from Patrick and Jugsujinda (1992).

Redox reactions are important to P solubility due to the high affinity of the oxidized form of iron (Fe(III)) for orthophosphate. As Table 1.1 indicates, Fe(III) will be utilized once the local supply of oxygen, nitrogen, and manganese have been reduced (Brady and Weil, 2008). The change in valence status as Fe is reduced from Fe(III) to Fe(II) is important because Fe(II) is soluble and the Fe-containing compounds will solubilize. Prolonged saturation in crop fields can result in reduced conditions that will mobilize P into the soil solution and be subject to leaching processes. In a laboratory incubation study, Sallade and Sims (1997) flooded soil cores for 21 d and

measured P in soil solution. Depending on the depth sampled, they observed three and four-fold increases of soluble P, with the greater solubilization rates occurring at greater depths where redox potential was lower.

Phosphorus solubilization due to the reductive dissolution of Fe(III)-containing compounds is also an important biogeochemical for in-lake controls of eutrophication. If the water overlying lake-bottom sediments becomes anaerobic, the sediments can release additional P, further exacerbating the eutrophication status of the lake. This was demonstrated by Smith et al. (2011), who observed that during a year (2008) in which algal blooms occurred in Lake Champlain, soluble P and cyanobacteria counts increased as lake conditions became more reduced. However, in summer 2007, no algal blooms occurred and the water at the sediment-water interface never became anoxic. In a laboratory microcosm study, Young and Ross (2001) observed that although porewater in flooded sediments became anoxic and 2-27 fold increases in porewater soluble P occurred, the overlying water remained aerobic. Due to this redox interface, the overlying water only exhibited about a four-fold increase relative to pre-flooding conditions. The authors concluded that as the majority of solubilized P and Fe(II) that crossed the interface, Fe(II) reverted back to its oxidized state and immediately resorbed the newly liberated P.

1.3 Hydrologic Processes

1.3.1. Soil Water Budget

As evidenced by the previous discussion of redox reactions, the behavior of P is strongly influenced by the moisture status of the soil. In addition to the influence of water on chemical reactions in soil, water movement strongly impacts the potential for P transport via soil erosion and subsurface drainage. The affinity for P to be adsorbed to soil can result in large P export from fields during runoff and erosion events.

The simplest description of a soil water budget is demonstrated by Equation 1.1.

Soil Water Flux = Precipitation – Evapotranspiration – Soil Storage [Eq. 1.1]

Equation 1.1 Basic calculation for a soil water budget. From Brady and Weil 2008.

The total amount of potential discharge from a field is ultimately influenced by its climate and soil characteristics. The effect of climate is reflected in the amount and distribution of rainfall and physical factors (e.g., temperature, humidity, solar radiation, wind) that influence evapotranspiration rates (Brady and Weil, 2008). The quantity and intensity of the precipitation has a major impact on the soil water budget as it influences the type of runoff processes that will occur (Kirkby, 1988). Up to 50% of water inputs may be lost to groundwater annually in humid regions (Brady and Weil, 2008).

Evapotranspiration (ET) is a term for the combined processes of evaporation of water to the atmosphere directly from the soil (and plant surfaces) and transpiration, the translocation of water from the soil for use and cooling before exiting the stomata to the atmosphere. An estimated 12% of the earth's precipitation returns to the atmosphere

via terrestrial ET (Eagleson, 1978). Evapotranspiration calculations are made by comparing potential ET (PET) to actual ET (AET) (Brady and Weil, 2008). Potential ET is the maximum rate at which water vapor will be lost if soil water content is not limiting and is based on crop type and climatic variables (solar radiation, temperature, relative humidity, cloud cover, and wind speed) that affect the vapor pressure gradient between the soil/vegetation and the atmosphere. PET is typically calculated by applying a correction factor to the amount of water that will evaporate from a pan. Potential ET equals AET when the soil water content is not limiting. When there is a soil moisture deficit, ET will be less than PET and dependent on the available soil water. AET is impacted not only by climatic variables and soil moisture storage, but also on the type and growth stage of the plant (Allen et al., 1989; Penman, 1948).

The amount of water retained by the soil or lost to runoff processes is largely dependent upon the relative proportion of sand, silt, and clay. The texture of a soil partially imparts its porosity, the total volume in a soil not occupied by solid particles (Brady and Weil, 2008). Although land use and management factors (e.g., tillage, compaction) influence porosity by impacting soil structure, some general assumptions can be made regarding the relationship between texture and porosity (Dexter, 1988; Pagliai et al., 2004). Finer-textured soils have greater total porosity than coarser-textured soils and have a greater soil water storage capacity. However, the water content available to vegetation is not necessarily greater due to the inability of plants to remove water from the smallest pores. The permanent wilting point is the water content of a soil below which plants cannot remove water and will fail to recover once

the soil is rewetted. This results from the inability of most plants to create suction greater than the -1500 kPa required to remove the most tightly held water molecules (Brady and Weil 2008). According to the USDA Agricultural Research Service Soil Water Characteristics Tool (v. 6.02.74), a clay soil (50% clay) will have 48.8% porosity by volume and a maximum of 1.45 in ft^{-1} of plant available water. However, a silty clay loam (20% clay) will have very similar porosity, 48.2% by volume, but have roughly 50% more plant available water, for a total of 2.21 in ft^{-1}.

1.3.2. Runoff Processes

There are various pathways precipitation can take upon reaching the land surface. The type of pathway is determined by a variety of factors including rainfall intensity and duration, geographic setting, soil characteristics, and antecedent moisture conditions. Dunne and Leopold (1978) identify and define the characteristics of the different storm runoff processes. These processes are Hortonian overland flow, subsurface storm flow, return flow, and direct precipitation onto saturated areas. Direct precipitation onto saturated areas can occur regardless of the mechanism responsible for generating overland flow. An awareness that these processes vary widely in both spatial and temporal domains has given rise to the concept of variable source area (VSA) hydrology (Needelman et al., 2004). Under VSA hydrology, only a small percent of the landscape is responsible for producing storm flows. When combined with P source areas, these locations are termed critical source areas (CSAs) because approximately 80% of P losses originate from 20% of the landscape (Sharpley et al. 2009).

Hortonian overland flow occurs when the infiltration capacity of a soil is exceeded by the precipitation rate and water begins to accumulate on the surface. Overland flow will initiate if there is appropriate slope to conduct the water once the topographical irregularities of the land surface have filled with water (depression storage). The volume of overland flow and its velocity increase as distance downslope increases and a greater area contributes to the flow (Kirkby, 1988). Precipitation onto the sheet of overland flow also adds to the total volume of surface runoff. Dunne and Leopold (1978) refer to this as direct precipitation onto saturated areas (DPS). The energy of overland flow has the potential to move large amounts of topsoil (Kleinman et al., 2006). Depending on the distance to a receiving water body, overland flow may runoff directly to surface water or accumulate in depressions at a lower elevation where it resides until the water table lowers, allowing it to infiltrate and be consumed by evapotranspiration processes (Dunne and Black, 1970b).

A second type of overland flow is saturation excess overland flow. This occurs when precipitation exceeds the storage capacity of the soil, often in downslope areas where there is a shorter distance to the water table and thus lower storage capacity. Saturation excess overland flow is termed return flow because it is subsurface water that returns to the surface where the water table rises above the ground level (Dunne, 1983). This can often occur near the base of slopes where horizontal subsurface flows emerge from the hillside where the water table is at a height greater than the base of the slope.

In some cases, subsurface storm flows (i.e., subsurface flow that occurs in excess of normal baseflow conditions) may occur. These flows tend to occur when a coarse-textured soil overlies an impermeable layer (Gburek and Sharpley, 1998). An impermeable layer is defined as having less than 10% of the conductivity of the overlying layer (NRCS, 2001). As a result of this resistance to vertical flow, the majority of subsurface flow will move downslope over the impermeable layer until it reaches a stream channel. Subsurface storm flow is often at least 100 times slower than overland flow but can still dominate the storm hydrograph in many cases (Dunne and Black, 1970a). Increased subsurface storm flow due to an impermeable layer can also impact the volume of saturation excess overland flow. Gburek et al. (2006) observed about three times the surface runoff in a watershed with fragipan soils (compacted subsurface layer) compared to a similar nearby watershed that experienced nearly identical rainfall.

Soil characteristics are an important factor in determining runoff processes. As previously discussed, soils consisting of finer textured soils will generally have greater total porosity. Soil texture is also related to the development of soil structure. Dexter (1998) defines soil structure as "the spatial heterogeneity of the different components or properties of soil." Good soil structure (i.e., soil with a well-distributed range of stable, well-developed pore sizes) is influenced by the clay and organic matter properties that allow for the formation of stable aggregates (Dexter, 1998; Pagliai et al., 2004). The large reactive surface area of organic matter and the products formed by biological activity act as glue to enhance soil structure (Bronick and Lal, 2005). Soil aggregation

allows for large inter-aggregate pore spaces and facilitates rapid infiltration and drainage (Azooz and Arshad, 1996).

Cultivated fields, particularly those planted with row crops, may suffer from poor infiltration rates (Burch et al., 1987; Needelman et al., 2004). This is a consequence of the high disturbance of soil structure, low organic matter, and minimal rain interception rates due to low vegetative cover. Tillage practices destroy the soil's ability to form aggregates due to mechanical disruption (Pagliai et al., 2004) and increased rates of organic matter mineralization (Balesdent et al., 1990). A corn field may only intercept 7% of total rainfall as compared with 43% under a maple and beech tree canopy (Haynes, 1954; Kittridge, 1948). This increases the total amount of water volume available to generate runoff and exposes the soil surface to the high kinetic energy of raindrops. The energy of the raindrops can lead to soil particle detachment, surface crusting and further reduction of infiltration (le Bissonnais, 1996). The cumulative effects of soil particle detachment and erosive forces of the overland flow scouring the topsoil have the potential to erode large amounts of exposed soil (Young and Wiersma, 1973). This situation results in both agronomic and environmental impacts as the fertile topsoil is lost for crop growth and is often deposited in an undesirable location, particularly if it is carried to surface waters (Sharpley et al., 1992).

An important factor in the development of soil structure is the formation of macropores. Macropores are formed from the moisture dependent shrink/swell properties of clays and biopores created by root channels, earthworm burrows, and

other soil biota (Simard et al., 2000). They are often collectively referred to as preferential flow pathways as a means of differentiating the flow that occurs in these pores from the matrix flow (i.e., uniform flow through intra-aggregate pore spaces) that occurs in the majority of the soil profile (Simard et al., 2000). Beven and Germann (1982) note that the pore diameter size that defines a macropore is arbitrary and many different definitions exist in the literature, with typical values ranging from 75 µm – 3000 µm (Haygarth et al., 2000; Simard et al., 2000). The main properties that differentiate macropores from the rest of the soil matrix is that these pores are large enough to have no significant capillary forces, are the first pores to empty during periods of flow, and are responsible for a disproportionate amount of flow relative to their volume (Beven and Germann, 1982; Simard et al., 2000). Quantifying their extent and the amount of water that flows through these pathways is difficult and many studies have relied on the use of tracers to follow water movement.

Finally, antecedent moisture conditions also influence hydrologic runoff pathways. Less rainfall will be required to induce saturation excess overland flow when following a rain event that already raised the water table and reduced available soil moisture storage in the vadose zone (Skaggs, 1994; Gburek and Sharpley, 1998). Conversely, when a storm occurs with low antecedent moisture conditions in soils with shrink/swell clays, infiltration rates may be above normal as there are large preferential flow pathways open for rapid infiltration (Hardie et al., 2011) and increasing rates of subsurface storm flows versus overland flows (Kleinman et al., 2006).

Once the soil is saturated, the major factors controlling subsurface water movement are the hydraulic gradient and hydraulic conductivity. The relationship between these variables is described by Darcy's Law as seen in Equation 2.

$$\frac{Q}{A} = -K_s \frac{\Delta H}{L} \qquad \text{[Eq. 2]}$$

Equation 1.2 Darcy's Law for describing water flux in a porous medium.

This states that the volumetric flow rate per unit of saturated cross-sectional area (Q/A) is a function of the difference in hydraulic head (height of the water table) between two points (hydraulic gradient, ΔH/L) and the saturated hydraulic conductivity constant (K_s) of a given medium (Radcliffe and Simunek, 2010). Saturated hydraulic conductivity is extremely variable and largely determined by soil texture, structure, and the existence of preferential flow pathways. However, due to the variability of these factors in the field, ranges of K_s are given according to soil texture classes. For example, the NRCS hydraulic conductivity classes list the range of K_s for a loamy sand to be 42.34-141.14 μm s^{-1} versus 1.41-4.24 μm s^{-1} for a clay loam (NRCS, 2015).

In unsaturated soils, the Richard's equation is generally used to estimate transient water fluxes under steady-state conditions. Richard's equation was developed to account for changes in soil moisture and matric potential (negative pressure due to empty pores) on water fluxes (Radcliffe and Simunek, 2010). Numerical iterative methods are generally used to solve Richard's equation and are computationally intensive (Pachepsky, 2003). However, in field soils with high macroporosity and preferential flow pathways, the assumption of steady-state conditions may not be applicable much of the time.

1.4. Agricultural Drainage

1.4.1. History and Status of Agricultural Drainage

The practice of artificial water drainage for the benefit of agricultural production has a long history. Herodotus wrote about drainage in Egypt in the 5th century B.C. and Cato described drainage techniques necessary in Roman times around 160 B.C. In the United States, much of the productive farmland in the Midwest was originally swamp. As the nation was in the midst of westward expansion in the 19th century, the Swamp Land Acts of 1849 and 1850 were enacted by the federal government (Skaggs and van Schilfgaarde, 1999). This legislation allowed the federal government to turn over wetlands to individual states, who in turn, could sell the land to settlers, as long as the proceeds were used for drainage. These actions were motivated by the inhospitable conditions of the swamps where swarms of mosquitoes and associated diseases such as malaria thrived. Drainage of these areas had the two-fold benefits of providing easier passage for westward migration and providing large amounts of highly productive land for agriculture (Skaggs et al., 1994).

Skaggs et al. (1994) estimate that natural drainage processes are insufficient on about 25% of cropland in the United States and Canada. For some states, estimates exceed 50%. Agricultural drainage practices are generally classified as to whether they facilitate surface or subsurface drainage processes. Surface drainage generally involves land grading and ditching to prevent depressional storage (Carter, 1999). Subsurface drainage is dominated by artificial tile drainage and the two terms are often used interchangeably. Currently, the term tile drainage is an anachronism due to

technological advances. When the practice was first introduced, fired clay tiles, and later concrete tiles, were buried underground where they functioned as a conduit for the collection and transport of excess water in the field. Presently, perforated corrugated PVC pipe is used in place of the clay tiles (Schwab and Fouss, 1999). Many different options exist with regard to engineering tile drainage systems (i.e., depth of tiles, grade, lateral spacing) and are largely dependent on field conditions and desired drainage capacity (Madramootoo, 1999). In the northeast, field tiles are typically 10 cm in diameter and connect to main lines ranging from 15 to 25 cm in diameter that typically drain to a ditch or directly to a stream. While the USDA minimum cover for subsurface tile drains is 0.61 m, many drainage installations target a depth of 1 m below the soil surface with a minimum grade of 0.1% (Madramootoo, 1999). Lateral spacing between tiles in the northeast ranges from 7.6 m to 23 m. Most tile drainage today is installed by subsurface drainage machines that plow pipe directly into the soil at a given grade using laser leveling or GPS technology (Broughton and Fouss, 1999; Wright and Sands, 2001).

The first use of tile drainage is claimed by England in 1810 (Fraser and Fleming, 2001). John Johnston of Seneca, NY brought the technology with him from Scotland and the success it brought him soon popularized the practice in North America (Smith and Massey, 1987). Skaggs et al. (1994) estimate that as of 1985, 45 million ha and 31 million ha in the U.S. and Canada respectively, have been artificially drained. They further estimate that of those 45 million ha in the U.S., 30 million ha have improved subsurface drainage. These numbers have probably increased since then as

improvements in technology have simplified installation and made the practice even more economically sound. However, difficulties in determining where these practices have been installed make estimation of their use challenging. The effectiveness of geographic information systems and other technologies is currently being investigated (Sugg, 2007).

The well-documented agronomic advantages of implementing drainage practices, particularly tile drainage, have resulted in the loss of about 50% of the wetlands in the United States (Skaggs and van Schilfgaarde, 1999). Increased public awareness of the benefits of wetlands for water quality and wildlife purposes has resulted in a backlash against drainage practices as they are still commonly viewed as destructive to these ecosystems. However, since the Swampbuster provisions in the 1985 and 1990 Food Security Acts, the conversion of wetlands for agricultural production has been prohibited (Blann et al., 2009). As Skaggs and van Schilfgaarde (1999) point out, the majority of subsurface installation now occurs in areas that have been farmed for decades. Additionally, without the conversion of land that occurred in the 19th and mid-20th century, a large percent of the land base used to produce our food would not be available. The ever-increasing pressure placed on our resources by growing populations requires an objective and thorough assessment of the risks and benefits of the methods with which we produce our food supply.

1.4.3. Benefits of Agricultural Drainage

The agronomic benefits of improved drainage have been well documented in the literature. Brady and Weil (2008) define the "ideal" soil as that consisting of 45%

minerals, 5% organic matter, 25% water, and 25% air. Tile drainage aids in accelerating the rate at which gravitational water from precipitation and/or snowmelt events is removed from the profile and thus allows increased respiration and root growth of the vegetation (Fraser and Fleming, 2001). Increased availability of oxygen has positive implications for both the biological community and the physical structure of the soil (Evans and Fausey, 1999; Fraser and Fleming, 2001). Soil temperatures are directly related to the moisture content due to the high specific heat of water. Soil temperatures should reach a minimum of 50° F prior to planting for healthy seed germination of many crops. When soil temperatures are less than this critical point, the seed will absorb water but not germinate and the moisture levels will result in the seed rotting in the soil (Al-Darby and Lowery, 1986). The risk of saturated soil conditions is not limited to germination, but persists especially during the early vegetative growth of crops. Lal and Taylor (1969) observed significant losses in corn yield when plots were exposed to intermittent flooding periods as well as consistently shallow (15 and 30 cm) water tables.

Improved drainage in heavy soils also allows for greater trafficability of fields. The use of heavy tractors and trucks on saturated soils results in soil compaction. Soil compaction destroys the structure of the soil by decreasing pore sizes and disrupting the connectivity of pores. Decreasing the porosity of the soil limits the vertical extent of root growth (Pagliai, 2004). Therefore, even though water and nutrient levels should be adequate, the limited root growth diminishes the plant's ability to scavenge available nutrients. By increasing the removal rate of water in the spring, farmers are able to

work their fields earlier. This extension of the growing season allows farmers to choose from a wider choice of crops and crop varieties as well as increasing yields at harvest. Crop yield benefits seen in Table 1.2 demonstrate the potential yield benefits of maintaining high soil quality and longer growing seasons.

Table 1.2: Crop yield increases following installation of tile drainage. From Colwell, 1978.

Crop	Average Yield before tile drainage	Average yield after tile drainage	Yield increase	
	tonne/ha	tonne/ha	tonne/ha	%
Grain corn	4.14	5.58	1.44	34.8
Soybeans	1.96	2.59	0.63	32.1
Wheat	1.77	2.61	0.84	47.5
Oats	1.60	2.35	0.75	46.9
Hay	4.10	5.20	1.10	26.8

1.4.3. Effects of Drainage on P Forms and Losses

Installation of tile drainage substantially alters natural field hydrology, biogeochemical conditions and nutrient transport potential. Faster infiltration rates due to greater soil water storage can reduce surface runoff by 34% (Bengtson et al., 1988), 55% (Istok and Kling, 1983), and up to 100% in some cases (Macrae et al., 2007). Madison et al. (2014) found that subsurface drainage accounted for 66-96% of the total water yield from four sites with differing management. Reviews of the literature found that not only is the pathway of drainage altered, but the total water yield from fields tends to increase with increases between 10-25% reported in the literature (Skaggs et al., 1994; King et al., 2015a). Tile drainage also increases the hydrologic connectivity of landscapes. As a result, locations that previously were hydrologically isolated from

surface waters now have a direct, unfiltered connection. This can increase the dispersal of nutrient loads as well as alter the hydrologic dynamics of the entire watershed (Schilling and Helmers, 2008).

For many years, tile drainage was considered to be a conservation practice due to its role in the reduction of surface runoff and erosion (Skaggs and van Schilfgaarde, 1999). However, research has demonstrated that tile drainage increases nitrate-N export potential compared to undrained conditions (Dinnes et al., 2002). More recent studies at the field and watershed scales show tile drains contribute to more P loss at the field scale than previously assumed (King et al., 2015; Smith et al., 2015). Although P concentrations tend to be lower in subsurface runoff than in surface runoff, increased total water yield from tile drainage can result in similar loading rates (King et al., 2014b). Estimates of total P export from tiles range from 0.2 to 2.4 kg ha^{-1} (King et al., 2015; Sharpley, 2000). Although these losses reflect only a small percentage of the total P applied to agricultural fields, the Ohio Phosphorus Task Force estimates loads of 0.6 to 1.1 kg ha^{-1} are sufficient to cause algal blooms in the western Lake Erie Basin (King et al., 2015a).

Losses of P generated by overland flow processes tend to be dominated by particulate P (PP) due to the affinity of orthophosphate for soil particles (Sharpley et al., 2003). Particulate P losses account for about 80% of P transported in overland flow from cultivated land (Sharpley et al., 1992). Sediment losses can be particularly extreme during intense rainfalls if rill and gully erosion occur due to the lack of adequate vegetative cover and adequate soil organic matter to protect and anchor

cultivated soils (Gilliam et al., 1999; Haygarth and Jarvis, 1999). Studies in Louisiana and Ohio conducted by Bengtson (1990) reported decreases of 42% and 36% in sediment export over 6 yr following the installation of tile drainage. Dissolved P (DP) losses may occur during overland flow as well. These losses are most likely to occur on P saturated soils and when rainfall events occur shortly following surface application of fertilizers such as liquid manure, which is high in soluble forms of P (King et al., 2015a). Withers et al. (2003) noted that about 60% of the total P losses occurred within the first 7 d post-application.

In general, P losses via subsurface pathways tend to occur in dissolved forms due to the inherent ability of the soil matrix to act as a filter for solid particles. However, limited levels of P reach the groundwater as a result of the high rates of P sorption by soil particles. Most vertical movement of DP occurs in preferential flow pathways (Simard et al., 2000). Although fine-textured soils have more reactive surfaces to bind P, their ability to preferential flow pathways prevents consistent correlations between P losses and texture. Most of the subsurface transport of P to surface waters, including PP, occurs when these preferential flow paths deliver P directly to tile drains that bypass the soil matrix and limit P sorption (King et al., 2015a). Evidence of this 'bypass flow' can be seen in the hydrographs and chemographs of storm events wherein discharge and P concentration peaks in tile flow coincide strongly with the onset of precipitation, rather than having a more delayed response (Smith et al., 2015b). The results of a three-year study showed 70% of total P losses in tile drainage were PP (Bottcher et al., 1981). Vidon and Cuadra (2011)

determined macropore flow to be responsible for 43-50% of total P losses in tile drainage during large storms (>6 cm bulk precipitation) and 11-17% of total P losses in small storms (< 3 cm bulk precipitation).

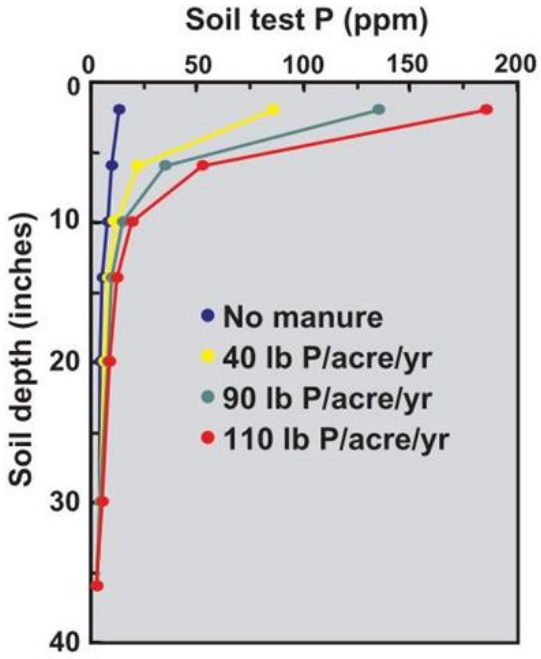

Figure 1.3: Stratification of STP (Mehlich-3) by depth in the soil profile. From Sharpley et al., 2003.

Elevated rates of DP losses in subsurface runoff may occur with long-term saturation following heavy rainfall if the water table remains elevated long enough to stimulate the reductive dissolution of Fe-phosphates (Pierzynski et al., 2005a). Soil P in agricultural fields tends to be highly stratified with depth due to tillage and fertilization (Penn et al., 2007; Sharpley et al., 2003). Higher P concentrations tend to reside in the tilled horizon (Ap) and strongly decrease with depth (Figure 1.3). There is an even

smaller depth of enrichment when no-till practices are employed as soils are not annually turned over by plow.

This stratification of P in the profile can present environmental risks as these P-rich surface particles are preferentially eroded. Sharpley (1980) refers to this as the P enrichment ratio and observed the process in a laboratory study with simulated rain. The ratio represents the relationship between the soil test P (STP) for a given location and the STP present in eroded sediment following runoff events. The results also demonstrated that runoff events following nutrient applications results in an even larger ratio. Enrichment ratios of a fine loam were determined to be 2.43 and 6.29 following P additions of 0 and 100 kg ha^{-1} respectively.

In soils with minimal P sorption capacity (e.g., sands) and a long history of over-application of P, substantial downward movement can occur. The P sorption capacity of a soil is an essential factor in determining the fate of applied P. The degree of P saturation (DPS) is the ratio between the extractable P to the sum of extractable Fe and Al. When soils have a high DPS, the risks of P losses due to desorption is elevated (Young and Ross, 2001). Additionally, when reactive surfaces for P sorption are limited, P will more readily migrate through the profile (Maguire and Sims, 2002).

Desorption of orthophosphate to soil solution and soil-water extracts designed to mimic runoff tends to exhibit a two-stage, curvilinear pattern with respect to STP. Some researchers have referred to this rapid increase in P release at a given STP (estimated by split-line regression) as the critical "change point". Numerous studies have seen this change point occur between 42 and 70 kg Olsen-P ha^{-1} (Heckrath et al.,

1995; Hesketh and Brooks, 2000; Smith et al., 1995; Smith et al., 1998). McDowell and Sharpley (2001) found a change point at 193 mg Mehlich-3 P kg^{-1}. The Mehlich-3 extraction method is roughly twice as efficient as the Olsen extraction so their finding equates to approximately 96 kg Olsen-P ha^{-1} (King et al., 2015a; Wolf and Baker, 1985).

The lack of consistent results in the literature regarding the effects of tile drainage on water quality reflects the inherent variability of soil conditions, hydrology, and biogeochemical processes. This variability is further intensified by the variety of management techniques employed in the field. In order to be widely effective, the development of best management practices must reflect the potential variety of responses and weigh the advantages and disadvantages of different management decisions. Targeting these practices where VSA hydrology and P sources intersect (i.e., CSAs) will be essential to maintain economically viable crop production while protecting our water resources (Sharpley et al., 2009).

1.5. Research Objectives

The objective of this study was to quantify differences in runoff water yield and associated P losses between artificially drained and undrained field plots. The following hypotheses were tested:

I. Mean surface runoff volumes will be lower for the tile-drained plots compared to the naturally-drained plots.

II. The reduction in surface runoff volumes will result in lower mean sediment losses for the tile-drained plots compared to the naturally-drained plots.

III. The reduction in sediment losses will result in lower mean total phosphorus losses for the tile-drained plots compared to the naturally-drained plots.

CHAPTER 2: MATERIALS AND METHODS

2.1. Site Description and Timeline of Field Activities

The experimental site is located within a 1.65 ha field in Clinton County at the Lake Alice Wildlife Area in Chazy, NY (44°52'30.49"N; 73°28'51.08"W). The land is leased and managed by the William H. Miner Agricultural Research Institute in Chazy, NY. Clinton County experiences an average of 80 cm yr^{-1} of precipitation and an average growing season of 130 d. Prior to the establishment of the trial, the field had been managed as a cool season grass field *(Phalaris arundinacea*) with no recent history of crop rotations. The field was harvested approximately one time per year, did not receive any nutrient applications, and had no prior history of improved drainage.

The research plots were established across a relatively uniform hill slope (5%) that transitions from an excessively drained outwash soil (Colosse-Trout River complex; sandy-skeletal, mixed, frigid Entic Haplorthods) on the upslope to a very poorly drained silty clay series (Adjidaumo; fine, mixed, active, nonacid, frigid Mollic Endoaquepts) at the toeslope (Trevail et al., 2006). Plots were approximately 45.7 m long by 22.9 m wide with plot lengths oriented up and down the slope. The transverse slope was < 1% and field observations indicated no evidence of mixing of surface water flows among adjacent plots under a range of runoff events, including snowmelt. Soil samples were taken from the upper three soil horizons (Ap, Bw, B/C) from the middle of each plot and sent to the University of Maine Soil Testing Service for agronomic testing following Cornell University soil testing methods (Morgan soil test extractant). The approximate depths of the horizons across all four plots were: Ap horizon: 0-30

cm, Bw horizon: 30-51 cm, B/C horizon: 51-91 cm. The B/C horizon extended beyond 91 cm, however soil pits were only excavated to that depth.

2.2. Experimental Design

Four experimental plots were constructed in 2012-2013 to enable the individual collection of surface and subsurface runoff (Figure 2.1). Field preparations for plot installation began in the summer of 2012. Woody vegetation along the upslope field border was removed to homogenize the field and create equivalent plot dimensions. Three artificial subsurface tile drainage lines were installed parallel with the field slope and centered in each plot during the fall of 2012. Average tile installation depths were approximately 1 m below the soil surface. Each plot drained to a 15 cm (i.d.) PVC pipe that connected to individual concrete manholes where subsurface and surface drainage water is sampled and flows are measured. The undrained treatment was accomplished by plugging the end of the tile line with 100 mm Cherne Original® Gripper Plugs in the manholes of the undrained plots.

To collect surface water runoff from each plot, 30 cm (i.d.) PVC pipe was cut in half and installed in shallow excavated trenches at the bottom of each plot. Surface water collection trenches flowed via gravity into each manhole where flow was sampled and gauged. To stabilize the disturbed soil following installation of the collection trenches, a 1 m wide layer of gravel was deposited along the length of the trenches. Minimal collection of sediment was observed in the gravel strips throughout the duration of the study. Installation of the surface runoff collectors was delayed by

the onset of winter and wet field conditions in spring 2013 and was completed in summer 2013 once field conditions were dry enough to resume construction.

The grass sod was terminated in fall 2013 with glyphosate application. Liquid dairy manure was applied in fall 2013 at a rate of approximately 15 Mg ha^{-1} in the fall followed by primary tillage with a disk harrow. In May 2014, the field was disk harrowed again prior to planting corn (*Zea mays* L.) for silage June 2014 at a population of approximately 84,000 seeds ha^{-1}. At planting, 168 kg ha^{-1} of a 23-12-18 dry fertilizer was applied through the planter. The field was harvested in fall 2014, followed by manure application at a rate of approximately 15 Mg ha^{-1}. A snow storm in early December 2014 prevented incorporation of the applied manure. Monitoring efforts for the study began in fall 2013, but due to low precipitation rates, no runoff was generated and data collection began in April 2014, continuing through June 2015.

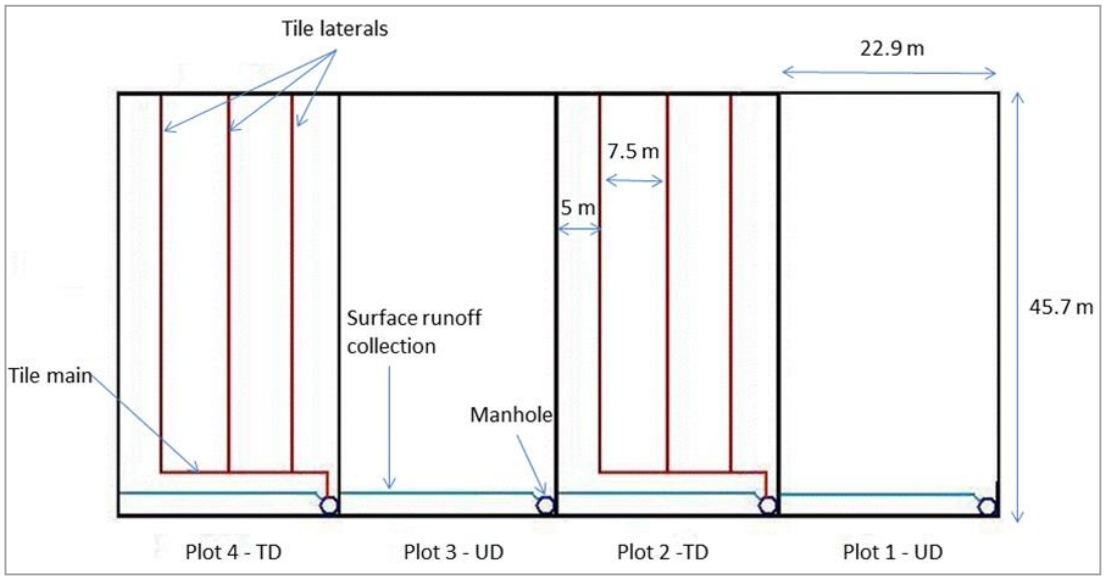

Figure 2.1: Schematic of plot layout at the Lake Alice Wildlife Area, Chazy, NY.

In May 2015, 22 shallow groundwater wells (2 cm diameter, 91 cm screen) were installed at a depth of 1.2 m to monitor the water table across two of the three shared boundaries between treatments. The wells were installed across the boundary of plots 1 and 2 and the boundary of plots 3 and 4. Figure 2.2 shows the locations of wells along the shared boundaries. Water table elevation contour maps were generated using R statistical software (R Foundation for Statistical Computing, Vienna, Austria) for both arrays of wells at each time-point to determine the predominant direction of water flow. Water table equipotential lines were determined with the Akima package (v. 0.5-12), which utilizes a bilinear spline interpolation method. The maps for plots 3 and 4 only contained the lower two transects of wells as the water table never rose to the height of the single well furthest upslope.

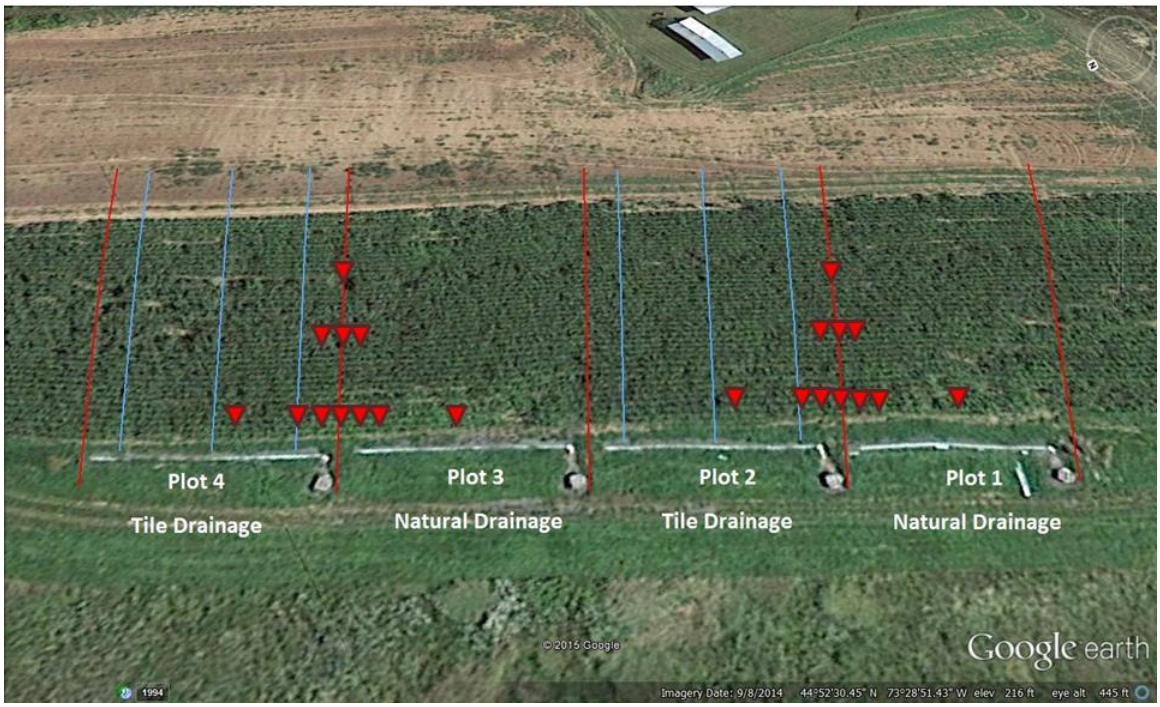

Figure 2.2: Shallow groundwater well locations. Wells are indicated by red triangles, red lines indicate plot boundaries and blue lines indicate tile lines. In each array, wells are labeled A-G (left to right) for the downslope transect of wells, H-J for the mid-slope transect of wells (left to right), and well K is furthest upslope.

2.3. Water Flow Measurements

Surface and subsurface runoff flows were measured with a five gallon bucket modified with a v-notch weir to enable stage-discharge relationships to be determined. Each bucket was equipped with a 5 cm diameter stilling well which housed a HOBO U20 Water Level Logger (Onset Computer Corporation, Bourne, MA). An additional water level logger was located at the study site to provide barometric correction to transform pressure readings to water depth. Loggers were programmed to record measurements at 5-min intervals except when winter temperatures remained consistently below freezing. In order to prevent damage, data loggers were removed from the field during these conditions when there was a minimal chance of water flow.

The v-notch weir buckets were developed and calibrated in the laboratory. A rating curve was developed using a series of peristaltic pumps to deliver a precise water flow rate into each bucket-HOBO logger for a given time period. Pressure readings were then transformed to water height inside buckets and plotted as a function of measured flow (estimated by the time to fill a known volume) to develop stage-discharge relationships for each bucket. The laboratory results showed a strong curvilinear relationship (mean $R^2 = 0.99$) and therefore the bucket-logger combinations were used in the field study. New rating curves for each bucket-logger combination were developed in the field using the 5-min interval pressure readings and measured flows across a range of flow rates. Flow rates were measured in duplicate for each observation using the time to fill a known volume to estimate instantaneous discharge.

Cubic regression models were fit to field measured flows (Fig. 2.3) using JMP PRO 11.2 (SAS Institute Inc., Cary, NC) and used to predict water runoff flows.

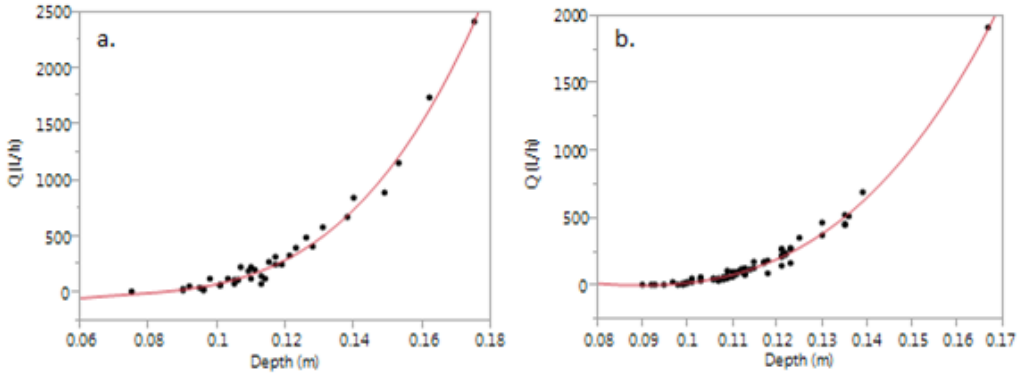

Summary of Fit

RSquare	0.986
RSquare Adj	0.985
Root Mean Square Error	60.42
Mean of Response	342.71
Observations (or Sum Wgts)	38

Summary of Fit

RSquare	0.987
RSquare Adj	0.986
Root Mean Square Error	30.75
Mean of Response	173.16
Observations (or Sum Wgts)	65

Figure 2.3: Rating curves developed in the field for a.) Plot 1 surface flow bucket, Flow (L/h) = -253.784 + 12814.592*Depth + 259905.13*(Depth - 0.11437)^2 + 2092942.2*(Depth - 0.11437)^3, and b.) Plot 2 tile flow bucket, Flow (L/h) = -1114.649 + 10826.456*Depth + 308017.64*(Depth - 0.11358)^2 + 2200297.4*(Depth - 0.11358)^3.

2.4. Water Sampling

Water samples were generally collected weekly during periods of low flow. During low intensity, continuous precipitation events, samples were collected 2-3 times per day. Runoff from high intensity precipitation and snowmelt events was sampled hourly using ISCO 6712 automated samplers (Teledyne ISCO, Lincoln, NE), hereafter referred to as autosamplers. Grab samples were immediately transported to the laboratory at Miner Institute and refrigerated. Samples collected by the autosamplers remained in the autosampler carousel until the 24-hour sampling cycle was completed.

Soluble reactive P (SRP) was determined within 48 hours of collection after membrane filtration (<0.45μm) by the ascorbic acid-ammonium molybdate colorimetric method (Murphy and Riley, 1962; APHA, 1989) using a spectrophotometer (Thermo Fisher Scientific Inc., Waltham, MA, US). Total P (TP) was also determined colorimetrically before filtration following sulfuric acid/persulfate digestion (APHA, 1989). Unreactive P (UP) was estimated as the numerical difference between TP and SRP and represents a combination of particulate P (PP) and dissolved organic P (DOP). Water samples were also analyzed for total suspended solids (TSS) with Proweigh filters (Environmental Express, Charleston, SC) according to Standard Methods 2540 (APHA 1989).

2.5. Water Yield and Load Calculations

The HOBO loggers were downloaded every 2-4 weeks and the depth readings were converted to flow rates according to the equations for each location listed in Table 2.1. The 5 min interval flow rates were then summarized to mean hourly flows. Hourly flow volumes were summed for each event and the duration of the study. Water yield for each plot is expressed as volumetric depth (mm), which was calculated by dividing the runoff water volume by plot area. Load estimates for each time interval and bucket were calculated by multiplying the hourly mean flows by the corresponding SRP, TP, UP, and TSS concentrations. When autosamplers were used for sample collection, hourly SRP, TP, and TSS concentrations were multiplied by the corresponding hourly mean flows to achieve hourly loading data. Event and total loads for P fractions were expressed as g ha^{-1} and TSS loads as kg ha^{-1}. For less frequent

sampling, SRP, TP, and TSS concentrations were assumed to be constant from halfway between the previous sample and subsequent sample for each collection time point and these estimates were multiplied by the corresponding flows (King et al. 2015b).

Table 2.1: Rating curve equations for each runoff collection location, where y = flow (L/h), x = water depth (m), RMSE = root mean square error, and n = number of observations.

Source	Rating Curve Equation	R^2	RMSE	n
Plot 1 Surface Flow	$y = -1253.784 + 12814.592x + 259905.13*(x-0.11437)^2 + 2092942.2*(x-0.11437)^3$	0.99	60.4	38
Plot 2 Surface Flow	$Y = -1179.754 + 13110.917x + 188035.1*(x-0.10615)^2 + 2618310.9*(x-0.10615)^3$	0.98	261.3	40
Plot 2 Tile Flow	$Y = -1114.649 + 10826.456x + 308017.64*(x-0.11358)^2 + 2200297.4*(x-0.11358)^3$	0.99	30.7	65
Plot 3 Surface Flow	$Y = -977.8281 + 10684.031x + 258932.18*(x-0.10245)^2 + 2368245.2*(x-0.10245)^3$	0.92	52.9	58
Plot 4 Surface Flow	$Y = -774.6562 + 7816.3228x + 186538.03*(x-0.11068)^2 + 1179312.4*(x-0.11068)^3$	0.98	58.7	19
Plot 4 Tile Flow	$Y = -888.0222 + 10038.702x + 231885.28*(x-0.10525)^2 + 5207383.1*(x-0.10525)^3$	0.98	34.3	65

Load estimates were calculated by event and for the total duration of data collection. For the undrained treatment, plot level loads were the summation of surface flow loads, whereas the tile-drained treatment was the sum of the tile drain and surface flow loads. Flow-weighted mean concentrations (FWM) were calculated for SRP, TP, UP, and TSS for each event and cumulatively for the entire study by dividing the total load by the total water yield. The water yield as a percent of total rainfall (rain recovery) was also calculated for each event in addition to cumulative totals. To differentiate the groundwater component of tile flows from the storm flows, the average subsurface water yield from each plot in the 24 h preceding a storm event was subtracted from the hourly subsurface yields over the duration of the storm event. The

groundwater component accounted for 0-36% of total drainage volume depending on the precipitation characteristics and antecedent moisture conditions. Precipitation data was collected from a RainWise Inc. (Bar Harbor, ME) weather station 1.7 km from the experimental plots, operated by the Network for Environment and Weather Applications (NEWA).

While most runoff events were captured during 2014-2015, some water yield estimates during colder times of the year were precluded due to freezing. This was due to the difficulty of keeping the water in the collection buckets from freezing when flows were minimal or absent. When freezing occurred, the water depth data from the loggers was unusable as the presence of ice changed the depth of water or completely encapsulated the logger in ice. As such, water yields were not quantified during freeze/thaw cycles that occurred during March and April 2015. Nutrient loading estimates are typically reported by hydrologic year (October-September), however, the monitoring period did not encompass two full years (April 20, 2014 to June 30, 2015). Cumulative data from the 13 months will be referred to as the cumulative total for the purposes of this paper.

2.6. Statistical Analysis

Runoff plots were arranged in a randomized complete block design to account for potential differences in treatment responses and drainage treatments were randomly assigned to plots within each block. The plots were blocked with respect to landscape position, with the two southernmost plots (plots 1 and 2) and two northernmost plots

(plots 3 and 4) designated as the two blocks. Response variables measured included SRP, TP, UP, TSS, and runoff water yields. Plot loads and FWM concentrations were reported for each variable in tile-drained (TD) and naturally-drained (UD) plots. Mean response was tested for differences by event (n=7) and for cumulative totals using JMP PRO 11.2 (SAS Institute Inc., Cary, NC). In addition, differences among response variables were assessed by hydrologic loss pathway (i.e., either surface runoff or tile-drain flow). A two-tailed t-test with blocking was used to test for treatment differences. Differences by hydrologic loss pathways were tested with a one-way analysis of variance (ANOVA) with blocking. When significant differences were found between hydrologic pathways, means were separated using Tukey's HSD test. Significance for all tests was declared at a P-value ≤ 0.05 and trends at a P-value ≤ 0.10.

CHAPTER 3: RESULTS AND DISCUSSION

3.1. Hydrology of Surface Runoff and Tile Discharge

3.1.1. Total Runoff Water Yield

Cumulative rainfall for the study was 1042 mm, excluding that which occurred between February 23, 2014 and April 9, 2015 (34 mm) when freeze/thaw cycles prevented accurate water yield data collection. Treatment means for water yield from the seven intensively sampled runoff events and the study total are listed in Table 3.1. Table 3.2 lists the mean water yields by hydrologic pathway for UD and TD for each event and cumulative monthly rainfall and mean runoff volumes. There was a significant difference in mean cumulative water yield from the tile-drained treatment (TD) and naturally-drained treatment (UD). The total water yield for TD was 560 mm (±155) and 166 mm (±75) for UD, which represents 53.8% and 16.0% of the total rainfall for TD and UD, respectively. The recovery rate for TD is greater than reported by King et al. (2015b) in Ohio, who observed that 28% of annual rain (1004 mm) was recovered in surface and subsurface drainage. Madison et al. (2014) reported drainage volumes for two chisel plowed corn fields for five consecutive years and precipitation recovery in drainage (surface and tiles) ranged from 18-52%. This range indicates that precipitation recovery can vary considerably from year to year.

The majority of total runoff (95%) in TD occurred in the tile drains. Overland flows only accounted for 25.8 mm (5%) of the mean water yield in TD, an 85% reduction from overland flows in UD. Overland flows only occurred during 6.4% of the total study duration in TD as compared to 13.5% in UD. Tile flow occurred in at

least one plot in TD 54.9% of the time. These results are supported by other studies in which there were drastic reductions or elimination of overland flows following the installation of tile drainage (Dolezal et al., 2001). Overland flow is rarely observed in tile-drained fields except during periods of high intensity storm events or when consistent rainfall and/or snowmelt exceed the drainage capacity of the field (King et al., 2015a). The reduction in overland flows associated with tile drains is generally limited to saturation excess overland flows as soil properties will have a greater role in controlling infiltration rates and the initiation of overland flows during high intensity precipitation (Needelman et al., 2004).

Table 3.1: Mean water yield by treatment for events and the study total. Bold values denote a significant difference in mean values between TD and UD.

Event Date	Treatment	Q (mm)	*SD*
5/16/2014	TD	**24.4**	8.0
5/16/2014	UD	**11.3**	4.2
6/3/2014	TD	10.9	1.8
6/3/2014	UD	4.7	3.7
6/11/2014	TD	**19.2**	2.0
6/11/2014	UD	**10.2**	1.1
6/24/2014	TD	**2.0**	1.3
6/24/2014	UD	**0.7**	1.0
8/13/2014	TD	**6.0**	1.7
8/13/2014	UD	**2.6**	0.1
12/25/2014	TD	50.3	17.2
12/25/2014	UD	30.5	23.8
5/31/2015	TD	**6.7**	0.3
5/31/2015	UD	**0.4**	0.5
Total	TD	**560.4**	155.1
Total	UD	**166.3**	75.6

Table 3.2: Mean water yield by treatment pathways for events and the study cumulative total. Means that significantly differ are highlighted in bold text. Means not connected by the same letter are significantly different. Values not highlighted with letters attached indicate a trend.

Event Date	Treatment	Pathway	Q (mm)	*SD*
5/16/2014	UD	Surface	11.3	4.6
5/16/2014	TD	Surface	8.9	12.0
5/16/2014	TD	Tile	15.4	4.0
6/3/2014	UD	Surface	4.7	3.7
6/3/2014	TD	Surface	2.8	3.1
6/3/2014	TD	Tile	8.1	1.3
6/11/2014	UD	Surface	10.2^{ab}	1.1
6/11/2014	TD	Surface	1.3^{b}	1.8
6/11/2014	TD	Tile	18.0^{a}	3.7
6/24/2014	UD	Surface	0.7	1.0
6/24/2014	TD	Surface	0.0	0.0
6/24/2014	TD	Tile	2.0	1.3
8/13/2014	UD	Surface	2.6	0.1
8/13/2014	TD	Surface	1.4	1.8
8/13/2014	TD	Tile	4.6	0.1
12/25/2014	UD	Surface	30.5^{ab}	23.8
12/25/2014	TD	Surface	4.4^{b}	5.8
12/25/2014	TD	Tile	45.9^{a}	11.5
5/31/2015	UD	Surface	$\mathbf{0.4^{b}}$	0.5
5/31/2015	TD	Surface	$\mathbf{0.5^{b}}$	0.6
5/31/2015	TD	Tile	$\mathbf{6.2^{a}}$	0.3
Total	UD	Surface	166.3^{ab}	75.6
Total	TD	Surface	25.8^{a}	32.4
Total	TD	Tile	534.5^{b}	187.5

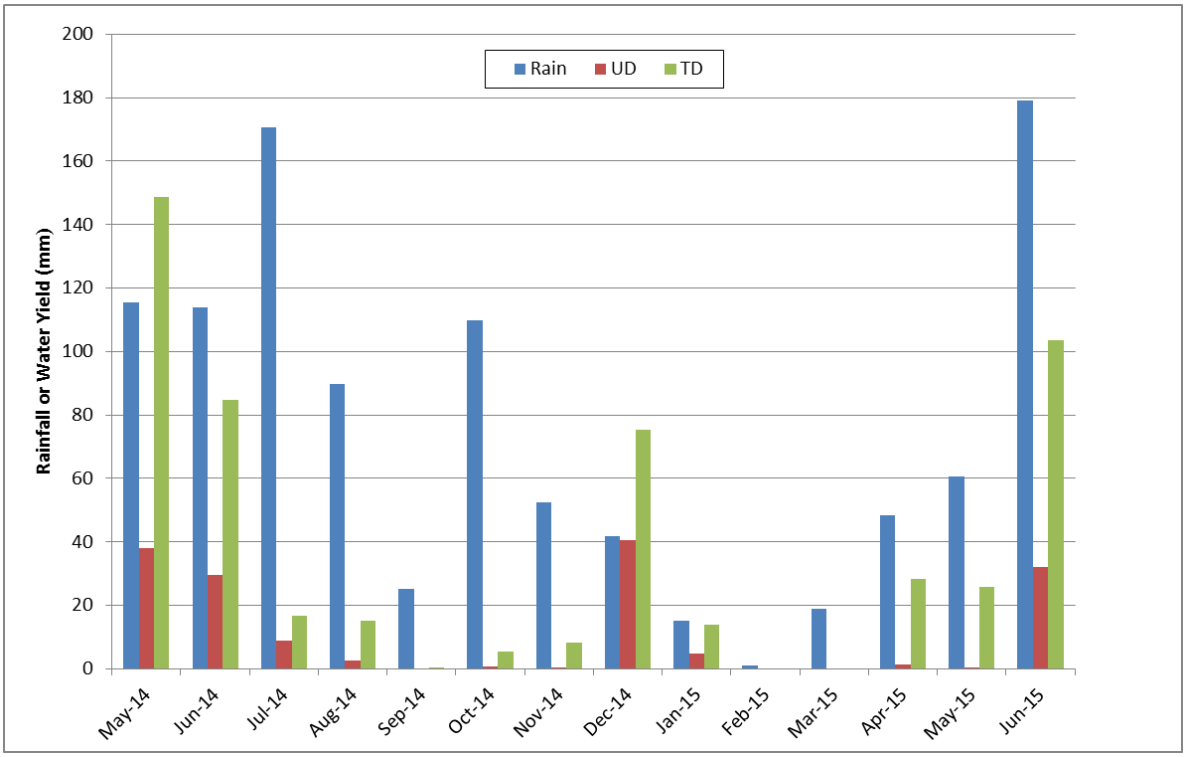

Figure 3.1: Monthly rainfall and mean water yield for UD and TD.

3.1.2. Runoff Events

The seven events intensively sampled for this study are listed in Table 3.3. The mean water yield from TD was significantly greater than UD in all events except the 6/3/14 and 12/25/14 events. Combined, the rain that fell during events accounted for 23% (242 mm) of the total rainfall over the study duration. Despite this small percentage, 36% and 74% of all overland flows in UD and TD, respectively, occurred during the events. In contrast, only 19% of the total water yield from the tiles occurred during events indicating that groundwater is a large component of tile flow. The 5/16/14 event resulted in 41 mm of rain in 4 h and was responsible for 35% (8.9 mm) of the overland flow from TD (Figure 3.2). A similar volume of overland flow drained

from UD during the event. However, the 11.3 mm of overland flow from UD only represents 6.8% of the total yield in UD. The nearly identical hydrologic response in both treatments for this event may indicate that the flow was infiltration excess flow rather than saturation excess flow. When overland flow occurs due to soil saturation, there should be a delay in response to the onset of precipitation. Also, the tiles in TD were flowing prior to the event, indicating that there were areas within the plots above field capacity. Due to the decreased drainage capacity in UD, soil moisture levels were likely higher compared to TD soils. Therefore, if overland flows were a result of saturation excess flows the onset of flows in UD would be expected prior to TD as a result of differing soil moisture storage capacities.

Table 3.3: Timeframes of the seven runoff events intensively sampled. Event duration, total rainfall, and recovery rate of rain in drainage for TD and UD are listed for each event. Recovery rates from the 12/24/14 event are inflated due to lack of water estimates from the melting snowpack.

Event Start	Event Finish	Duration	Rain	Rain Recovery (%)	
		h	mm	**TD**	**UD**
5/16/14 7:00 PM	5/17/14 11:59 PM	29	54.4	22.8	20.8
6/3/14 4:00 PM	6/4/14 3:59 PM	24	27.9	23.3	16.7
6/11/14 4:00 PM	6/14/14 4:59 PM	73	52.3	25.4	19.5
6/24/14 6:00 AM	6/26/14 8:59 AM	51	10.9	1.7	6.7
8/13/14 7:00 AM	8/14/14 11:59 PM	41	54.1	11.1	4.8
12/24/14 8:00 AM	12/26/14 11:59 PM	64	11.43	389.9	266.4
5/31/15 11:00 PM	6/2/15 7:59 AM	33	30.5	16.0	1.3

The percent of rain recovered in tile drain-flow was similar for the first three events (23%, 23%, and 25%, respectively). These events were the most hydrologically similar as they occurred in late spring when the tiles were flowing prior to the onset of precipitation. Smith et al. (2015) reported the percent recovery for two specific events

in Indiana (May 2010 and April 2011) to be 26% and 27%, only slightly greater than those reported here for the same approximate time of year.

The 5/31/14 event was similar to the first three events with respect to TD (16% rain recovery), though the antecedent moisture conditions (AMC) were not as high, as inferred from the minimal tile flow prior to the event, in comparison to the three events from spring 2014. The lower recovery rate in TD likely reflects the increased storage capacity of the soil. The high AMC common during the spring is also reflected in the difference in recovery rates in UD for the first three events relative to the other events (excluding snowmelt). The 6/24/14 event had both the lowest intensity and lowest rainfall amount, which is reflected in the low depth of drainage (10.9 mm) and rain recovery (1.7%). The increased storage capacity of the soil during drier periods is reflected in the 6/24/14 event and the 8/13/14 event, which experienced the lowest rainfall recovery rates. Drainage from the 12/24/14 event was primarily due to snowmelt, resulting in inflated recovery rates compared to the other rainfall-only events.

The 6/11/14 event was the only event in which there was a delay in overland flow in TD relative to UD (Figure 3.3). Overland flows for TD plots occurred 24 h after the onset of flows in UD. The rainfall totals for this event are similar to the other events sampled for this study, but occurred over a period of days, rather than hours. The rainfall characteristics (low intensity, longer duration) and delayed hydrologic response in TD conforms to the conditions that would be expected from saturation excess overland flows (Kirkby, 1988).

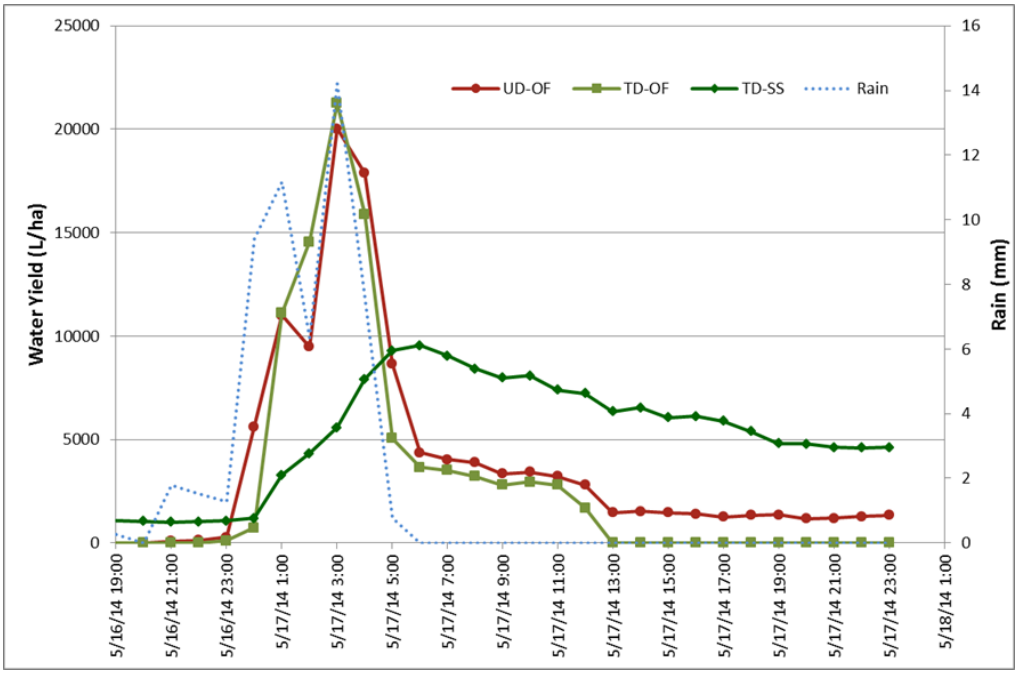

Figure 3.2: Water yield from the 5/16/14 rain event. UD-OF = overland flow from UD; TD-OF = overland flow from TD; TD-SS = subsurface tile flow from TD.

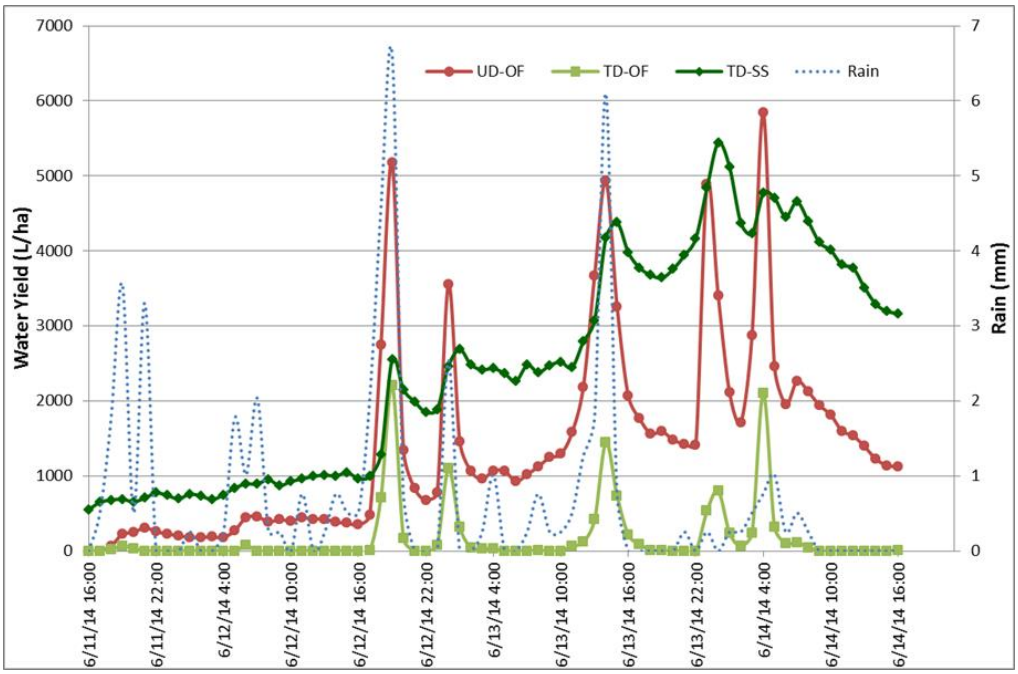

Figure 3.3: Water yield from the 6/11/14 rain event. UD-OF = overland flow from UD; TD-OF = overland flow from TD; TD-SS = subsurface tile flow from TD.

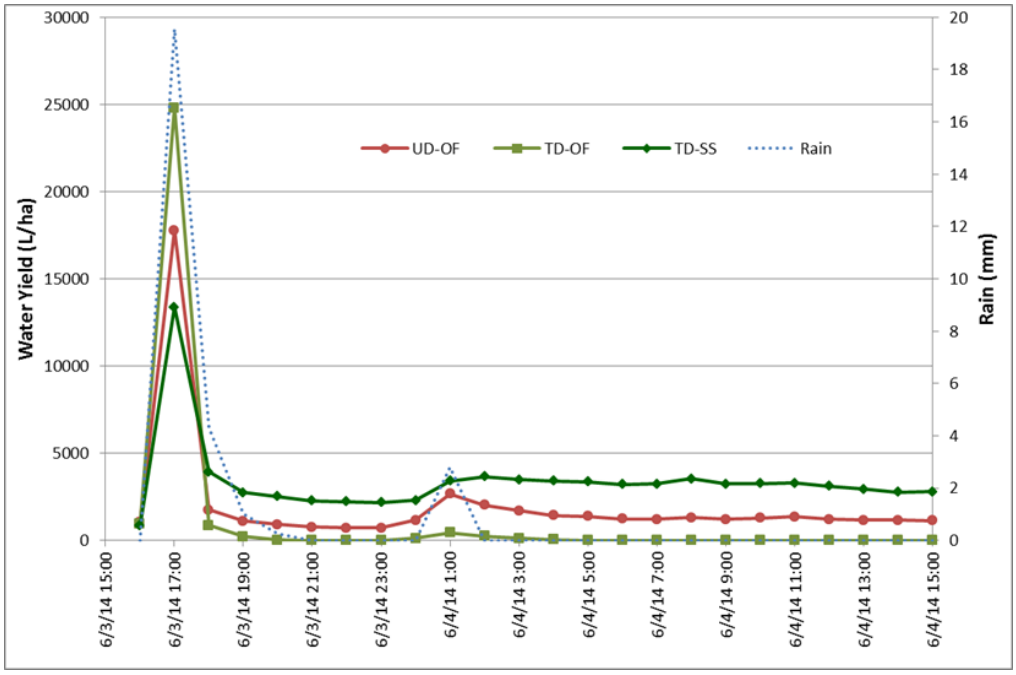

Figure 3.4: Water yield from the 6/3/14 rain event. UD-OF = overland flow from UD; TD-OF = overland flow from TD; TD-SS = subsurface tile flow from TD.

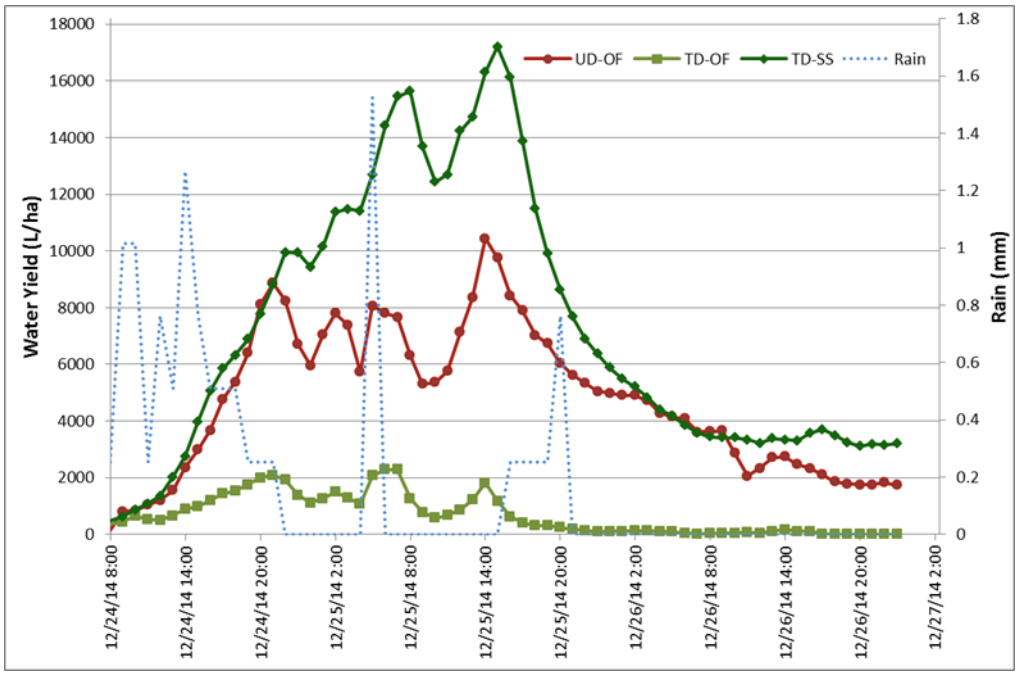

Figure 3.5: Water yield from the 12/25/14 snowmelt event. UD-OF = overland flow from UD; TD-OF = overland flow from TD; TD-SS = subsurface tile flow from TD.

Seasonality has been demonstrated in the literature to play a significant role in water yield in tile drains. The majority of annual rainfall occurs during the nongrowing season in many states in the Midwest and Northeast (Baker et al., 1975; Karl and Knight, 1998) and produces more runoff compared with warmer, drier months with higher rates of ET (Tan et al., 2002; Penman, 1948). Tan et al. (2002) reported that tile drain flow during the nongrowing season accounted for 64% of annual drainage. Despite the effect of the nongrowing season on annual water yield, a comprehensive literature review by King et al. (2015a) found few studies that measured runoff during this period.

The pronounced effect of snowmelt on runoff water yield was captured on the 12/24/14-12/26/14 event. Runoff from this event represented just 0.7% of the total study duration but contributed the most to total water yield, with 9% (50.3 mm) and 18% (30.5 mm) of the total from TD and UD, respectively. This event also contributed 17% (4.4 mm) of the total overland flow in TD, the second most by any single event. The potential for sustained elevated drainage rates following snowmelt is illustrated by the contrast of Figures 3.2 and 3.5. While the magnitude of the peaks is similar, the duration of flows greater than 5,000 L ha^{-1} h^{-1} is much greater in the 12/25/14 event than the 5/16/14 event. The persistence of elevated flows in the 12/25/14 event is even more notable considering the dry conditions in the four months preceding snowmelt in comparison to the 5/16/14 event when tiles had been consistently flowing in the preceding weeks.

Despite the immediate response of tile flow to snowmelt in the 12/25/14 event, as indicated by the simultaneous rising limbs of the overland flow and tile flow hydrographs, overland flow still occurred in TD plots. The peaks in drainage rates were similar between treatments with overland flow rates of 3249 L h^{-1} and 4250 L h^{-1} recorded in UD and TD, respectively. However, the duration of time at those rates was much less for TD than UD and reflected in the lower mean overland flow yield in TD of 5.8 mm, compared to 25.8 mm in UD. Previous work has also demonstrated the potential for snowmelt to create large volumes of overland flow (Rodzik et al., 2009). The large volume of water from snowmelt appears to have induced infiltration excess flows, followed by saturation excess flows due to continued snowmelt and periodic rainfall on 12/24/14 and 12/25/14, which helped to sustain elevated tile flows.

The 46 d period in late winter without water yield data (2/22/15-4/9/15) only accounted for 34 mm of rainfall. However, all of the spring snowmelt occurred during this period and large volumes of overland flow were drained. During this time, the zone of frozen soil presumably prevented infiltration and tile flow. Therefore, all of the water flow during this period occurred as overland flow. While the total volume was unable to be quantified, the highest manually recorded flow rates occurred during this period. The majority of the snow pack melted during a warm period in early March 2015, with large volumes of runoff in all plots observed on 3/11/15. A manual measurement of the overland flow draining from plot 2 (TD) was taken on 3/10/15 and measured 5760 L h^{-1}. The flow measured at this time in plot 1 (UD) was 1728 L h^{-1}, also among the highest observed flow rates. The measured flow rates on this date were

considerably greater for plots 1 and 2 than 3 (UD: 432 L h^{-1}) and 4 (TD: 630 L h^{-1}) due to landscape features that resulted in snow drifts accumulating in the southern half of the study area.

Similar flow rates to those observed 3/11/15 were observed during the 12/25/14 snowmelt event. The only other instances of flow rates of this magnitude were during the 5/16/14 event and the 6/3/14 event (Figure 3.4). The combination of high antecedent soil moisture conditions (inferred from tile flow drainage rates) and intense rainfall (>1.75 cm h^{-1}) resulted in brief (1-3 h) large spikes in drainage rates during these two events. In contrast to the 12/25/14 event, peak drainage rates were confined to the duration of high intensity precipitation. Despite occurring over just a 4 h period during peak rainfall for the 6/3/14 event, 11% (2.8 mm) of TD total overland flow for the study duration occurred. As previously mentioned, 35% of the overland flow in TD occurred in 12 h for the 5/16/14 event. These three events combined to represent 62% (16.1 mm) of the total overland volume for TD plots.

The contribution of these three events to the total water yield and the flow rates measured on 3/10/15 highlight the importance of continuous, year-round monitoring to fully understand the timing, magnitude, and characteristics of runoff events. By limiting the occurrence of overland flows to the more extreme and infrequent weather events, tile drainage may have implications for management strategies targeting these outlier events that are responsible for the majority of edge-of-field losses.

3.1.3. Water Table Monitoring

Shallow groundwater wells were installed in May 2015 (plot layout and well locations in Figs. 2.1 and 2.2) to monitor the elevation of the water table along TD-UD plot boundaries. Prior to a 4 d rain event (5/30/15-6/2/15) that delivered 5.1 cm of rain, field conditions were relatively dry and the water table only reached approximately half of the wells. Following this event, the water table remained sufficiently elevated to monitor in all locations except the well furthest upslope on the border of plots 3 and 4. Throughout the month of June during which monitoring occurred, the water table never reached this well.

During June 2015, 17.9 cm of rainfall occurred with only one instance of 3 consecutive days without rain (Table 4.2). Water table elevation at each of the wells was measured 18 times during June, with measurements taken two times per day following periods of heavy rain (Tables 4.3 and 4.4). Although the expectation was for the elevation of the water table to increase with distance from tile lines, this was not always the case. This may be due in part to the orientation of the tile laterals in the field. For the most efficient drainage, it is recommended that tiles be oriented perpendicular to the slope in order to intercept the movement of water downslope (Wright and Sands, 2009). The laterals in the experimental site were installed parallel with the slope in order to maintain a sufficient hydraulic gradient to drain all plots via gravity. This may have resulted in local variability of the water table as the tile drain-induced gradient may have been greater than the natural downslope gradient in certain areas.

The interpolated water table elevation contour maps for each array of wells displayed different patterns, but were relatively consistent (Figs. 4.12-4.40). The wells appear to be hydrologically connected as the water table responded to each rain event in a similar pattern. Additionally, the water table appeared to be relatively consistent with the topography and site characteristics. The maps for plots 1 and 2 indicate groundwater mounding around the mid-slope wells. This may be due to the soil characteristics and local topography. The soil transitions from poorly-drained silty clay at the toeslope of the plots to high permeability outwash soils upslope and to the east. Also, the plots terminate at the upslope position along a ridge, from which the land decreases in elevation to a small lake (Figure 4.41).

Following precipitation, the landscape features, in combination with rapid hydraulic conductivity of the outwash soils, may have caused the peak of the water table to move west to the mid-slope position as seen in Figures 3.6 and 3.7. As a result, the predominant direction of groundwater flow appears to be east and west of the groundwater mound and parallel to the plot boundaries. While the interpolated maps for events such as that in Figure 3.6 indicate potential for some lateral groundwater movement from plot 1 (UD) to 2 (TD), they also suggest groundwater in the vicinity of the plot boundary flows downslope with limited interaction with the tiles (Figure 3.7). Therefore, potential migration of groundwater from plot 1 to plot 2 that could be measured as tile flow in plot 2 should be minimal.

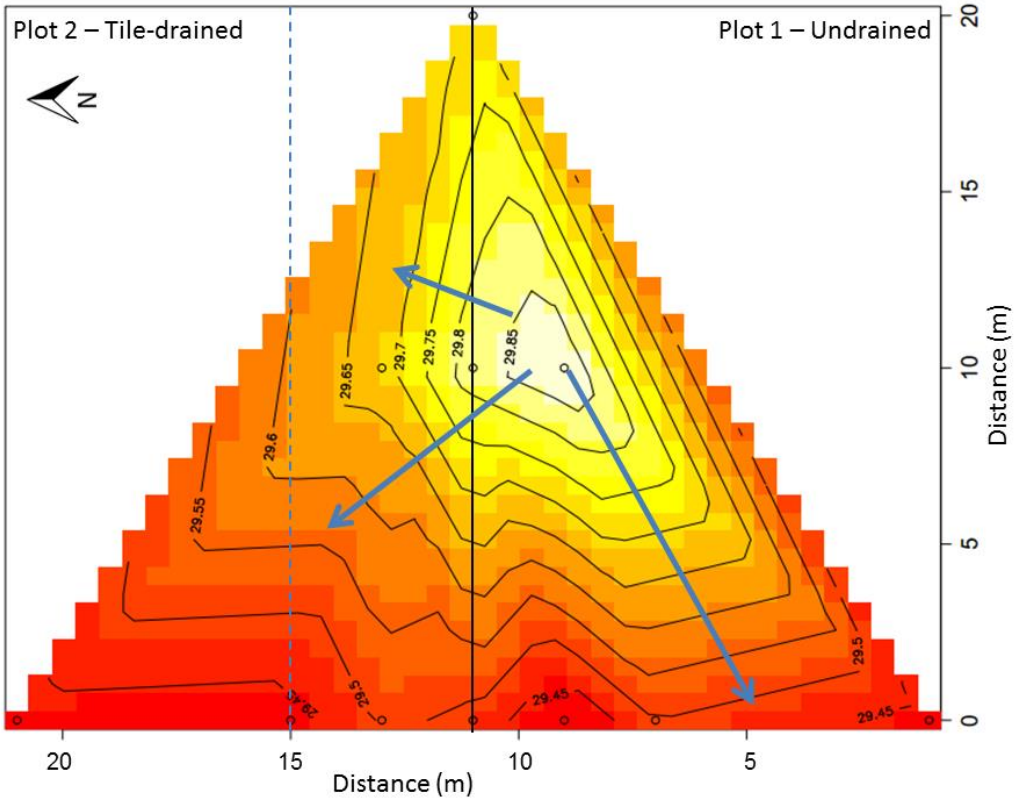

Figure 3.6: Water table contour map for plots 1 and 2 on 6/4/15. X and Y axes represent distance (m), central vertical black line indicates the plot boundary, dotted blue vertical line indicates the outer tile line, small circles indicate well locations, and blue arrows represent probable direction of groundwater flow.

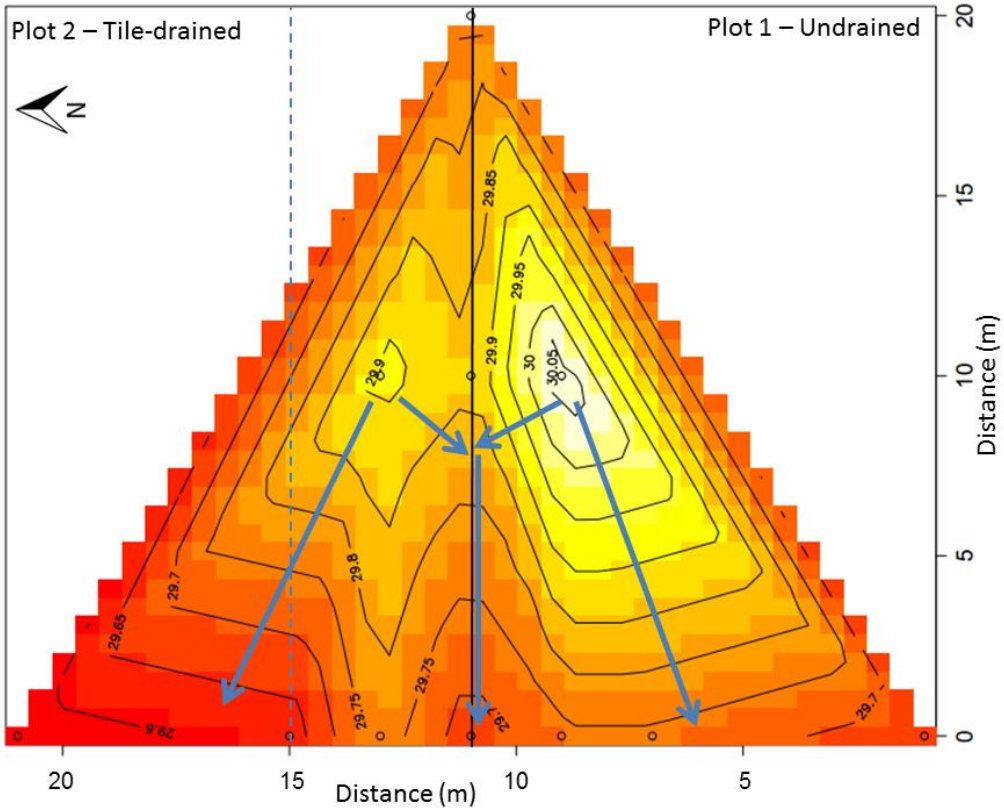

Figure 3.7: Water table contour map for plots 1 and 2 on 6/22/15 (10:00). X and Y axes represent distance (m), central vertical black line indicates the plot boundary, dotted blue vertical line indicates the outer tile line, small circles indicate well locations, and blue arrows represent probable direction of groundwater flow.

The interpolated water table elevations between plots 3 and 4 suggest limited groundwater flow across plot boundaries. The maps indicate the presence of a ridge along the boundary of the plots from which flows diverged. The location of the ridge varied with moisture conditions, moving into plot 3 during periods of water table draw-down. In some cases, flow lines suggest the potential for groundwater flow from plot 3 (UD) into plot 4 (TD), thus contributing some groundwater to the outside tile in plot 4 (Figure 3.8). However, the majority of the dates indicate limited potential for inter-plot groundwater flow (Figure 3.9).

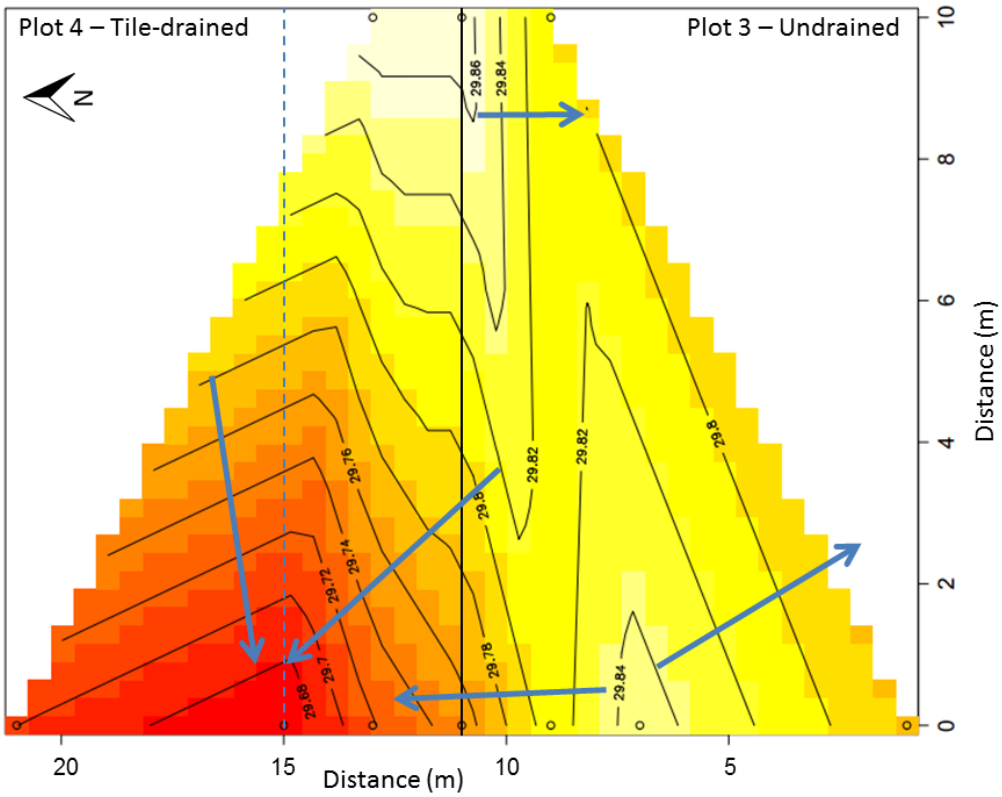

Figure 3.8: Water table contour map for plots 3 and 4 on 6/4/15. X and Y axes represent distance (m), central vertical black line indicates the plot boundary, dotted blue vertical line indicates the outer tile line, small circles indicate well locations, and blue arrows represent probable direction of groundwater flow.

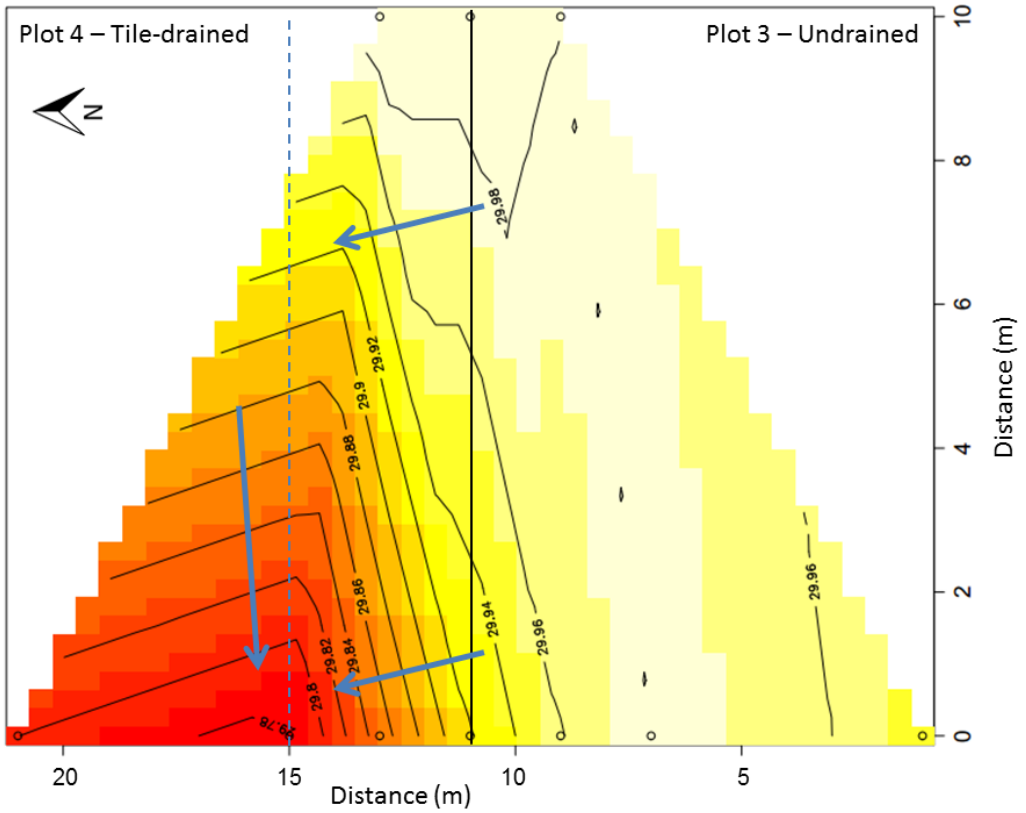

Figure 3.9: Water table contour map for plots 3 and 4 on 6/22/15 (17:00). X and Y axes represent distance (m), central vertical black line indicates the plot boundary, dotted blue vertical line indicates the outer tile line, small circles indicate well locations, and blue arrows represent probable direction of groundwater flow.

The water table elevation for each event was plotted for individual wells (Figure 3.10 and 3.11). The water table appeared to reach its maximum height at the plot boundary (well D) and remained at a relatively constant elevation in wells E, F, and G. Evidence of the possible channel along the boundary of plots 1 and 2 can be seen by the lower position of the water table at well I, in relation to wells H and J. In plots 3 and 4, the water table appears to peak at well E (2 m into plot 3), before decreasing in height at wells F and G. Overall, results suggest tile lines had minimal impact on overall UD soil moisture status and that the majority of subsurface drainage from each TD plot originated from within the plot boundaries. This assumption also implies that surface

runoff in UD plots were not underrepresented due to the interception of subsurface flows by tile drains in adjacent TD plots.

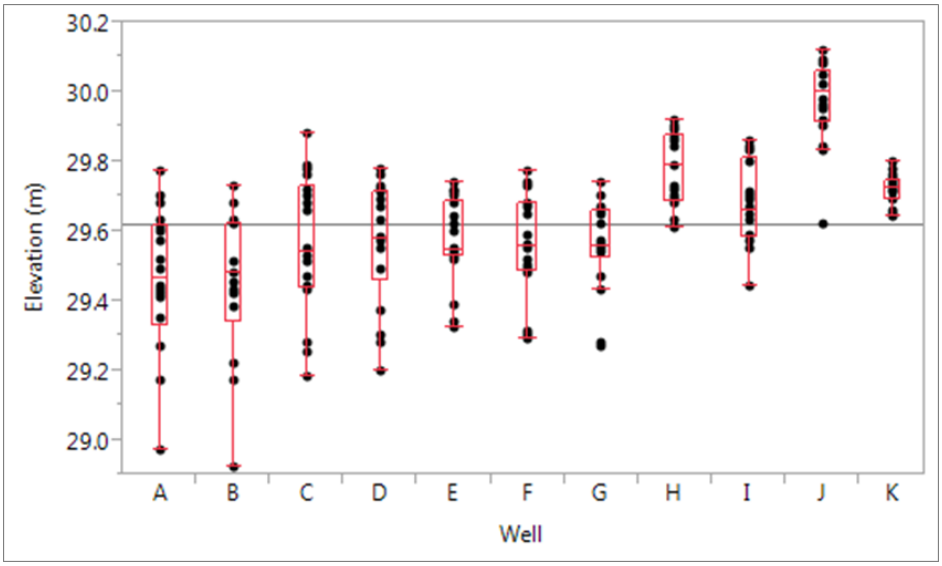

Figure 3.10: Box plot of water table elevations in groundwater wells across the shared boundary of plots 1 and 2. Each point represents the water table elevation at a specific time-point. Wells A-G represent the downslope transect of wells moving from TD to UD, H-J for the mid-slope transect of wells, and well K is furthest upslope.

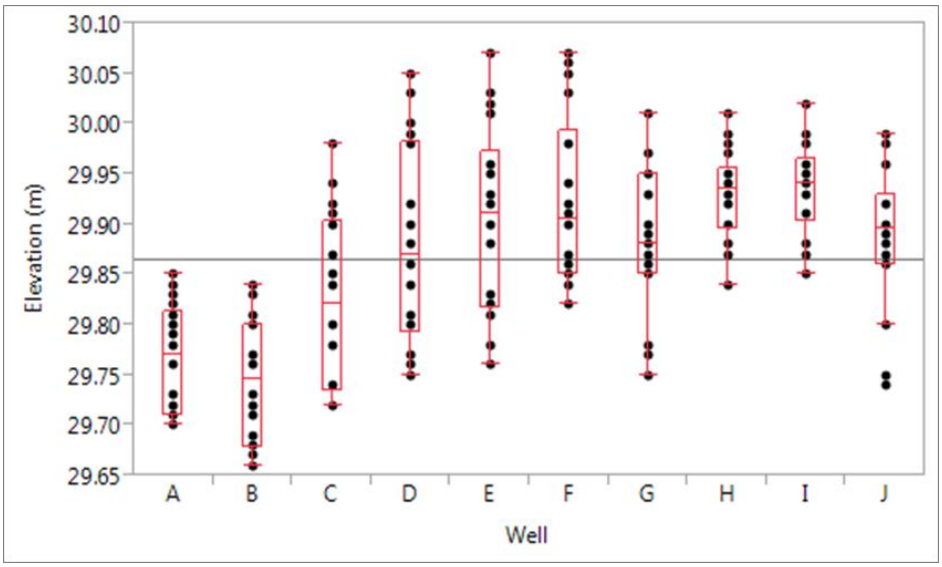

Figure 3.11: Box plot of water table elevations in groundwater wells across the shared boundary of plots 3 and 4. Each point represents the water table elevation at a specific time-point. Wells A-G represent the downslope transect of wells moving from TD to UD, H-J for the mid-slope transect of wells, and well K is furthest upslope.

3.2. Soil Analysis

Results from the soil samples taken at the start of the study were averaged by plot, from which treatment means were calculated. Results confirmed that pH, organic matter, Morgan-P were similar between plots (Figure 3.12). All horizon means within each treatment were in the low range (0.5-2.0 mg P kg^{-1}) for P availability with respect to UVM field crop guidelines (Jokela et al., 2004) with 0.78 mg kg^{-1} ± 0.04 in TD and 0.90 mg kg^{-1} ± 0.42 in UD in the Ap horizon. Mean soil pH of the Ap horizon was 5.5 ± 0.3 and 5.6 ± 0.1 for TD and UD, respectively; therefore sorption processes should be similar between treatments. The percent organic matter of the Ap was also similar between treatments (TD = 3.2 ± 0.2; UD = 3.1 ± 0.1).

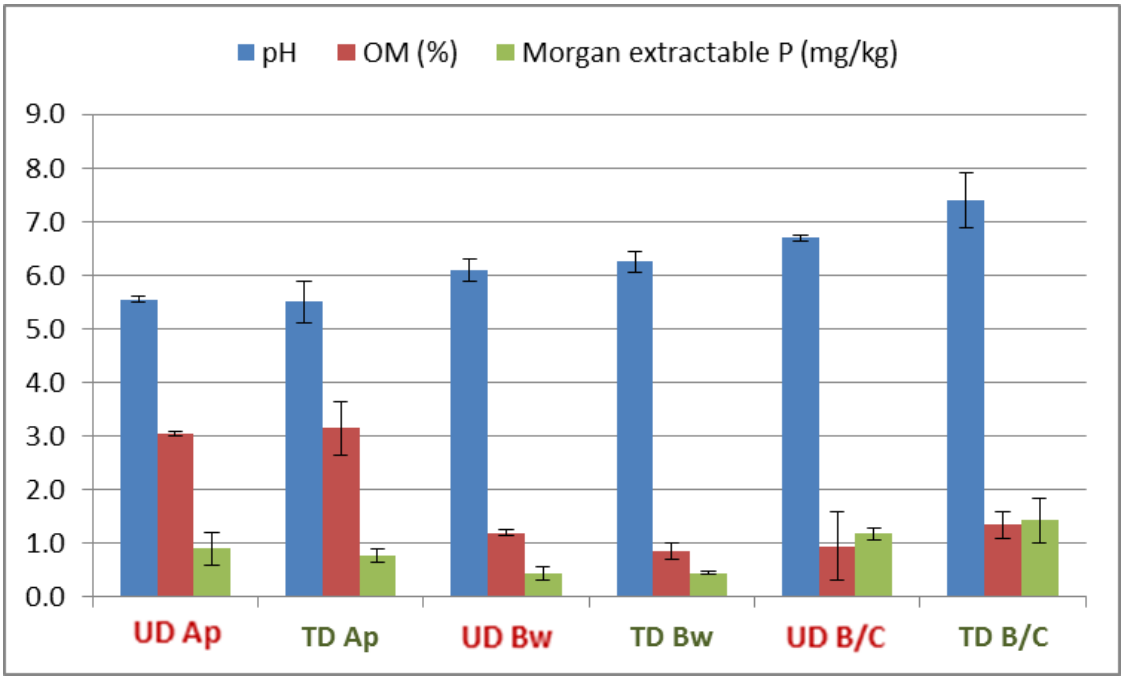

Figure 3.12: Select soil test results for upper three soil horizons sampled from each plot, averaged by treatment assignment.

3.3. Phosphorus and Sediment Loads in Runoff

3.3.1. Cumulative Phosphorus and Sediment Loads

Loads were calculated for P fractions (SRP, UP, and TP) and TSS for the study duration and the seven events. Loads were calculated by treatment (Table 3.4) and by hydrologic pathway for each treatment (Table 3.5). There were no treatment differences in TP lost during the study with 233.9 g ha^{-1} lost from TD and 230.9 g ha^{-1} lost from UD. Although these loads are from 13 months of field observations, they are still less than those reported in a review by King et al. (2015a) that found that annual TP loads from tile drains typically vary from 0.4 to 1.6 kg ha^{-1} y^{-1}. The relatively low TP loss in tile-drain flows may be partially due to the low STP at this site and correspondingly lower P release potential. Numerous studies have shown strong correlations between STP and DP concentrations in surface and subsurface runoff (Maguire and Sims, 2002; McDowell and Sharpley, 2001; Pote et al., 1996).

The low STP in this field may have implications for the response of the plots to runoff events. Agricultural fields with repeated P applications in excess of crop uptake are often high in STP and when this P-rich topsoil is eroded, P exports can be substantial (McDowell and Sharpley, 2001). However, event data for the study site shows that TP and TSS loads may be decoupled and not always related. Although 2.5 times more TSS was exported by UD (118.8 kg ha^{-1}) than TD (46.0 kg ha^{-1}) in May 2014, TP exports by UD (32.1 g ha^{-1}) were three times less than TD (96.1 g ha^{-1}) (Figs. 3.13 and 3.14). The majority of TP was UP during this time period in both TD (85%) and UD (92%). Unreactive P represents a combination of PP and dissolved organic P

(DOP) and may have accounted for the apparent decoupling of TP and TSS during this time period. It is possible that manure applied the previous fall contributed DOP that was transported in surface and tile drainage runoff and measured as UP. Beauchemin et al. (1998) sampled tile drainage flows from twenty-seven sites within an intensively cropped region in Quebec, Canada and observed that DOP could account for up to 79% of TP concentrations.

Table 3.4: Event and cumulative mean losses of SRP, UP, TP, and TSS for TD and UD treatments. Bold values denote a significant difference in mean values between TD and UD.

Event Date	Treatment	SRP g ha^{-1}	UP g ha^{-1}	TP g ha^{-1}	TSS kg ha^{-1}
5/16/2014	TD	13.63	62.23	72.95	42.67
5/16/2014	UD	1.30	14.25	15.55	113.21
6/3/2014	TD	0.49	15.73	16.22	14.47
6/3/2014	UD	0.50	5.21	5.70	9.91
6/11/2014	TD	0.47	3.87	4.34	1.21
6/11/2014	UD	2.07	7.40	9.48	7.21
6/24/2014	TD	0.04	0.13	0.17	0.01
6/24/2014	UD	0.02	0.06	0.08	0.04
8/13/2014	TD	1.62	2.45	4.08	**0.33**
8/13/2014	UD	1.73	2.49	4.22	**0.84**
12/25/2014	TD	51.58	14.00	65.58	1.21
12/25/2014	UD	110.45	27.75	138.19	2.70
5/31/2015	TD	0.86	0.90	1.76	0.18
5/31/2015	UD	0.15	0.20	0.34	0.05
Total	TD	84.19	149.67	233.87	65.45
Total	UD	130.78	100.09	230.87	168.82

Table 3.5: Event and cumulative mean losses of SRP, UP, TP, and TSS for hydrologic pathways in TD and UD treatments. Bold values denote a significant difference in mean values between TD and UD. Means not connected by the same letter are significantly different.

Event Date	Treatment	Pathway	SRP g ha^{-1}	UP g ha^{-1}	TP g ha^{-1}	TSS kg ha^{-1}
5/16/2014	UD	surface	1.30	14.25	15.55	113.21
5/16/2014	TD	surface	13.12	47.18	60.31	36.04
5/16/2014	TD	tile	0.50	15.05	12.64	6.63
6/3/2014	UD	surface	0.50	5.21	5.70	9.91
6/3/2014	TD	surface	0.36	10.87	11.23	13.63
6/3/2014	TD	tile	0.13	4.86	4.99	0.84
6/11/2014	UD	surface	1.87	6.54	8.41	2.32
6/11/2014	TD	surface	0.13	0.94	1.08	0.34
6/11/2014	TD	tile	0.39	2.88	3.27	0.29
6/24/2014	UD	surface	0.02	0.06	0.08	0.04
6/24/2014	TD	surface	0.01	0.06	0.07	0.00
6/24/2014	TD	tile	0.03	0.07	0.10	0.01
8/13/2014	UD	surface	1.73	2.49	4.22	**0.84**[a]
8/13/2014	TD	surface	1.27	1.17	2.44	**0.17**[b]
8/13/2014	TD	tile	0.35	1.28	1.63	**0.16**[b]
12/25/2014	UD	surface	110.45	27.75	138.19	2.70
12/25/2014	TD	surface	11.28	2.08	13.36	0.21
12/25/2014	TD	tile	40.30	11.92	52.22	1.00
5/31/2015	UD	surface	0.15	0.20	0.34	0.05
5/31/2015	TD	surface	0.56	0.25	0.81	0.02
5/31/2015	TD	tile	0.30	0.66	0.96	0.16
Total	UD	surface	130.79	100.08	230.87	162.29
Total	TD	surface	34.01	68.51	102.52	50.99
Total	TD	tile	50.17	81.17	131.35	14.46

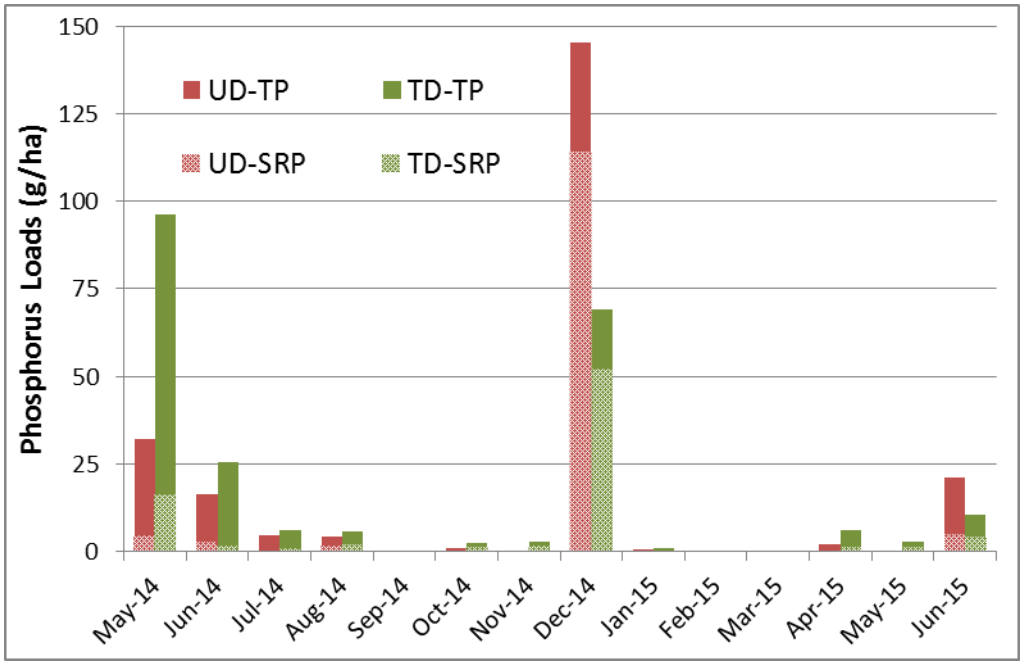

Figure 3.13: Monthly SRP and TP loads for each treatment. UD is shown in red and TD is shown in green. Lighter colors represent SRP, darker colors represent TP.

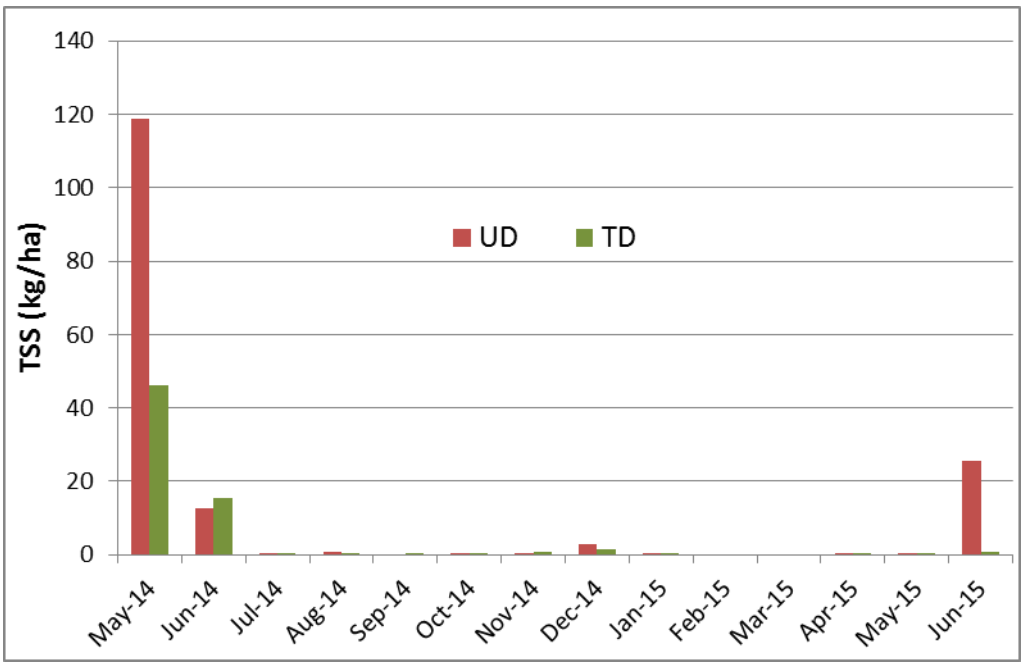

Figure 3.14: Monthly TSS loads for each treatment. UD is shown in red and TD is shown in green.

Approximately 78% of the TSS load from TD was in overland flow and this pathway only accounted for 56% of TP losses. If the STP were higher at this site, the TP loads could have potentially been much greater in both surface and tile runoff, but particularly for UD plots. For the present study, UD had 357% greater cumulative TSS losses than TD. It is possible that greater soil P saturation at the site could have resulted in substantially more P loss. Pote et al. (1996) found a high correlation (R^2 = 0.77) between SRP in surface runoff and the degree of soil P saturation using an acidified ammonium oxalate extraction (DPS = P_{ox} / (Fe_{ox} + Al_{ox}). Maguire and Sims (2002) found a similar correlation (R^2 = 0.78) between SRP concentrations in tile flow and DPS using the Mehlich-3 extraction. However, significant increases in SRP concentrations due to STP status have typically not been observed until STP concentrations are approximately four times greater than the recommended agronomic optimum (Klatt et al., 2002; King et al., 2015a).

While TP loads were similar between treatments, SRP loads were 130.8 g ha^{-1} in UD and 84.2 g ha^{-1} TD and represented 57% of TP losses from UD and 36% of TP in TD. Although there is growing awareness of the role of preferential flow pathways in conducting both DP and PP losses to tile drains (Kleinman et al., 2015), concerns regarding P loss from overland flows have still primarily focused on PP losses (Kleinman et al., 2011). The high proportion of SRP in UD demonstrates that SRP can be an important component of TP in surface runoff, regardless of the STP status of the field.

Concerns regarding the use of tile drainage systems have been raised due to their potential for DP transport (Daniel et al., 1998). If tiles are primarily exporting DP and account for most of the annual runoff from a field, tile drainage could contribute a disproportionate amount of P to TP loads. To better understand relationships among site hydrology, TSS, and P transport, it is necessary to differentiate P losses by hydrologic pathway. The speciation of P was similar between tile flow and overland flow, with SRP comprising 38% of tile flow and 33% of overland flow. Not only was the high proportion of SRP observed in UD surface flows not duplicated in TD surface flows, SRP did not dominate tile flows. The low percentage of SRP in the tiles may reflect the high P sorption capacity of the soil due to the high levels of reactive surface area in a fine-textured soil with low STP (Sims et al., 1998)

Bottcher et al. (1981) observed that greater than 70% of TP in tiles was due to PP during three years of monitoring P losses on a silty clay field. These high levels of PP in tile flow are indicative of preferential flow pathways providing a conduit for transport of soil particles from the surface and demonstrate that losses are highly site-specific. Uusitalo et al. (2001) observed PP (calculated as the difference between TP and SRP) as the major fraction of PP in tile drain-flow, with a range of 66-99% of TP as PP across four experimental sites. The work of Bottcher et al. (1981), Uusitalo et al. (2001), and that presented here all occurred on silty clay or clay soils which are more prone to the development of macropores than a more coarsely textured soil (Beven and Germann, 1982). Therefore, P speciation should not be assumed based on hydrologic

pathway alone since the combination of hydrology, soil characteristics, and management simultaneously influence P speciation and transport.

3.3.2. Phosphorus and Sediment Loads in Runoff Events

The high percentage of SRP in UD (57%) relative to the losses observed in TD (36%) can be explained by the influence of the 12/25/14 snowmelt event on the total loads (Figure 3.15). Total P losses were 65.6 g ha^{-1} and 138.2 g ha^{-1} from TD and UD, respectively. This single event was responsible for 28% of the cumulative TP losses from TD and 60% of TP losses from UD. The losses from UD in this event were dominated by the dissolved fraction, with 80% occurring as SRP. A similar SRP fraction was also lost by TD plots (79% of TP loss was SRP). Despite a similar distribution of P forms between treatments, the primary transport pathway was different, as 80% of TP losses from TD were from the tiles. There was no difference in the SRP fraction of TP in overland (84%) and tile flows (77%) for TD plots. Seasonal P speciation in surface and tile flows reported in the literature are inconsistent, with some reporting increased PP losses relative to DP in the winter (Chapman et al., 2001), while others found that DP dominated winter losses (Macrae et al., 2007; Stuntebeck et al., 2008).

The importance of the interaction between weather and manure management strategies on P transport is demonstrated by the 12/25/14 event. Following corn harvest and tillage, manure was broadcast on the field on 11/28/14 without incorporation prior to snowfall or a cover crop. Average temperatures remained at or below freezing following manure application. Therefore, any precipitation that fell occurred as snow

or sleet prior to the start of the rain on 12/23/14. During 12/23/14-12/25/14, 1.73 cm of rain fell and initiated snowmelt on 12/24/14 along with three consecutive days exceeding 40° F (12/24/15-12/26/14). The dry period preceding the 12/25/14 snowmelt may have influenced P exports as some studies have shown increased P availability when soils are rewetted following a dry period (Heathwaite and Dils, 2000; Venterink et al., 2002).

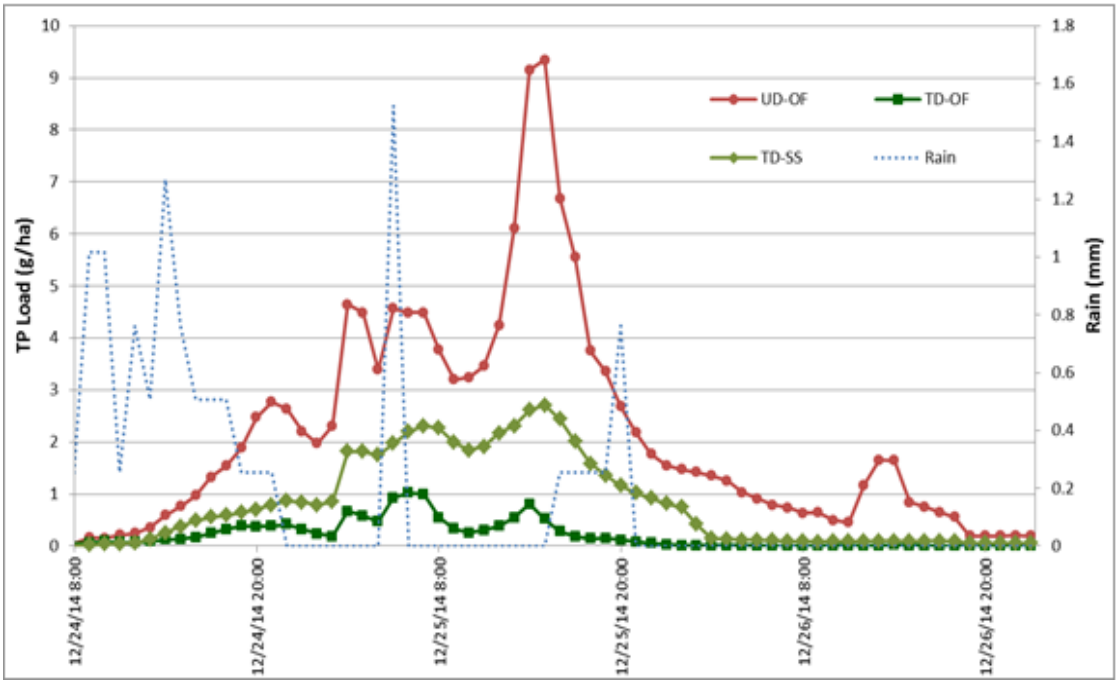

Figure 3.15: TP loads by hydrologic pathway for each treatment from the 12/25/14 event.

The combination of recently applied, unincorporated manure and weather conditions likely resulted in a large pool of labile P, vulnerable to runoff losses during a high flow event such as snowmelt. This combination of factors led to the largest export of SRP (110.5 g ha^{-1}) and TP (138.2 g ha^{-1}) from UD and the largest export of SRP (51.6 g ha^{-1}) from TD. Jamieson et al. (2003) observed similar losses during a 4 d

snowmelt event in a tile-drained field in southern Quebec that resulted in drainage depths of 164.8 mm combined from surface and subsurface pathways. They observed 166.4 g ha^{-1} of TP in surface flow and 98.2 g ha^{-1} in subsurface flow, accounting for 63 and 37% respectively, of the annual TP loads. Although these loads are somewhat higher than those observed in the 12/25/15 snowmelt, the snowmelt event captured by Jamieson et al. (2003) experienced a greater volume of discharge likely due to a larger volume of water in the snowpack.

The presence of a labile P source, combined with a high volume of runoff is likely the cause for the high loads in this event relative to other events. Just as the flow rates were highest during the 12/25/14 event and 3/11/15 grab samples, P concentrations were also much greater for these snowmelt events than the rest of the year. TP and SRP concentrations of the grab samples taken on 3/11/15 of the overland flows from all four plots were higher than at any other sampling time-point. The highest TP and SRP concentrations from UD were 2312 µg L^{-1} and 2128 µg L^{-1}, respectively. The maximum concentrations in TD were similar with 2632 µg L^{-1} and 2464 µg L^{-1} for TP and SRP, respectively. The 12/24/14 event had the second highest SRP concentrations among plots, although the concentrations were approximately four times less. The high concentrations on 3/11/15 may have also been influenced by the extent of soil freezing that occurred during a winter that saw temperatures well below average for the region. Temperatures in January and February were 3.6° F and 14.1° F below average, respectively (NRCC, 2015). Studies have demonstrated that freezing conditions may increase P availability, particularly as the surface residue and number

of freeze/thaw cycles increase (Messiga et al., 2010). Additionally, despite the volume of water and P loads transported during the 12/25/14 event, the P supply from the November manure application may not have been exhausted. Measured concentrations far exceed critical threshold levels cited for eutrophication (20-30 µg SRP L^{-1}) (King et al., 2015a) and 92% of TP was bioavailable as SRP (presumed to be mainly orthophosphate).

The 5/16/14 rainfall event also had a large impact on cumulative total P export from plots. This event delivered 5.4 cm of rain in just 9 h and the rainfall intensity resulted in the largest sediment losses of any single event. Although not statistically significant, TP losses were numerically greater in TD (73 g ha^{-1}) than UD (13.9 g ha^{-1}) despite greater TSS losses in UD. This event was responsible for 65% and 71% of cumulative total TSS lost from TD and UD, respectively. However, as Figure 3.16 illustrates, these losses occurred over a very short period of time and were largely confined to the duration of high intensity rainfall.

Although the magnitude of the losses in the surface runoff from both UD and TD in Figure 3.16 obscure the losses via tile flow, 85% of TSS lost through the tiles (6.6 kg ha^{-1}) occurred in this event. This may have been a legacy of the tile installation six months prior in December 2013. The disturbance of the soil during installation may have resulted in sediment settling into the recently installed tile drains and subsequent transport through the tile system during the high intensity event. Preferential flow pathways are also capable of delivering large amounts of sediment to tiles (Bottcher et

al., 1981), but in cultivated fields these losses are most often seen following dry periods that allow macropores to develop (King et al., 2015a).

The research plots were minimally tilled (one pass with a disk harrow) the previous fall and the tiles in TD plots had flowed continuously since early April 2014. However, prior to sod termination in fall 2013, the field had been managed as a long-term grass field. The absence of tillage likely promoted macropore and biopore development by root channels and soil biota throughout the soil profile (Beven and Germann, 1982), which can result in large TSS and PP loading in tile drains (Chapman et al., 2005; Geohring et al., 2001; Uusitalo et al., 2001). Although the field was tilled prior to corn establishment, this would only have disrupted the preferential flow pathways in the upper 20-30 cm of the soil profile, while the rest of the profile may have still allowed for the translocation of soil particles to the tile drains.

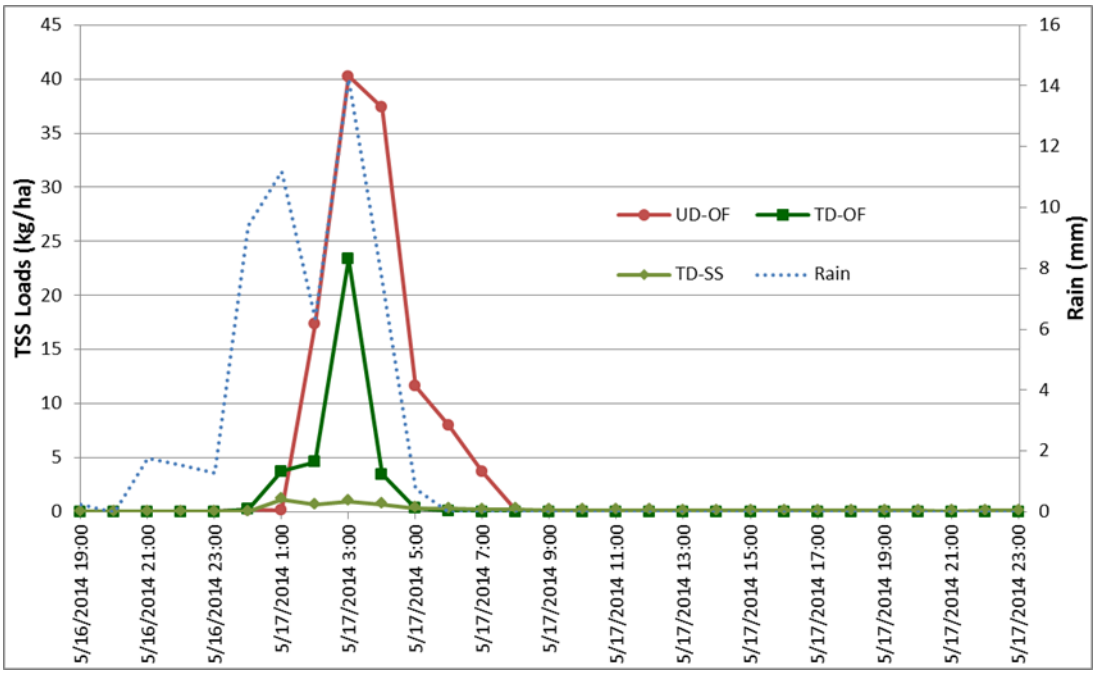

Figure 3.16: TSS loads by hydrologic pathway for each treatment from the 5/16/14 event.

These results demonstrate the potential for the majority of losses to occur in during short time periods. Approximately 82%, 70%, and 92% of SRP, TP, and TSS losses respectively from TD occurred during the seven major runoff events. These percentages were similar in UD with 89%, 75%, and 83% of SRP, TP, and TSS losses, respectively occurring during events. Sharpley et al. (2008) observed a similar pattern during ten years of monitoring a 39.5 ha sub-watershed of Mahantango Creek in south-central Pennsylvania. From 1997-2006, storm flow only accounted for 32% of the watershed discharge, but was responsible for 65% and 80% of DP and TP exports, respectively. Additionally, 23% of TP exported during the study period was from just two storms with a 10-year return period. Although it can be difficult to predict when these losses will occur, continuing to monitor and understand the interactions among weather, field and soil conditions will help target best management practices to when and where they can be most effective.

3.4. Flow-Weighted Mean Concentrations

Flow-weighted mean (FWM) concentrations were calculated for the study duration and each event by treatment mean and by hydrologic pathway (Tables 3.6 and 3.7, respectively**).** Analysis of the data by treatment yielded a number of significant differences or trends with respect to individual events, particularly the 6/3/14 and 8/13/14 events. Notably, the FWM TSS concentrations were significantly greater in UD (291.1 mg L^{-1}; 32.0 mg L^{-1}) than TD (147.6 mg L^{-1}; 4.7 mg L^{-1}) for the 6/3/14 and 8/13/14 events, respectively. The differences in TSS FWM for these events are also

reflected in the significant difference in UP FWM between the treatments. Additionally, these events showed a trend for greater FWM TP in UD. Mean FWM TP for UD (160.9 μg L^{-1}) was approximately three times greater than in TD FWM TP (58.5 μg L^{-1}) for the 8/13/14 event.

Although the analysis of the total FWM for each fraction by treatment did not reveal significant differences, this may be due to the high variation in runoff processes and low replication. However, some general observations can be made regarding the data. Total FWM TP concentrations for both treatments exceeded the 20-30 μg L^{-1} threshold for eutrophication control in freshwater bodies, though TD is closer to this range (King et al., 2015a). Additionally, the EPA recommends that TDP concentrations in flowing waters not exceed 100 μg L^{-1} (USGS, 2015). The FWM TP from TD (49 μg L^{-1}) is 50% below, whereas UD is nearly twice (183 μg L^{-1}) this recommended concentration.

Analysis of the hydrologic pathways by treatment revealed few statistically significant differences despite large numerical differences in many cases. In general, the FWM in surface flows from TD and UD were similar, whereas the tile flows were always lower. For example, the total FWM SRP and FWM TP concentrations were 12.0 μg L^{-1} and 29.0 μg L^{-1}, respectively in TD tile-drain flows, whereas they were 110.2 μg $L^{-1}$and 183.0 μg L^{-1}, respectively in UD surface runoff.

The tile FWM SRP concentrations measured in this study are lower than others reported in tile drainage monitoring studies. King et al. (2015a) reported a range of TP FWM concentrations in monitored tiles of 100-230 μg L^{-1}, with a mean of 150 μg L^{-1}

and similar to other ranges reported in the literature (Gentry et al., 2007; Madison et al., 2014). The difference between FWM concentrations reported here and those in previous studies likely demonstrates the difference in the potential for P export from fields with low STP versus high STP.

Table 3.6: FWM concentrations for SRP, UP, TP, and TSS for each treatment. Means that significantly differ are highlighted in bold text. Values with an asterisk indicates a trend.

Event Date	Treatment	SRP FWM µg L^{-1}	UP FWM µg L^{-1}	TP FWM µg L^{-1}	TSS FWM mg L^{-1}
5/16/2014	TD	46.5	203.9	250.4	148.6
5/16/2014	UD	9.6	89.0	98.7	827.3
6/3/2014	TD	5.1	**161.5**	166.6*	**147.6**
6/3/2014	UD	9.7	**183.6**	193.2*	**291.1**
6/11/2014	TD	3.1	29.6	32.8	11.2
6/11/2014	UD	23.4	84.6	107.9	93.9
6/24/2014	TD	2.4	8.9	11.3	0.8
6/24/2014	UD	130.9	187.1	318.0	25.2
8/13/2014	TD	23.3	**35.2**	58.5*	**4.7**
8/13/2014	UD	66.1	**94.8**	160.9*	**32.0**
12/25/2014	TD	83.9	24.6*	108.4	**2.1**
12/25/2014	UD	260.4	71.4*	331.8	**7.9**
5/31/2015	TD	12.7	13.2	25.9	2.6
5/31/2015	UD	201.5	201.0	402.6	8.6
Total	TD	18.2	30.8	49.0	14.0
Total	UD	110.2	72.8	183.0	135.0

Table 3.7: FWM Concentrations for SRP, UP, TP, and TSS for treatment pathways. Means that significantly differ are highlighted in bold text. Means not connected by the same letter are significantly different.

Event Date	Treatment	Pathway	SRP FWM $\mu g\ L^{-1}$	UP FWM $\mu g\ L^{-1}$	TP FWM $\mu g\ L^{-1}$	TSS FWM $mg\ L^{-1}$
5/16/2014	UD	surface	**9.6[b]**	111.2	**98.7[b]**	827.3
5/16/2014	TD	surface	**137.9[a]**	528.0	**519.6[a]**	225.1
5/16/2014	TD	tile	**3.4[b]**	78.7	**93.3[b]**	44.9
6/3/2014	UD	surface	9.5	109.8	192.5	289.4
6/3/2014	TD	surface	10.0	390.8	310.8	325.7
6/3/2014	TD	tile	1.6	60.0	67.5	10.9
6/11/2014	UD	surface	19.5	64.0	87.4	24.0
6/11/2014	TD	surface	10.7	75.0	85.7	27.3
6/11/2014	TD	tile	2.3	16.0	19.3	1.8
6/24/2014	UD	surface	130.9	8.3	318.0	25.2
6/24/2014	TD	surface	30.0	186.0	192.1	15.9
6/24/2014	TD	tile	1.3	3.6	5.7	0.4
8/13/2014	UD	surface	66.1	95.4	160.9	**32.0[a]**
8/13/2014	TD	surface	63.5	84.9	117.7	**8.4[b]**
8/13/2014	TD	tile	7.6	27.6	35.4	**3.5[b]**
12/25/2014	UD	surface	260.4	91.1	331.8	7.9
12/25/2014	TD	surface	458.0	47.7	531.2	6.1
12/25/2014	TD	tile	74.9	26.0	98.5	1.9
5/31/2015	UD	surface	201.5	48.9	402.6	8.6
5/31/2015	TD	surface	90.6	54.4	144.4	5.1
5/31/2015	TD	tile	4.9	10.5	15.7	2.6
Total	UD	surface	110.2	59.2	183.0	135.0
Total	TD	surface	124.6	265.1	324.3	120.7
Total	TD	tile	12.0	15.2	29.0	3.0

3.5. Implications for Water Quality and Field Management

The results of this study indicate that in some cases, tile drainage may be beneficial in reducing P loading from fields. Although there was no statistical difference in TP exported between treatments, SRP and TSS loads were 36% and 61% lower from TD plots compared to UD. The literature reports mixed results relative to

tile drainage impacts on P loss. Eastman et al. (2010) reported increased TP losses in a tile-drained field relative to a naturally-drained field during two years of monitoring paired fields (clay loam, 160 kg Mehlich-3 P ha^{-1}) in the Pike River Watershed in southern Quebec (approximately 50 km from the Lake Alice experimental plots). The average TP loads from 2004 and 2005 were 2.9 kg ha^{-1} y^{-1} in the tiled field (66% from tile flow) and 0.9 kg ha^{-1} y^{-1} in the naturally-drained field (surface runoff only). Although these loads are much higher than those lost from TD (0.234 kg ha^{-1}) and UD (0.231 kg ha^{-1}) in our experiment, they are consistent with other reports with similarly elevated STP levels. A review of tile drainage research by King et al. (2015a) found a range of 0.4 to 1.6 kg TP ha^{-1} y^{-1} exported from tile drains. Gilliam et al. (1999) reported a slightly larger range (0.2 to 2.4 kg TP ha^{-1} y^{-1}) in an earlier review of agricultural drainage. The difference in TP exports from our site relative to many of those reported may be due to the very low STP status in comparison to other studies with higher STP fields (Heckrath et al., 1995; McDowell and Sharpley, 2001; Maguire and Sims, 2002; Sharpley et al., 2013).

Differences in STP affect potential P export risk from tile drainage flows. Long-term over-application of organic and inorganic fertilizers has been shown to result in excess P in the soil (Sharpley et al., 2003). However, research has demonstrated that the change-point above which P losses in runoff increase rapidly is well above optimum crop levels (Heckrath et al., 1995; Maguire and Sims, 2002). Preventing P accumulation and excessively high STP concentrations is critical since

considerable time is required to reduce soil P concentrations back down to optimum levels (Sharpley and Withers, 1994).

In addition to the quantity of P applications, the timing of these applications is also critically important. The impact of manure application in the non-growing season was demonstrated in the snowmelt event presented here. This type of high P load runoff event due to snowmelt and non-growing season conditions has been previously documented in other research, though relatively few studies have measured losses during winter and early spring. Coelho et al. (2012) observed a snowmelt event that contributed 80% of the annual TDP load (both surface and subsurface pathways) and Jamieson et al. (2003) observed 97% of annual TP lost during 4 d of spring snowmelt. Macrae et al. (2007) observed the highest concentrations of TP during a snowmelt event in fields that received manure. Gentry et al. (2007) observed a rain/snowmelt event following a late-fall broadcast application of inorganic P fertilizer that resulted in TP exports that represented 40% of the annual TP load for the receiving stream and 80% of the TP was SRP. Results from these studies indicate that the timing and method (e.g., broadcast with or without incorporation, injected) of nutrient applications relative to high-flow events are critical in determining loss risk potential from fields.

3.6. Study Limitations

The results of the 12/25/14 event and grab samples from March and early April 2014 demonstrate the importance of continuous year-round monitoring. The inability to calculate P and sediment loads exported during that period of both maximum flow

and P concentrations could be important from a water quality and cumulative P loss perspective. The difficulty in maintaining an ice-free environment around sampling equipment during periods of fluctuating freezing and non-freezing temperatures needs to be addressed to fully understand the implications of tile drainage on water quality. However, the exact techniques will likely be dependent on the specific location, cost, and infrastructure needs. The U.S. Geological Survey in cooperation with the University of Wisconsin Discovery Farms and Pioneer Farm has been conducting year-round edge-of-field research since 2001. They have experimented with numerous techniques to limit ice build-up and the best option (heat-tape at the flume exit) is still not entirely effective and requires a power source at the site (Stuntebeck et al., 2008).

Improvements to the study design could also be made. Although results from the groundwater well monitoring in June 2015 indicated that the influence of the tile lines would be minimal, the ability to have hydrologic isolation would ensure that measured surface and subsurface flows originated from within the plot boundaries. However, the effects may be minimal enough to not warrant the additional construction and expense. Also, although the snow depth was not measured, field observations indicated that snow preferentially accumulated in plots 1 and 2 in the 2014-2015 winter season. This drifting snow could also impact data collection of snowmelt events. Although this would be difficult to control in fields with exposure to high winds, the effects of snowmelt will be difficult to discern on a smaller scale system similar to our plots without adequate isolation. Additionally, the drainage from snowmelt in the Northeast is a significant portion of the annual water budget. In the future, snow

sampling to estimate the average water equivalency depth of the snowpack would provide more complete water budget calculations.

Another limitation of this study was the relatively short time frame in which it was conducted. Weather events, site conditions, and management strategies (e.g., crop, tillage practices) are all variable and with more events and years monitored, more sound conclusions can be reached. In this data set, the 12/24/15 and 5/16/14 events exert heavy influence on the conclusions drawn. However, if these are outlier events, they are overly represented and could lead to false conclusions as to the typical conditions of this site and its response to runoff events. The constraints imposed by the site also limited additional replication, which would have provided more statistical power in our analyses.

Additional sampling equipment and capabilities could also improve the data collection for this study. The available equipment precluded the ability to conduct flow-based sampling and instead a time-based sampling regime was followed. Although samples were taken hourly to capture variation in P over the runoff hydrograph, overland flows can be very ephemeral and important data could be missed by not sampling these transient flows. Finally, the installation of soil moisture sensors would also facilitate a better understanding of the impacts of AMC on the hydrology and P speciation during runoff events.

3.6. Conclusions

The results of this study indicate that the installation of tile drainage into agricultural fields will not necessarily result in additional P losses relative to an undrained field under similar management. The data supported the first two hypotheses that surface runoff volume would be lower from TD plots, and that this reduction in surface runoff would result in a concomitant reduction in TSS loadings. However, the third hypothesis, that lower TSS loads in TD would result in a concomitant reduction in TP, was not supported. This is likely due to the low STP at the site and therefore, low P content in eroded sediment, a result of the short history of nutrient additions to the field. However, while TP losses were nearly identical between treatments, SRP losses were substantially lower from TD plots, which could have positive water quality implications for Lake Champlain due to a reduction in bioavailable P transport. These conclusions must be tempered by the knowledge that this study only encompassed 13 months of monitoring and should be considered site-specific. Seasonal differences in P forms and mobility were demonstrated and additional years and improved monitoring during the non-growing season will provide additional information on the hydrology and P dynamics of the experimental site in order to develop more robust conclusions.

BIBLIOGRAPHY

Al-Darby, A.M. and B. Lowery. 1986. Evaluation of corn growth and productivity with three conservation tillage systems. Agron. J., 78:901-907.

Allen, R.G., M.E. Jensen, J.L. Wright, and R.D. Burman. 1989. Operational Estimates of Reference Evapotranspiration. Agron. J. 81:650-662.

American Public Health Association. 1989. Phosphorus: 4500-P. *In:* L.S. Clesceri et al., editors, Standard methods for the examination of waste and wastewaters. 17th ed. Port City Press, Baltimore, MD. p. 4.166–4.181.

Arriaga, H., M. Pinto, S. Calsamiglia, and P. Merino. 2009. Nutritional and management strategies on nitrogen and phosphorus use efficiency of lactating dairy cattle on commercial farms: An environmental perspective. J. Dairy Sci. 92(1):204-215.

Azooz, R.H. and M.A. Arshad. Soil infiltration and hydraulic conductivity under long-term no-tillage and conventional tillage systems. Can. J. Soil Sci. 76:143-152.

Balesdent, J., A. Mariotti, and D. Boisgontier. Effect of tillage on soil organic carbon mineralization estimated from ^{13}C abundance in maize fields. Eur. J. Soil Sci. 41:587-596.

Baker, J.L., K.L. Campbell, H.P. Johnson, and J.J. Hanway. 1975. Nitrate, phosphorus, and sulfate in subsurface drainage water. J. Environ. Qual. 4:406–412.

Bartlett, R.J. and D.S. Ross. 2005. Chemistry of Redox Processes in Soils, in *Chemical Processes in Soils.* (eds. M.A. Tabatabai and D.L. Sparks), Soil Science Society of America, Inc. Madison, Wisconsin, pp461-488.

Beauchemin, S., R.R. Simard, and D. Cluis. 1998. Forms and Concentrations of Phosphorus in Drainage Water of Twenty-Seven Tile-Drained Soils. J. Environ. Qual. 27:721-728.

Bengtson, R.L., C.E. Carter, H.F. Morris, and S.A. Bartkiewiez. 1988. The influence of subsurface drainage practices on nitrogen and phosphorus losses in a warm humid climate. Trans. ASAE. 31. 729-733.

Bengtson, R.L., L.M. Southwick, G.H. Willis, and C.E. Carter. 1990. The influence of subsurface drainage practices on herbicide losses. Trans. ASAE. 33:415:418.

Beven, K. and P. Germann. 1982. Macropores and Water Flow in Soils. Water Resour. Res. 18:1311-1325.

Blann, K.L., J.L. Anderson, G.R. Sands, and B. Vondracek. 2009. Effects of Agricultural Drainage on Aquatic Ecosystems: A Review. Crit. Rev. Environ. Sci. Technol. 39:909-1001.

Bottcher, A.B., E.J. Monke, and L.F. Huggins. 1981. Nutrient and sediment loadings from a subsurface drainage system. Trans. ASABE 24:1221– 1226.

Brady, N. C., and R. R. Weil. 2008. The Nature and Properties of Soils. 14th ed. Prentice Hall, Upper Saddle River, N. J.

Bronick, C.J. and R. Lal. 2005. Soil structure and management: a review. Geoderma. 124:3-22.

Broughton, R.S. and J.L. Fouss. Subsurface Drainage Installation Machinery and Methods, in *Agricultural Drainage*. (eds. R.W. Skaggs and J. van Schilfgaarde), ASA-CSA-SSSA, Madison, Wisconsin, pp.963-1004.

Burch, G.J., R.K. Bath., I.D. Moore, and E.M. O'Loughlin. 1987. Comparative hydrological behaviour of forested and cleared catchments in southeastern Australia. J. Hydrol., 90: 19-42.

Cade-Menun, B.J. 2005. Characterizing phosphorus in environmental and agricultural samples by ^{31}P nuclear magnetic resonance spectroscopy. Talanta, 66:359-371.

Carter, C.E. 1999. Surface Drainage, in *Agricultural Drainage*. (eds.R.W. Skaggs and J. van Schilfgaarde), ASA-CSA-SSSA, Madison, Wisconsin, pp.1023-1050.

Chapman, A.S., I.D.L. Foster, J.A. Lees, and R.A. Hodgkinson. 2005. Sediment delivery from agricultural land to rivers via subsurface drainage. Hydrol. Processes. 19:2875:2897.

Chacon, N., W.L. Silver, E. A. Dubinsky, D.F. Cusack. 2006. Iron reduction and soil phosphorus solubilization in humid tropical forests soils: the roles of labile carbon pools and an electron shuttle compound. Biogeochemistry, 78:67-84.

Coelho, B.B., R. Murray, D. Lapen, E. Topp, and A. Bruin. 2012. Phosphorus and sediment loading to surface waters from liquid swine manure application under different drainage and tillage practices. Agr. Water Manage. 104:51-61.

Colwell H.T.M. 1978. The economics of increasing crop productivity in Ontario and Quebec by tile drainage installation. Canadian Farm Economics. 13(3):1-7.

Condron, L.M., B.L. Turner, B.J. Cade-Menun. 2005. Chemistry and Dynamics of Soil Organic Phosphorus, in in *Phosphorus: Agriculture and the Environment*. (eds J.T. Sims and A.N. Sharpley), ASA-CSA-SSSA, Madison, Wisconsin, pp87-122.

Correll, D.L. 1998. The Role of Phosphorus in the Eutrophication of Receiving Waters: A Review. J. Environ. Qual. 27:261-266.

Daniel, T.C., A.N. Sharpley, J.L. Lemunyon. 1998. Agricultural Phosphorus and Eutrophication: A Symposium Overview. J. Environ. Qual. 27:251-257.

Dexter, A.R. 1988. Advances in Characterization of Soil Structure. Soil Till. Res. 11:199-238.

Dinnes, D.L., D. L. Karlen, D.B. Jaynes, T.C. Kaspar, J.L. Hatfield. 2002. Nitrogen Management Strategies to Reduce Nitrate Leaching in Tile- Drained Midwestern Soils. Agron. J. 94:153-171.

Dolezal, F., Z. Kulhavy, M. Soukup, and R. Kodesova. 2001. Hydrology of tile drainage runoff. Phys. Chem. Earth B 26:623–627.

Dunne, T. 1983. Relation of Field Studies and Modeling in the Prediction of Storm Runoff. J. Hydrol. 65:25-48.

Dunne, T. and R.D. Black. 1970a. An experimental investigation of runoff production in permeable soils. Water Resour. Res. 6:478-490.

Dunne, T. and R.D. Black. 1970b. Partial-area contributions to storm runoff in a small New England watershed. Water Resour. Res. 6:1296-1311.

Dunne, T. and L.B. Leopold. 1978. Water in Environmental Planning. W.H. Freeman and Company, San Francisco, CA.

Eagleson, P.S. 1978. Climate, Soil, and Vegetation: Introduction to Water Balance Dynamics. Water Resour. Res. 14(5):705-712.

Eastman, M., A. Gollamudi, N. Stampfli, C.A. Madramootoo, and A. Sarangi. 2010. Comparative evaluation of phosphorus losses from subsurface and naturally drained agricultural fields in the Pike River watershed of Quebec, Canada. Agric. Water Manage. 97:596–604.

Essington, M.E. 2004. Soil and Water Chemistry: An Integrative Approach., CRC Press, Boca Raton, FL.

Evans, R.O. and N.R. Fausey. 1999. Effects of Inadequate Drainage on Crop Growth and Yield, in *Agricultural Drainage*. (eds. R.W. Skaggs and J. van Schilfgaarde), ASA-CSA-SSSA, Madison, Wisconsin, pp.13-54.

Foy, R.H. 2005. The return of the phosphorus paradigm; agricultural phosphorus and eutrophication, in *Phosphorus: Agriculture and the Environment*. (eds J.T. Sims and A.N. Sharpley), ASA-CSA-SSSA, Madison, Wisconsin, pp. 1021-1068.

Fraser, H. and R. Fleming. 2001. Environmental benefits of tile drainage: Literature review. www.ridgetownc.uoguelph.ca/research/documents/fleming_drainage.pdf

Frossard, E., L.M. Condron, A. Obserson, S. Sinaj, J.C. Fardeau. 2000. Processes Governing Phosphorus Availability in Temperate Soils. J. Environ. Qual. 29(1):1-15.

Gburek, W.J. and A.N. Sharpley. 1998. Hydrologic Controls on Phosphorus Loss from Upland Agricultural Watersheds. J. Environ. Qual. 27:267-277.

Gburek, W.J., B.A. Needelman, and M.S. Srinivasen. 2006. Fragipan controls on runoff generation: Hydropedological implications at landscape and watershed scales. Geoderma. 131:330-344.

Gentry, L.E., M.B. David, T.V. Royer, C.A. Mitchell, and K.M. Starks. 2007. Phosphorus transport pathways to streams in tile-drained agricultural watersheds. J. Environ. Qual. 36:408–415.

Geohring, L.D., O.V. McHugh, M.T. Walter, T.S. Steenhuis, M.S. Akhtar, and M.F. Walter. 2001. Phosphorus transport into subsurface drains by macropores after manure applications: Implications for best manure management practices. Soil Sci. 166:896–909.

Gilliam, J.W., J.L. Baker, and K.R. Reddy. 1999. Water Quality Effects of Drainage in Humid Regions, in *Agricultural Drainage*. (eds. R.W. Skaggs and J. van Schilfgaarde), ASA-CSA-SSSA, Madison, Wisconsin, pp.801-830.

Goldberg, S., J.A. Davis, and J.D. Hem. 1996. The Surface Chemistry of Aluminum Oxides and Hydroxides, in *The Environmental Chemistry of Aluminum*. (ed. G. Sposito), CRC Press, Boca Raton, FL, 272-318.

Hardie, M.A., W.E. Cotching, R.B. Doyle, G. Holz, S. Lisson, K. Mattern. 2011. Effect of antecedent soil moisture on preferential flow in a texture-contrast soil. J. Hydrol. 398:191-201.

Harrison, A.F. 1987. Soil organic phosphorus: a review of world literature. C.A.B. International, Wallingford, U.K., p. 257.

Haygarth, P.M and S.C. Jarvis. 1999. Transfer of Phosphorus from Agricultural Soils. Adv. Agron. 66:195-249.

Haygarth, P.M., and A.N. Sharpley. 2000. Terminology for Phosphorus Transfer. J. Environ. Qual. 29:10-15.

Haynes, J.L. 1954. Ground rainfall under vegetative canopy of crops. J. Amer. Soc. Agron. 46:67-94.

Heathwaite, A.L., and R.M. Dils. 2000. Characterising phosphorus loss in surface and subsurface hydrological pathways. Sci. Total Environ. 251-252:523-538.

Heckrath, G., P.C. Brooks, P.R. Poulton, and K.W.T. Goulding. 1995. Phosphorus leaching from soils containing different phosphorus concentrations in the Broadbalk experiment. J. Environ. Qual. 24:904–910.

Hesketh, N., and P.C. Brooks. 2000. Development of an indicator for risk of phosphorus leaching. J. Environ. Qual. 29:105–110.

Istok, J.D., and Kling, G.F. 1983. Effect of subsurface drainage on runoff and sediment yield from an agricultural watershed in Western Oregon, USA. J. Hydrol. 65:279-291.

Jamieson, A., C.A. Madramootoo, and P. Enright. 2003. Phosphorus losses in surface and subsurface runoff from a snowmelt event on an agricultural field in Quebec. Can. Biosyst. Eng. 45:1.1-1.7.

Jokela, B., F. Magdoff, R. Bartlett, S. Bosworth, and D. Ross. 2004. Nutrient Recommendations for Field Crops in Vermont. University of Vermont Extension.

Karl, T.R. and R.W. Knight. 1998. Secular Trends of Precipitation Amount, Frequency, and Intensity in the United States. B. Am. Meteorol. Soc. 79:231-241.

King, K.W., M.R. Williams, M.L. Macrae, N.R. Fausey, J. Frankenberger, D.R. Smith, P.J.A. Kleinman, and L.C. Brown. 2015a. Phosphorus Transport in Agricultural Subsurface Drainage: A Review. J. Environ. Qual. 44(2):467-485.

King, K.W., M.R. Williams, and N.R. Fausey. 2015b. Contributions of Systematic Tile Drainage to Watershed-Scale Phosphorus Transport. J. Environ. Qual. 44:486-494.

Kirkby. M. 1988. Hillslope Runoff Processes and Models. J. Hydrol. 100:315-339.

Kittridge, J. 1948. Forest Influences: The Effects of Woody Vegetation on Climate, Water and Soil. Mcgraw-Hill, New York, NY.

Klatt, J.G., A.P. Mallarino, and B.L. Allen. 2002. Relationship between soil P and P in surface runoff and subsurface drainage: An overview of ongoing research. North Central Extension-Industry Soil Fertility Conference, vol. 18. Des Moines, IA. p. 183–189.

Kleinman, P.J.A., M.S. Srinivasan, C.J. Dell, J.P. Schmidt, A.N. Sharpley, R.B Bryant. 2006. J. Environ. Qual. 35:1248:1259.

Kleinman, P.J.A., A.N. Sharpley, A.R. Buda, R.W. McDowell, and A.L. Allen. 2011. Soil controls of phosphorus in runoff: Management barriers and opportunities. Can. J. Soil Sci. 91:329-338.

Kleinman, P.J.A., D.R. Smith, C.H. Bolster, and Z.M. Easton. 2015. Phosphorus Fate, Management and Modeling in Artificially Drained Systems. J. Environ. Qual. 44:460-466.

Lal, R. and G.S. Taylor. 1969. Drainage and Nutrient Effects in a Field Lysimeter Study: I. Corn Yield and Soil Conditions. Soil Sci. Soc. Ameri. Proc. 33:937-941.

Le Bissonnais, Y. 1996. Aggregate stability and assessment of soil crustability and erodibility: I. Theory and methodology. Eur. J. Soil Sci. 47:425–437.

Liu, J., Y. Hu, J. Yang., D. Abdi, B.J. Cade-Menun. 2014. Investigation of Soil Legacy Phosphorus Transformation in Long-Term Agricultural Fields Using Sequential Fractionation, P K-edge XANES and Solution P NMR Spectroscopy. Environ. Sci. Tech. 49(1):168-176.

Macrae, M.L., M.C. English, S.L. Schiff, and M. Stone. 2007. Intra-annual variability in the contribution of tile drains to basin discharge and phosphorus export in a first-order agricultural catchment. Agr. Water Manage. 92:171–182.

Madison, A.M., M.D. Ruark, T.D. Stuntebeck, M.J. Komiskey, L.W. Good, N. Drummey, E.T. Cooley. 2014. Characterizing phosphorus dynamics in tile-drained agricultural fields of eastern Wisconsin. J. Hydrol. 519:892-901.

Madramootoo, C.A. Planning and Design of Drainage Systems, in *Agricultural Drainage*. (eds. R.W. Skaggs and J. van Schilfgaarde), ASA-CSA-SSSA, Madison, Wisconsin, pp.871-892.

Maguire, R.O. and J.T. Sims. 2002. Soil Testing to Predict Phosphorus Leaching. J. Environ. Qual. 31:1601-1609.

McDowell, R.W., and A.N. Sharpley. 2001. Approximating phosphorus release from soils to surface runoff and subsurface drainage. J. Environ. Qual. 30:508–520.

McDowell, R.W. and R.M. Monaghan. 2015. Extreme Phosphorus Losses in Drainage from Grazed Dairy Pastures on Marginal Land. J. Environ. Qual. 44:545-551.

Messiga, A.J., N. Ziadi, C. Morel, L.E. Parent. 2010. Soil phosphorus availability in no-till versus conventional tillage following freezing and thawing cycles. Can. J. Soil Sci. 90:419-428.

Myers, C.F., J. Meek, S. Tuller, A. Weinberg. 1985. Nonpoint sources of water pollution. J. Soil Water Conserv. 40:14-18.

Needelman, B.A., W.J. Gburek, G.W. Petersen, A.N. Sharpley, P.J.A. Kleinman. 2004. Surface Runoff along Two Agricultural Hillslopes with Contrasting Soils. Soil Sci. Soc. Am. J. 68:914-923.

NRCC. 2015. Northeast Regional Climate Center. http://www.nrcc.cornell.edu/

NRCS. 2001. Water Management (Drainage), *in Part 650 Engineering Field Handbook*. http://directives.sc.egov.usda.gov/OpenNonWebContent.aspx?content=17551.wba.

NRCS, 2015. Saturated Hydraulic Conductivity. Natural Resources Conservation Service. www.nrcs.usda.gov.

Olander, L.P. and P.M. Vitousek. 2005. Short-term controls over inorganic phosphorus during soil and ecosystem development. Soil Biol. Biochem., 37:561-659.

Pachepsky, Y., D. Timlin, and W. Rawls. Generalized Richards' equation to simulate water transport in unsaturated soils. J. Hydrol. 272:3-13.

Pagliai, M., N. Vignozzi, S. Pellegrini. 2004. Soil structure and the effect of management practices. Soil Till. Res. 79:131-143.

Penman, H.L. 1948. Natural evaporation from open water, hare soil and grass. Proc. R. Soc. Lond. A Math. Phys. Sci.193(1032):120-145.

Penn, C.J., R.B. Bryant, P.J.A. Kleinman, and A.L. Allen. 2007. Removing dissolved phosphorus from drainage ditch water with phosphorus sorbing materials. Journal of Soil and Water Conservation 62(4):269-276.

Pierzynski, G.M. 1991. The chemistry and mineralogy of phosphorus in excessively fertilized soils. Crit. Rev. Environ. Control 21:265-295.

Pierzynski, G.M., and T.J. Logan. 1993. Crop, Soil, and Management Effects on Phosphorus Soil Test Levels: A Review. J. Prod. Agric. 6(4):513-520.

Pierzynski, G.M. 2000. Methods of Phosphorus Analysis for Soils, Sediments, Residuals, and Waters. Southern Cooperative Series Bulletin No. 396. http://www.soil.ncsu.edu/sera17/publications/sera17-2/pm_cover.htm

Pierzynski, G.M., R.W. McDowell, and J.T. Sims. 2005a. Chemistry, Cycling, and Potential Movement of Inorganic Phosphorus in Soils, in *Phosphorus: Agriculture and the Environment*. (eds J.T. Sims and A.N. Sharpley), ASA-CSA-SSSA, Madison, Wisconsin, pp. 53-86.

Pierzynski, G.M., J.T. Sims, and G.M. Vance. 2005b. Soils and Environmental Quality. 3rd ed. Taylor & Francis, Boca Raton, FL.

Pote, D.H., T.C. Daniel, A.N. Sharpley, P.A. Moore, Jr., D.R. Edwards, and D.J. Nichols. 1996. Relating extractable soil phosphorus to phosphorus in runoff. J. Environ. Qual. 60:855–859.

Radcliffe, D.E. and J. Simunek. 2010. Soil Physics with HYDRUS: Modelling and Applications. CRC Press, Boca Raton, FL.

Reddy, K.R., R.G. Wetzl, and R.H. Kadlec. 2005. Biogeochemistry of Phosphorus in Wetlands, in *Phosphorus: Agriculture and the Environment.* (eds J.T. Sims and A.N. Sharpley), ASA-CSA-SSSA, Madison, Wisconsin, pp. 263-316.

Rodzik, J., T. Furtak, and W. Zglobicki. 2009. The impact of snowmelt and heavy rainfall runoff on erosion rates in a gully system, Lublin Upland, Poland. Earth Surf. Process. Landsforms. 34:1938-1950.

Sallade, Y.E. and J.T. Sims. 1997. Phosphorus Transformations in the Sediments of Delaware's Agricultural Drainageways: II. Effect of Reducing Conditions on Phosphorus Release. J. Environ. Qual. 26:1579-1588.

Schilling, K.E. and M. Helmers. 2008. Tile drainage as karst: Conduit flow and diffuse flow in a tile-drained watershed. J. Hydrol. 349:291-301.

Schindler, D.W. Factors regulating phytoplankton production and standing crop in the world's freshwaters. 1977. Limnol. Oceanogr. 23(3):478-486.

Schindler, D.W., and T. Ruszczysnki. 1978. Phosphorus input and its consequences for phytoplankton standing crop and production in the Experimental Lakes Area and in similar lakes. J. Fish. Res. Bd. Can. 35(2):190-196.

Schindler, D.W., R.E. Hecky, D.L. Findlay, M.P. Stainton, B.R. Parker, M.J. Paterson, K.G. Beaty, M. Lyng, and S.E.M. Kasian. 2008. Eutrophication of lakes cannot be controlled by reducing nitrogen input: results of a 37 year whole ecosystem experiment. PNAS. 105(32):11254–11258.

Schwab, G.O. and J.L. Fouss. 1999. Drainage Materials, in *Agricultural Drainage*. (eds. R.W. Skaggs and J. van Schilfgaarde), ASA-CSA-SSSA, Madison, Wisconsin, pp.911-926.

Sharpley, A.N. 1980. The Enrichment of Soil Phosphorus in Runoff Sediments. J. Environ. Qual. 9:521-526.

Sharpley, A.N., S.J. Smith, O.R. Jones, W.A. Berg, and G.A. Coleman. 1992. The Transport of Bioavailable Phosphorus in Agricultural Runoff. J. Environ. Qual. 21:30-35.

Sharpley, A.N., S.C. Chapra, R. Wedepohl, J.T. Sims, T.C. Daniel, and K.R. Reddy. 1994. Managing Agricultural Phosphorus for Protection of Surface Waters: Issues and Options. J. Environ. Qual. 23:437:451.

Sharpley, A.N. and P.J.A. Withers. 1994. The environmentally-sound management of agricultural phosphorus. Fertilizer Research. 39:133-146.

Sharpley, A.N., B. Foy, and P. Withers. 2000. Practical and Innovative Measures for the Control of Agricultural Phosphorus Losses to Water: An Overview. J. Environ. Qual. 29:1-9.

Sharpley, A.N., R.W. McDowell, and P.J.A. Kleinman. 2001. Phosphorus loss from land to water: integrating agricultural and environmental management. Plant and Soil. 237: 287-307.

Sharpley, A.N., T. Daniel, T. Sims, J. Lemunyon, R. Stevens, and R. Parry. 2003. Agricultural Phosphorus and Eutrophication, 2nd Edition. U.S. Department of Agriculture, Agricultural Research Service, ARS-149, 44 pp.

Sharpley, A.N., P.J.A. Kleinman, A.L. Heathwaite, W.J. Gburek, G.J. Folmar, and J.P. Schmidt. 2008. Phosphorus Loss from an Agricultural Watershed as a Function of Storm Size. J. Environ. Qual. 37:362-368.

Sharpley, A.N., P.J.A. Kleinman, P. Jordan, L. Bergstrom, and A.L. Allen. 2009. Evaluating the success of phosphorus management from field to watershed. J. Environ. Qual. 38:1981-1988.

Sharpley, A.N., H.P. Jarvie, A. Buda, L. May, B. Spears, and P. Kleinman. 2014. Phosphorus Legacy: Overcoming the Effects of Past Management Practices to Mitigate Future Water Quality Impairment. J. Environ. Qual. 42(5):1308-1326.

Simard, R.R., S. Beauchemin, and P.M. Haygarth. 2000. Potential for Preferential Pathways of Phosphorus Transport. J. Environ. Qual. 29:97-105.

Sims, J.T., G.M. Pierzynski. 2005. Chemistry of Phosphorus in Soils, in *Chemical Processes in Soils.* (eds. M.A. Tabatabai and D.L. Sparks), Soil Science Society of America, Inc. Madison, Wisconsin, pp151-192.

Sims, J.T., R.R. Simard, and B.C. Joern. 1998. Phosphorus Loss in Agricultural Drainage: Historical Perspective and Current Research. J. Environ. Qual. 27:277-293.

Skaggs, R.W., M.A. Breve, J.W. Gilliam. Hydrologic and Water Quality Impacts of Agricultural Drainage. Crit. Rev. Environ. Sci. Technol. 24:1-32.

Skaggs, R.W. and J. van Schilfgaarde. 1999. Introduction, in *Agricultural Drainage*. (eds. R.W. Skaggs and J. van Schilfgaarde), ASA-CSA-SSSA, Madison, Wisconsin, pp.3-10.

Smeltzer, E. and S. Quinn. 1996. A Phosphorus Budget, Model, and Load Reduction Strategy for Lake Champlain. 12(3):381-393.

Smil, V. 2000. Phosphorus in the Natural Environment : Natural Flows and Human Interferences. Annual Rev. Energy Environ. 25:53-88.

Smith, D.R., K.W. King, L. Johnson, W. Francesconi, P. Richards, D. Baker, and A.N. Sharpley. 2015. Surface Runoff and Tile Drainage Transport of Phosphorus in the Midwestern United States. J. Environ. Qual. 44:495-502.

Smith, K.A., A.G. Chalmers, B.J. Chalmers, and P. Christie. 1998. Organic manure phosphorus accumulation, mobility, and management. Soil Use Manage. 14:154–159.

Smith, L. "Missisquoi Bay Sediment Phosphorus Cycling: the Role of Organic Phosphorus and Seasonal Redox Fluctuations". 2009. Graduate College Dissertations and Theses. Paper 217. http://scholarworks.uvm.edu/graddis/217

Smith, L., M.C. Watzin, G. Druschel. 2011. Relating sediment phosphorus mobility to seasonal and diel redox fluctuations at the sediment-water interface in a eutrophic freshwater lake. Limnol. and Oceanogr. 56(6):2251-2264.

Smith, R.V., S.D. Lennox, C. Jordan, R.H. Foy, and E. McHale. 1995. Increase in soluble phosphorus transported in drainflow from a grassland catchment in response to soil phosphorus accumulation. Soil Use Manage. 11:204– 209.

Smith, S.C. and D.T. Massey. 1987. A Framework for Future Farm Drainage Policy: The Environmental and Economic Setting, in *Farm Drainage in the United States. History, Status, and Prospects. Misc. Pub. No. 1455.* (ed. G.A. Pavelis), Economic Research Service, Department of Agriculture, Washington, D.C., pp1-12.

Smith, V.H., G.D. Tilman, J.C. Nekola. 1999. Eutrophication: impacts of excess nutrient inputs on freshwater, marine, and terrestrial ecosytems. Environmental Pollution. 100:179-196.

Sollins, P., G.P. Robertson, G. Uehara. 1988. Nutrient Mobility in Variable- and Permanent-Charge Soils. Biogeochemistry, 6(3):181-199.

Stuntebeck, T.D., M.J., Komiskey, D.W. Owens, and D.W. Hall. 2008. Methods of data collection, sample processing, and data analysis for edge-of-field, streamgaging, subsurface-tile, and meteorological stations at Discovery Farms and Pioneer Farm in Wisconsin, 2001-7: U.S. Geological Survey Open-File Report 2008-1015, 51p.

Sugg, Z. 2007. Assessing U.S. Farm Drainage: Can GIS Lead to Better Estimates of Subsurface Drainage Extent? World Resources Institute. August:1-8.

Syers, J.K., R.F. Harris, and D.E. Armstrong. 1973. Phosphate Chemistry in Lake Sediments. J. Environ. Qual., 2(1):1-14.

Tan, C.S., C.F. Drury, W.D. Reynolds, J.D. Gaynor, T.Q. Zhang, and H.Y.F. Ng. 2002. Effect of long-term conventional tillage and no-tillage systems on soil and water quality at the field scale. Water Sci. Technol. 46:183–190.

Tiessen, H., J.W.B. Stewart, and C.V. Cole. 1984. Pathways of Phosphorus Transformations in Soils of Differing Pedogenesis. Soil Sci. Soc. Am. J. 48:853-858.

Tilman, D., K.G. Cassman, P.A. Matson, R. Naylor, S. Polasky. 2002. Agricultural sustainability and intensive production practices. Nature. 418:671-677.

Trevail, T. 2006. Soil Survey of Clinton County, New York. USDA-NRCS.

Turner, B.L., M.J. Paphazy, P.M. Haygarth, and I.D. McKelvie. 2002. Phil. Trans. R. Soc. Lond. 357:449-469.

Turner, B.L. 2005. Organic phosphorus transfer from terrestrial to aquatic environments, in *Organic phosphorus in the environment*. (eds. B.L. Turner, E. Frossard, D.S. Baldwin), CABI Publishing, Wallingford, U.K., pp. 169-294.

Uusitalo, R., E. Turtola, T. Kauppila, and T. Lilja. 2001. Particulate Phosphorus and Sediment in Surface Runoff and Drainflow from Clayey Soils. J. Environ. Qual. 30:589-595.

Venterink, H.O., T.E. Davidsson, K. Kiehl, and L. Leonardson. 2002. Impact of drying and re-wetting on N, P and K dynamics in a wetland soil. Plant and Soil. 243:119-130.

Vidon, P., and P.E. Cuadra. 2011. Phosphorus dynamics in tile-drain flow during storms in the US Midwest. Agric. Water Manage. 98:532–540.

Wang, S., X. Jin, H. Zhao, X. Zhou, F. Wu. 2007. Effect of organic matter on the sorption of dissolved organic and inorganic phosphorus in lake sediments. Colloids and Surfaces A: Physicochemical and Engineering Aspects. 297:154-162.

Withers, P.J.A., B. Ulen, C. Stamm, and M. Bechmann. 2003. Incidental phosphorus losses – are they significant and can they be predicted? J. Plant Nutr. Soil Sci. 166:459-468.

Withers, P.J.A., H.P. Jarvie, R.A. Hodgkinson, E.J. Palmer-Felgate, A. Bates, M. Neal, R. Howells, C.M. Withers, and H.D. Wickham. 2009. Characterization of phosphorus sources in rural watersheds. J. Environ. Qual. 38:1998–2011.

Wolf, A.M. and D.E. Baker. 1985. Comparisons of soil test phosphorus by Olsen, Bray P1, Mehlich I and Mehlich III methods. Commun. Soil Sci. Plant Anal. 16:467-484.

Wright, J. and G. Sands. 2001. Planning an Agricultural Subsurface Drainage System. University of Minnesota Extension. www.irrigationtoolbox.com.

Wright, J. and G. Sands. 2009. Planning an agricultural subsurface drainage system. University of Minnesota Extension. http://www.extension.umn.edu/

Young, R.A. and J.L. Wiersma. The Role of Rainfall Impact in Soil Detachment and Transport. Water Resour. Res. 9:1629:1636.

Young, E.O. and D.S. Ross. 2001. Phosphate Release from Seasonally Flooded Soils: A Laboratory Microcosm Study. J. Environ. Qual. 30:91-101.

Young, E.O., D.S. Ross, C. Alves, T. Villars. 2012. J. Soil Water Conserv. 67(1):1-7.

APPENDICES

Table 4.1: Nitrate-N loads exported from each treatment during four runoff events.

Event	TD g ha^{-1}	UD g ha^{-1}
6/11/2014	688.6	546.7
8/13/2014	477.2	111.5
12/25/2014	3190.3	1252.7
5/31/2015	501.7	29.3

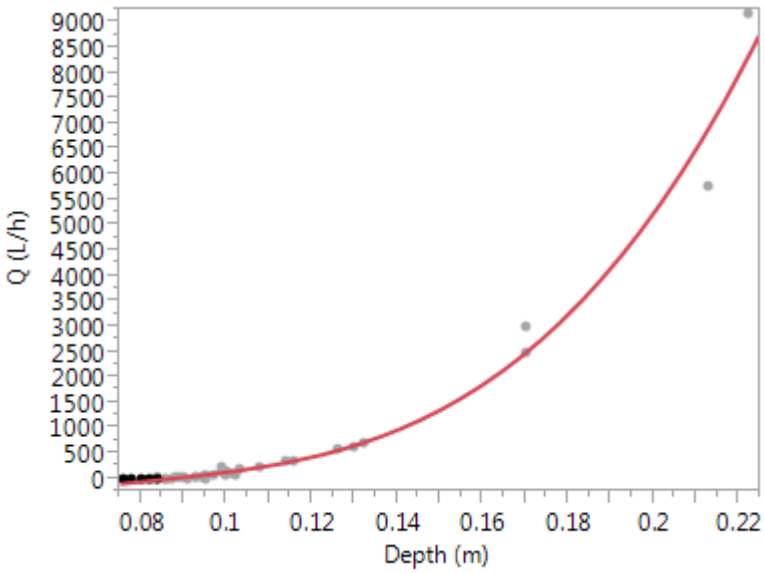

Summary of Fit

RSquare	0.979
RSquare Adj	0.977
Root Mean Square Error	265.29
Mean of Response	631.54
Observations (or Sum Wgts)	39

Figure 4.1: Rating curve developed in the field for Plot 2 surface flow bucket. Flow (L/h) = -1179.754 + 13110.917*Depth + 188035.1*(Depth - 0.10615)^2 + 2618310.9*(Depth - 0.10615)^3

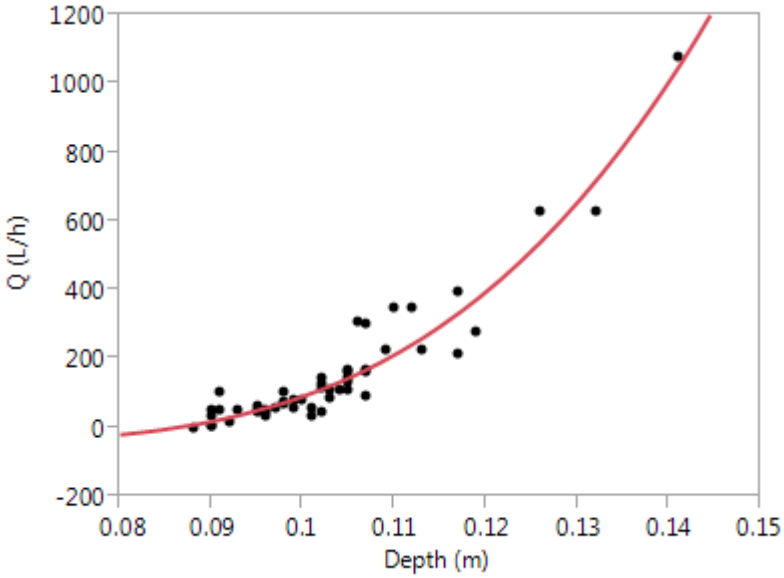

Summary of Fit

RSquare	0.920
RSquare Adj	0.915
Root Mean Square Error	52.89
Mean of Response	147.68
Observations (or Sum Wgts)	58

Figure 4.2: Rating curve developed in the field for Plot 3 surface flow bucket. Flow (L/h) = -977.828 + 10684.031*Depth + 258932.18*(Depth - 0.10245)^2 + 2368245.2*(Depth - 0.10245)^3

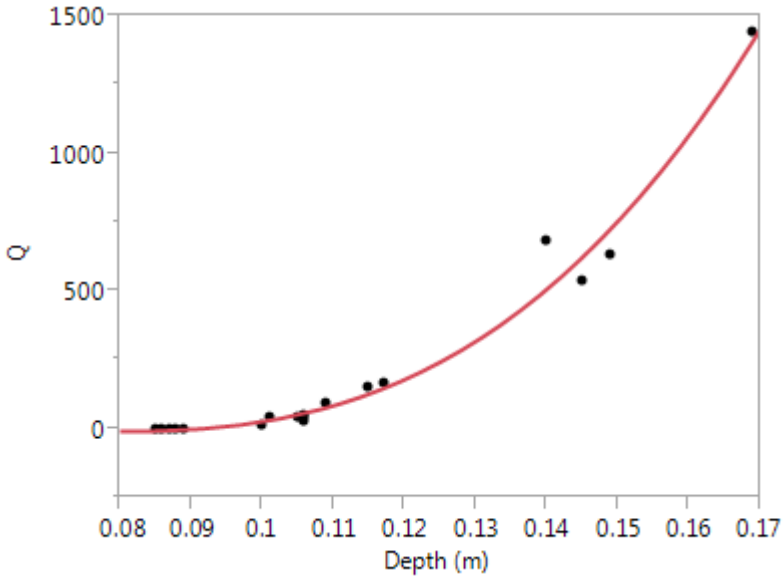

Summary of Fit

RSquare	0.979
RSquare Adj	0.975
Root Mean Square Error	58.73
Mean of Response	206.14
Observations (or Sum Wgts)	19

Figure 4.3: Rating curve developed in the field for Plot 4 surface flow bucket. Flow (L/h) = -774.6562 + 7816.3228*Depth + 186538.03*(Depth - 0.11068)^2 + 1179312.4*(Depth - 0.11068)^3

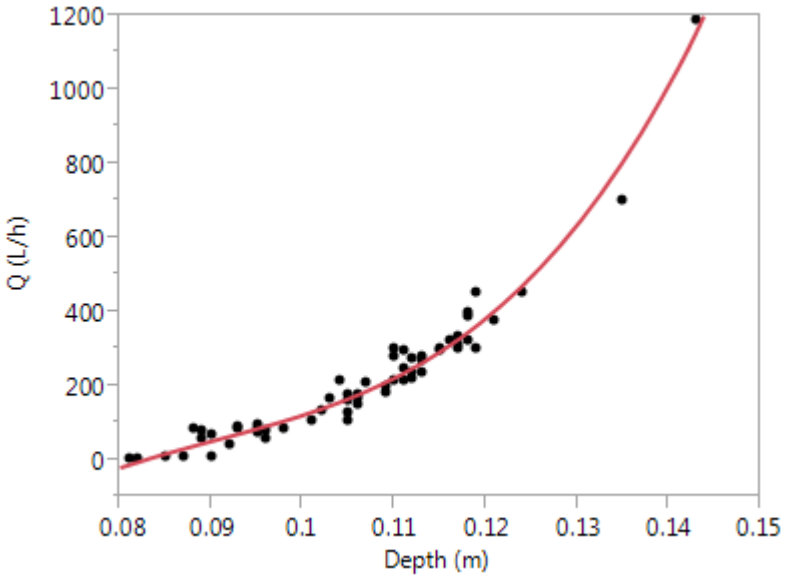

Summary of Fit

RSquare	0.977
RSquare Adj	0.976
Root Mean Square Error	34.282
Mean of Response	217.156
Observations (or Sum Wgts)	65

Figure 4.4: Rating curve developed in the field for Plot 4 tile flow bucket. Flow (L/h) = -888.0222 + 10038.702*Depth + 231885.28*(Depth - 0.10525)^2 + 5207383.1*(Depth - 0.10525)^3

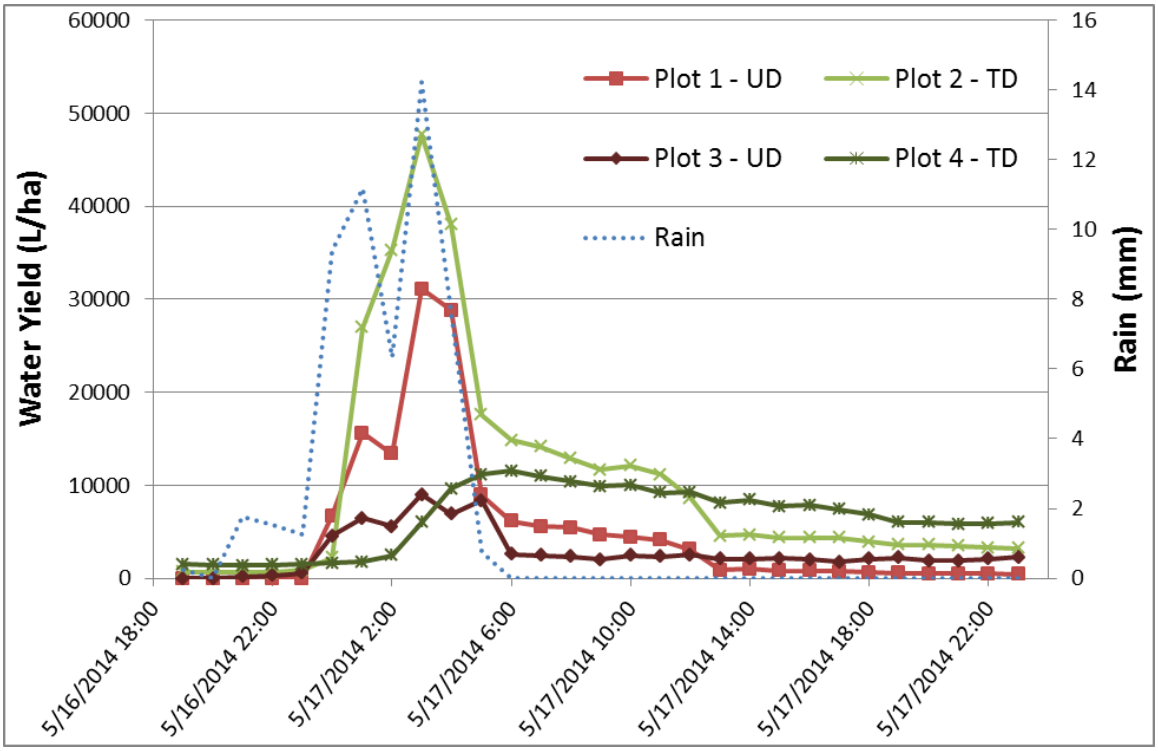

Figure 4.5: Total water yield by plot for the 5/16/14 rain event.

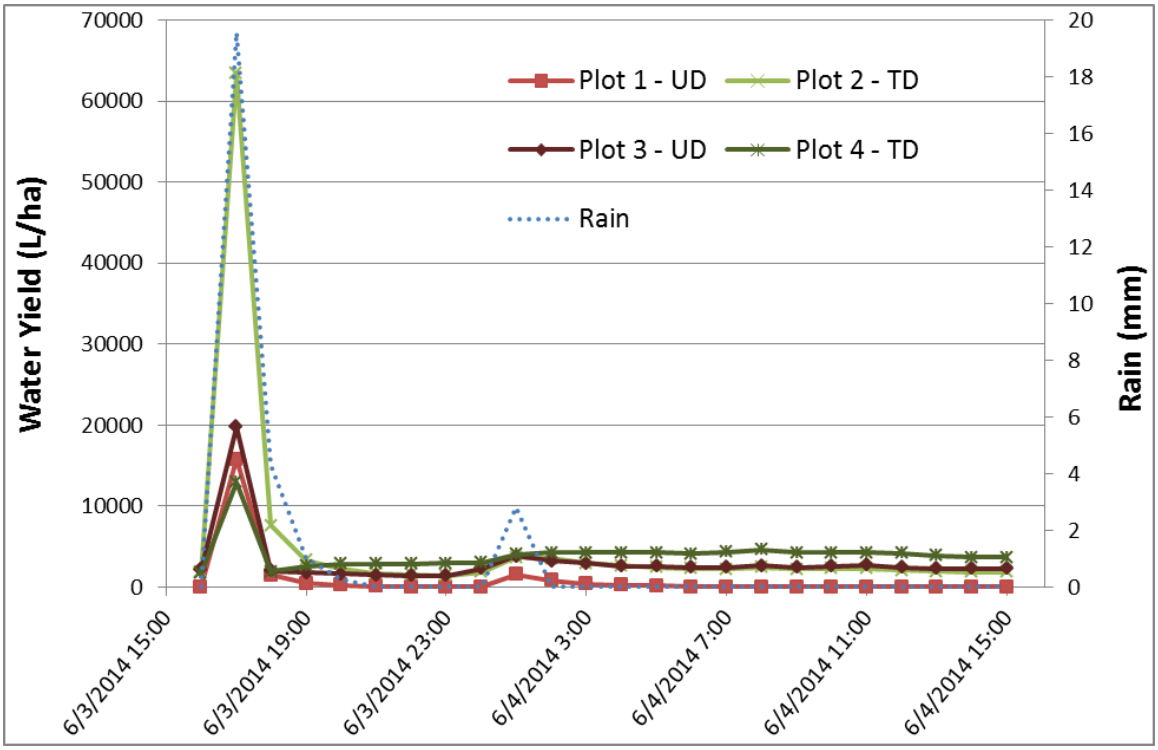

Figure 4.6: Total water yield by plot for the 6/3/14 rain event.

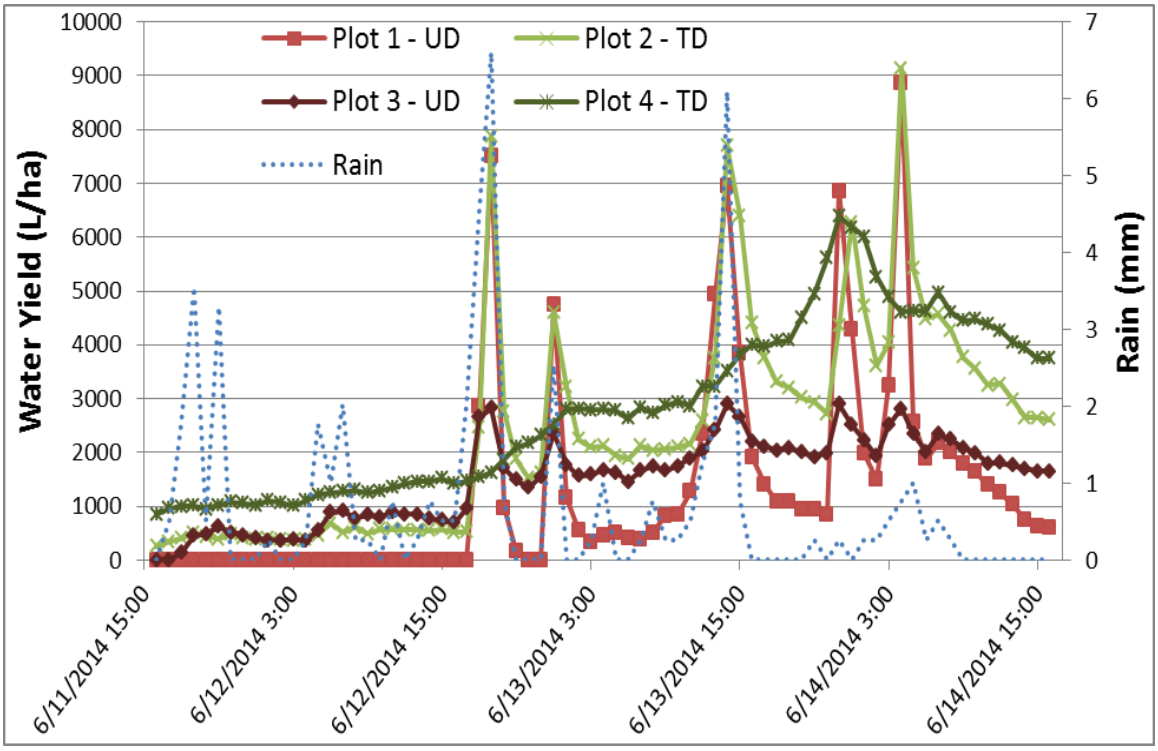

Figure 4.7: Total water yield by plot for the 6/11/14 rain event.

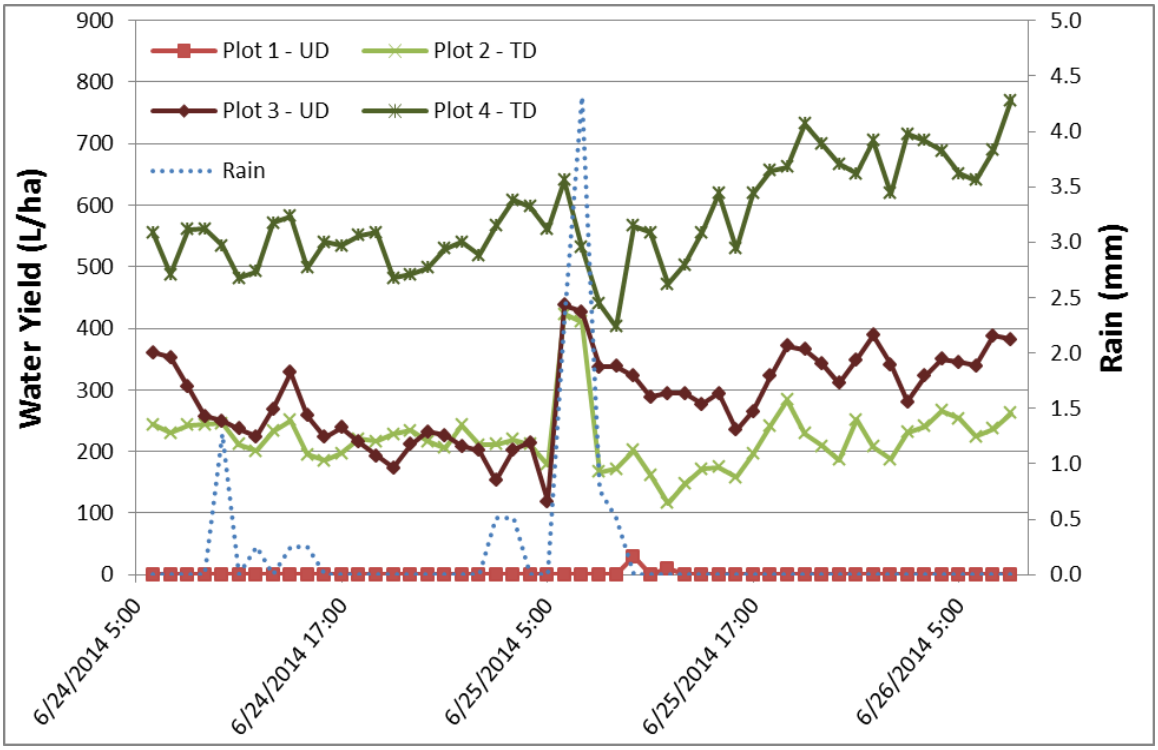

Figure 4.8: Total water yield by plot for the 6/24/14 rain event.

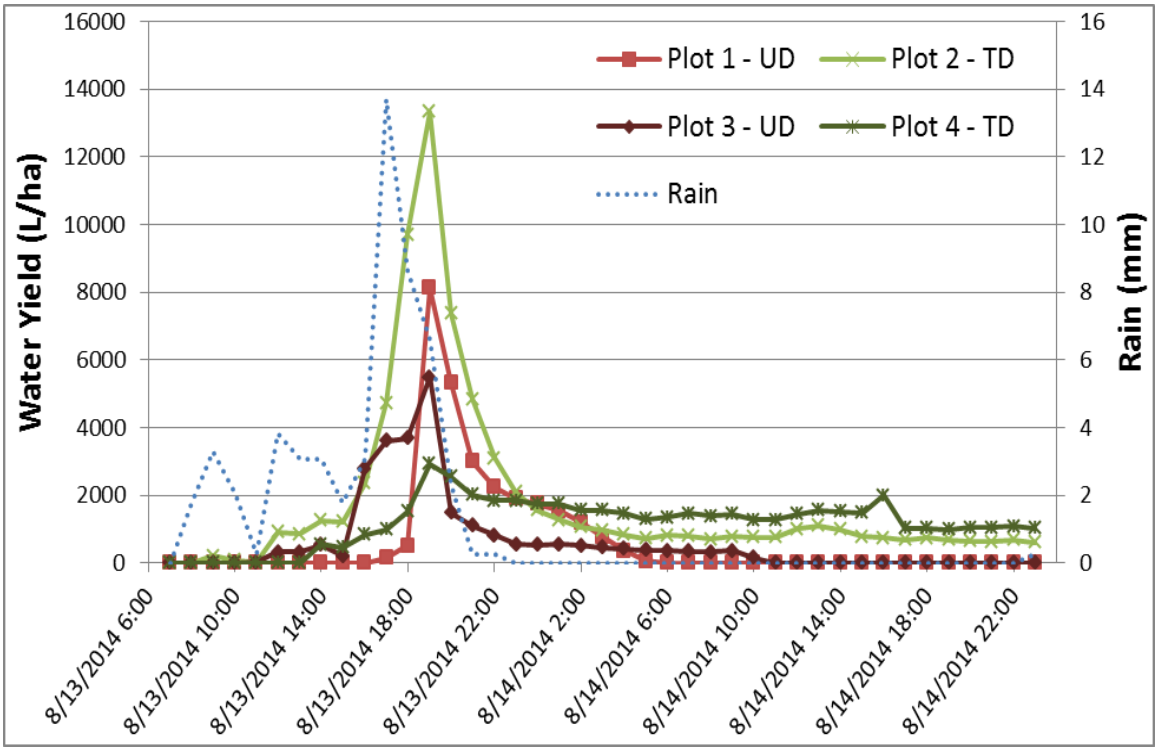

Figure 4.9: Total water yield by plot for the 8/13/14 rain event.

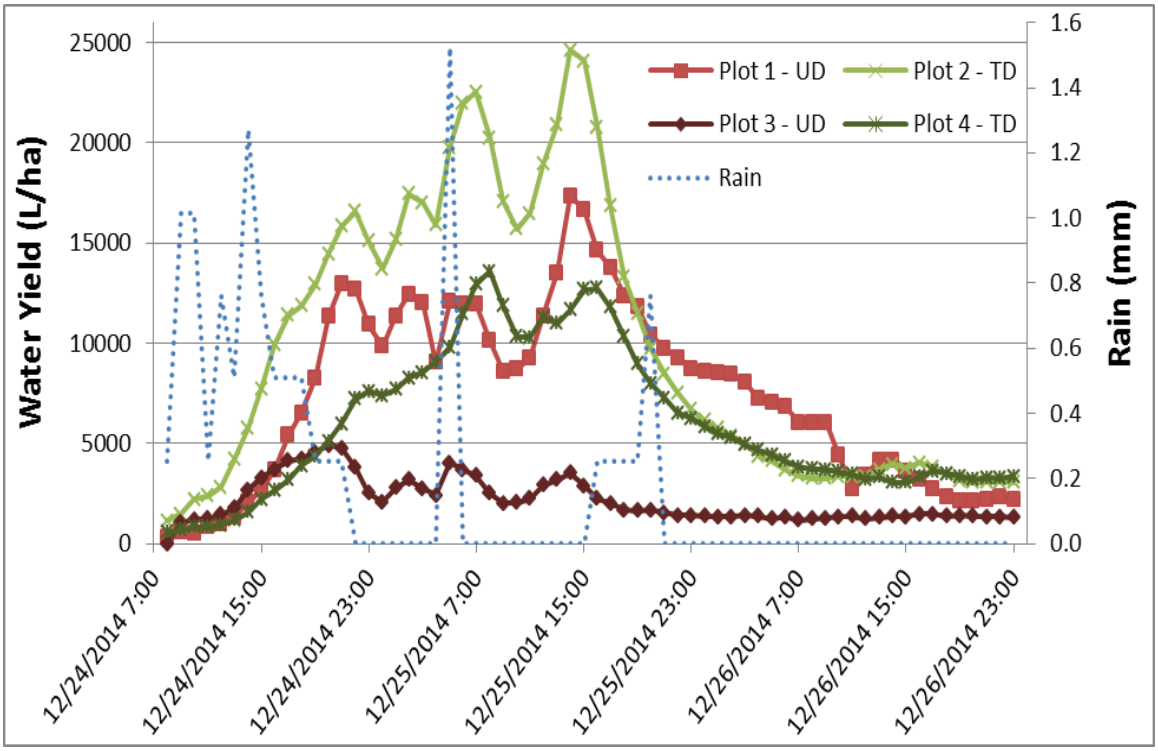

Figure 4.10: Total water yield by plot for the 12/25/14 rain event.

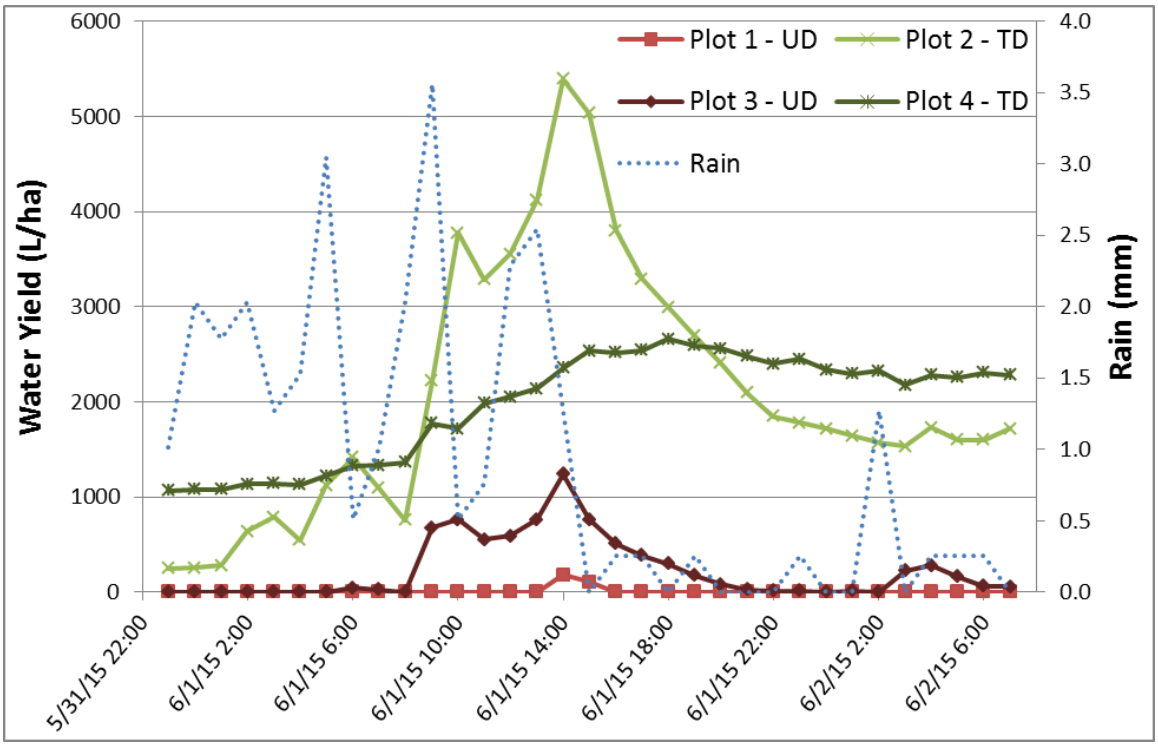

Figure 4.11: Total water yield by plot for the 5/31/15 rain event.

Table 4.2: Daily rainfall totals 5/30/15-6/30/15.

Date	Rain (mm)
5/30/2015	27.94
5/31/2015	2.29
6/1/2015	27.94
6/2/2015	2.29
6/3/2015	0.00
6/4/2015	0.00
6/5/2015	4.57
6/6/2015	0.25
6/7/2015	0.00
6/8/2015	7.62
6/9/2015	16.51
6/10/2015	9.40
6/11/2015	0.00
6/12/2015	19.56
6/13/2015	3.30
6/14/2015	0.00
6/15/2015	0.76
6/16/2015	10.67
6/17/2015	0.00
6/18/2015	10.67
6/19/2015	0.00
6/20/2015	0.00
6/21/2015	15.24
6/22/2015	19.30
6/23/2015	5.33
6/24/2015	3.56
6/25/2015	0.00
6/26/2015	0.00
6/27/2015	0.00
6/28/2015	19.30
6/29/2015	1.27
6/30/2015	1.52

Table 4.3: Water table elevation (m) at each well in plots 1 (UD) and 2 (TD) during June 2015.

	Well										
Date/Time	A	B	C	D	E	F	G	H	I	J	K
6/2/15 09:00	28.97	28.92	29.18	29.20	29.53	29.30	29.55	29.87	29.57	30.02	.
6/2/15 17:00	29.17	29.17	29.43	29.37	29.55	29.52	29.62	29.84	29.65	30.02	.
6/4/15 12:00	29.43	29.42	29.51	29.49	29.39	29.50	29.43	29.68	29.84	29.90	29.71
6/8/15 13:30	29.27	29.22	29.25	29.28	29.32	29.29	29.27	29.61	29.44	29.83	29.65
6/9/15 11:00	29.27	29.22	29.28	29.30	29.34	29.31	29.28	29.63	29.44	29.84	29.64
6/10/15 07:45	29.61	29.63	29.76	29.69	29.54	29.67	29.54	29.90	29.65	30.05	29.71
6/10/15 16:00	29.68	29.62	29.66	29.71	29.62	29.65	29.65	29.84	29.67	30.05	29.73
6/11/15 11:00	29.70	29.62	29.70	29.72	29.60	29.68	29.66	29.79	29.71	30.02	29.74
6/12/15 17:30	29.52	29.48	29.55	29.55	29.53	29.55	29.55	29.72	29.59	29.96	29.72
6/13/15 12:00	29.77	29.73	29.88	29.78	29.71	29.77	29.74	29.92	29.84	30.09	29.80
6/15/15 09:00	29.44	29.45	29.47	29.55	29.54	29.49	29.47	29.69	29.63	29.92	29.73
6/17/15 10:00	29.42	29.43	29.53	29.63	29.52	29.56	29.56	29.68	29.59	29.62	29.69
6/19/15 09:30	29.35	29.38	29.44	29.55	29.53	29.48	29.54	29.70	29.55	29.95	29.66
6/22/15 10:00	29.57	29.62	29.78	29.67	29.74	29.74	29.67	29.92	29.86	30.09	29.75
6/22/15 17:00	29.63	29.62	29.68	29.73	29.72	29.68	29.70	29.86	29.83	30.12	29.78
6/23/15 14:30	29.60	29.68	29.79	29.76	29.68	29.73	29.66	29.89	29.80	30.08	29.76
6/24/15 14:00	29.49	29.48	29.53	29.58	29.64	29.55	29.57	29.73	29.69	29.95	29.73
6/29/15 11:00	29.41	29.51	29.72	29.57	29.70	29.59	29.55	29.79	29.70	29.98	29.69

Table 4.4: Water table elevation (m) at each well in plots 3 (UD) and 4 (TD) during June 2015.

	Well										
Date/Time	A	B	C	D	E	F	G	H	I	J	K
6/2/15 09:00	29.82	29.80	29.98	30.05	30.03	30.03	29.87	29.95	29.94	29.90	.
6/2/15 17:00	29.79	29.77	29.85	29.98	29.93	29.94	29.95	29.94	29.93	29.89	.
6/4/15 12:00	29.70	29.66	29.72	29.75	29.81	29.85	29.78	29.87	29.87	29.80	.
6/8/15 13:30	29.70	29.66	29.72	29.75	29.78	29.82	29.75	29.84	29.85	29.74	.
6/9/15 11:00	29.70	29.66	29.72	29.76	29.76	29.82	29.77	29.84	29.85	29.75	.
6/10/15 07:45	29.84	29.83	29.92	30.00	29.95	29.94	29.88	29.95	29.95	29.90	.
6/10/15 16:00	29.79	29.77	29.84	29.90	29.93	29.92	29.90	29.95	29.94	29.90	.
6/11/15 11:00	29.76	29.73	29.80	29.86	29.90	29.91	29.89	29.93	29.94	29.89	.
6/12/15 17:30	29.73	29.71	29.78	29.81	29.83	29.90	29.85	29.88	29.88	29.86	.
6/13/15 12:00	29.83	29.81	29.90	29.98	30.01	30.05	29.97	29.98	29.98	29.96	.
6/15/15 09:00	29.71	29.67	29.72	29.77	29.81	29.87	29.85	29.90	29.91	29.87	.
6/17/15 10:00	29.71	29.68	29.74	29.80	29.83	29.85	29.85	29.90	29.91	29.86	.
6/19/15 09:30	29.71	29.72	29.78	29.84	29.88	29.90	29.88	29.92	29.95	29.88	.
6/22/15 10:00	29.85	29.84	29.94	30.03	30.07	30.07	30.01	30.01	30.02	29.99	.
6/22/15 17:00	29.80	29.77	29.85	29.92	29.96	29.98	29.95	29.99	29.99	29.98	.
6/23/15 14:30	29.81	29.80	29.91	29.99	30.02	30.06	29.97	29.97	29.99	29.96	.
6/24/15 14:00	29.72	29.69	29.74	29.80	29.82	29.84	29.86	29.92	29.96	29.90	.
6/29/15 11:00	29.78	29.76	29.87	29.88	29.92	29.86	29.93	29.95	29.95	29.92	.

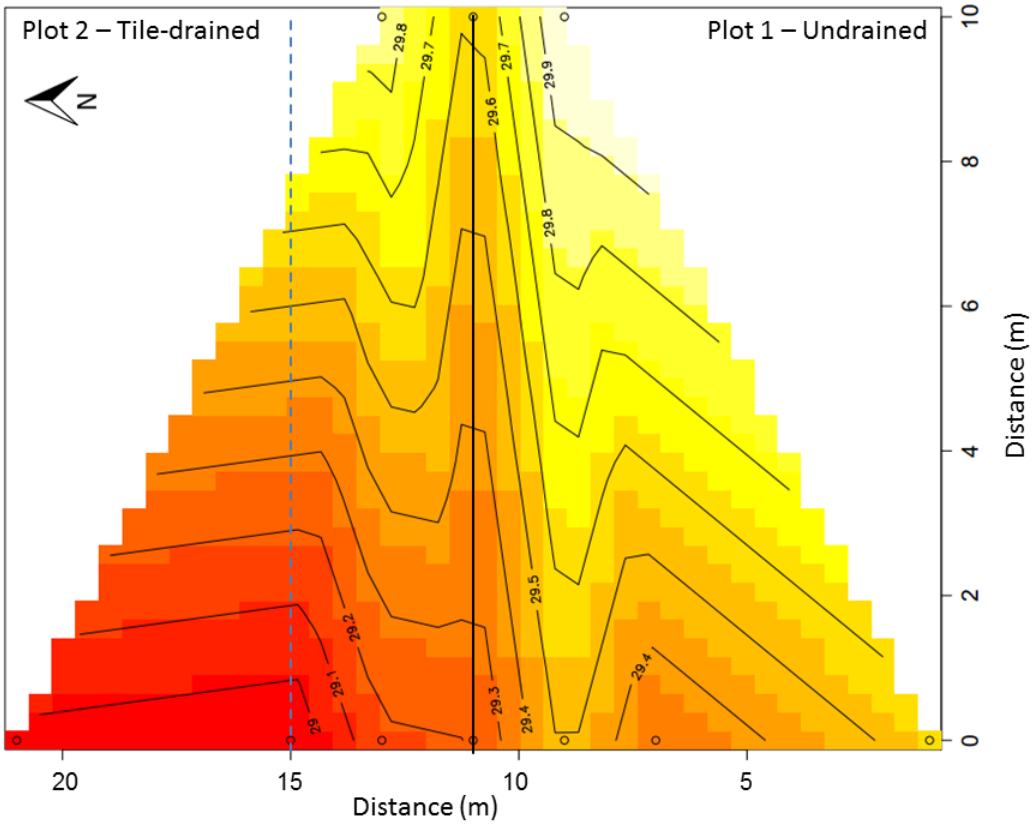

Figure 4.12: Water table contour map for plots 1 and 2 on 6/2/15 (09:00). X and Y axes represent distance (m), central vertical black line indicates the plot boundary, dotted blue vertical line indicates the outer tile line, and small circles indicate well locations.

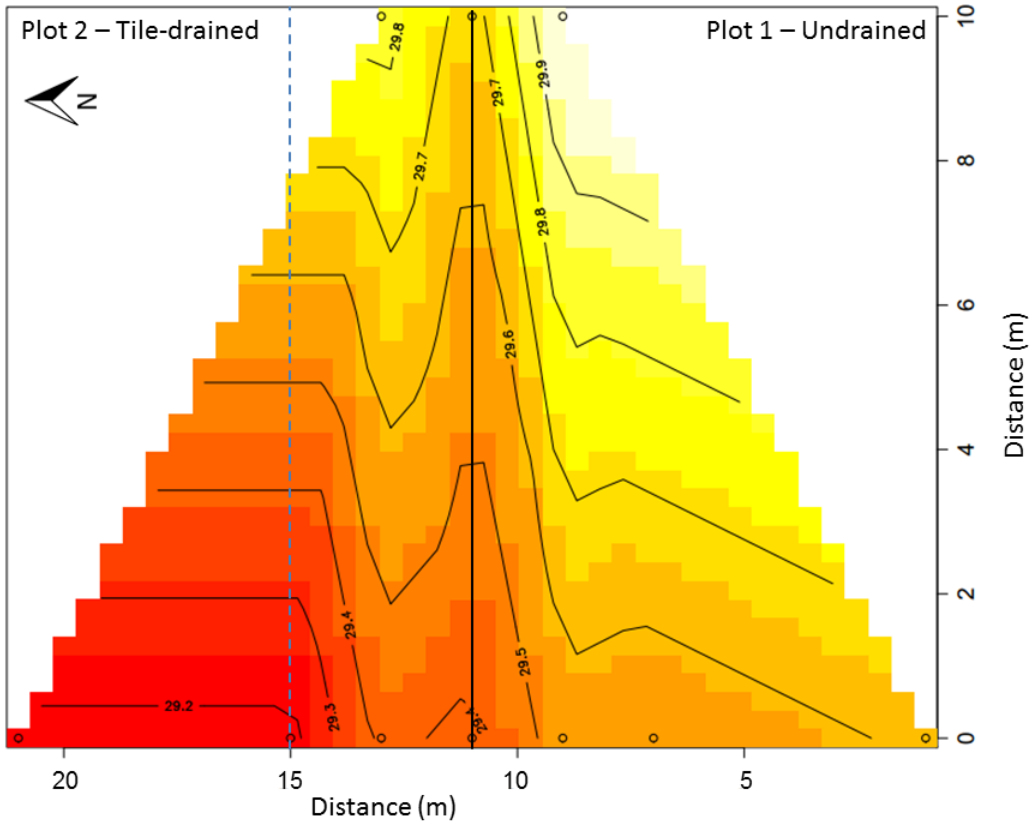

Figure 4.13: Water table contour map for plots 1 and 2 on 6/2/15 (17:00). X and Y axes represent distance (m), central vertical black line indicates the plot boundary, dotted blue vertical line indicates the outer tile line, and small circles indicate well locations.

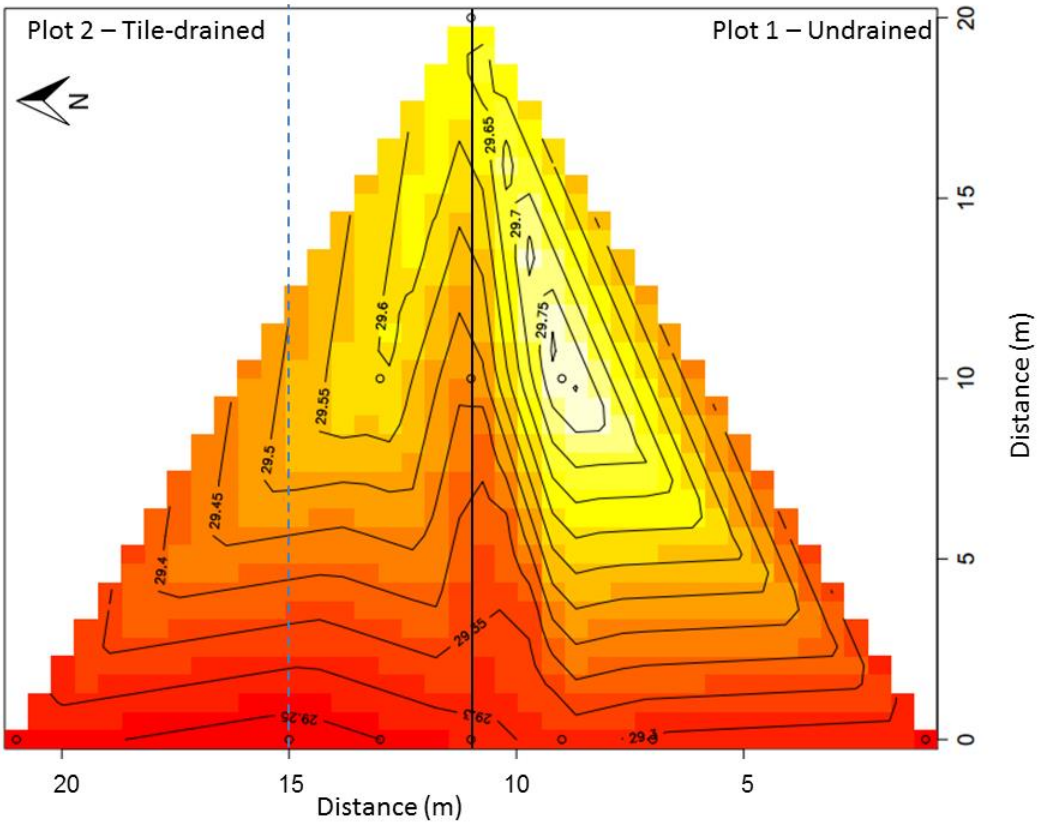

Figure 4.14: Water table contour map for plots 1 and 2 on 6/8/15. X and Y axes represent distance (m), central vertical black line indicates the plot boundary, dotted blue vertical line indicates the outer tile line, and small circles indicate well locations.

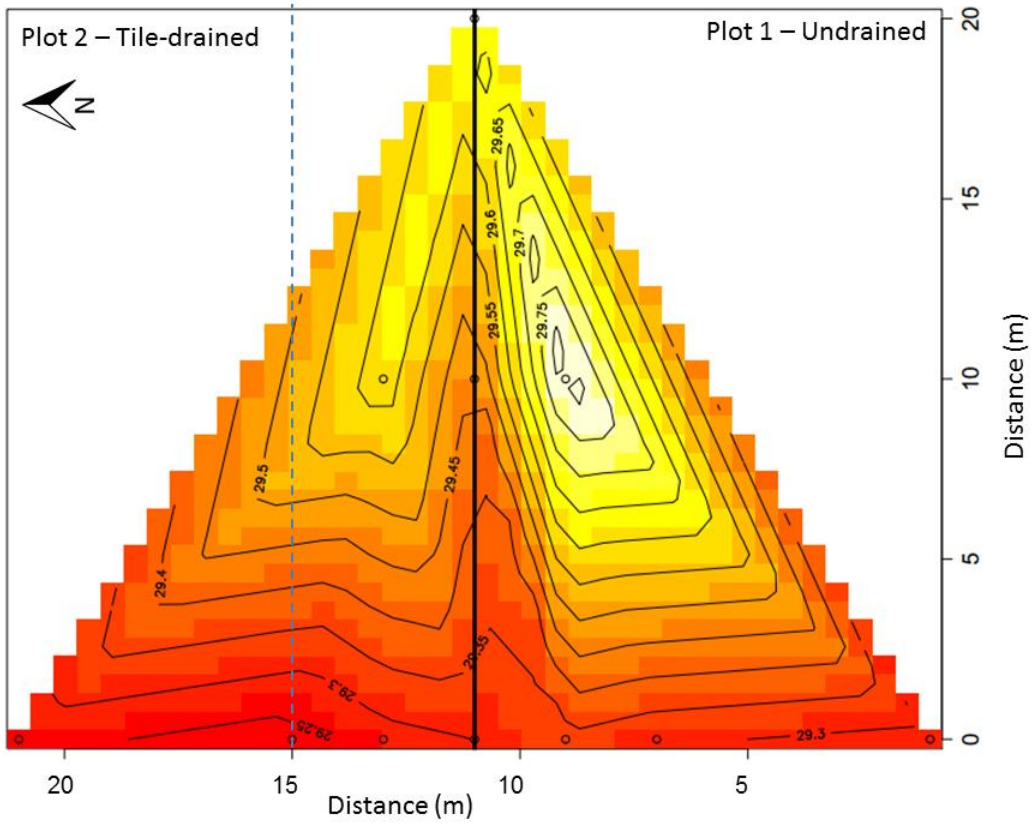

Figure 4.15: Water table contour map for plots 1 and 2 on 6/9/15. X and Y axes represent distance (m), central vertical black line indicates the plot boundary, dotted blue vertical line indicates the outer tile line, and small circles indicate well locations.

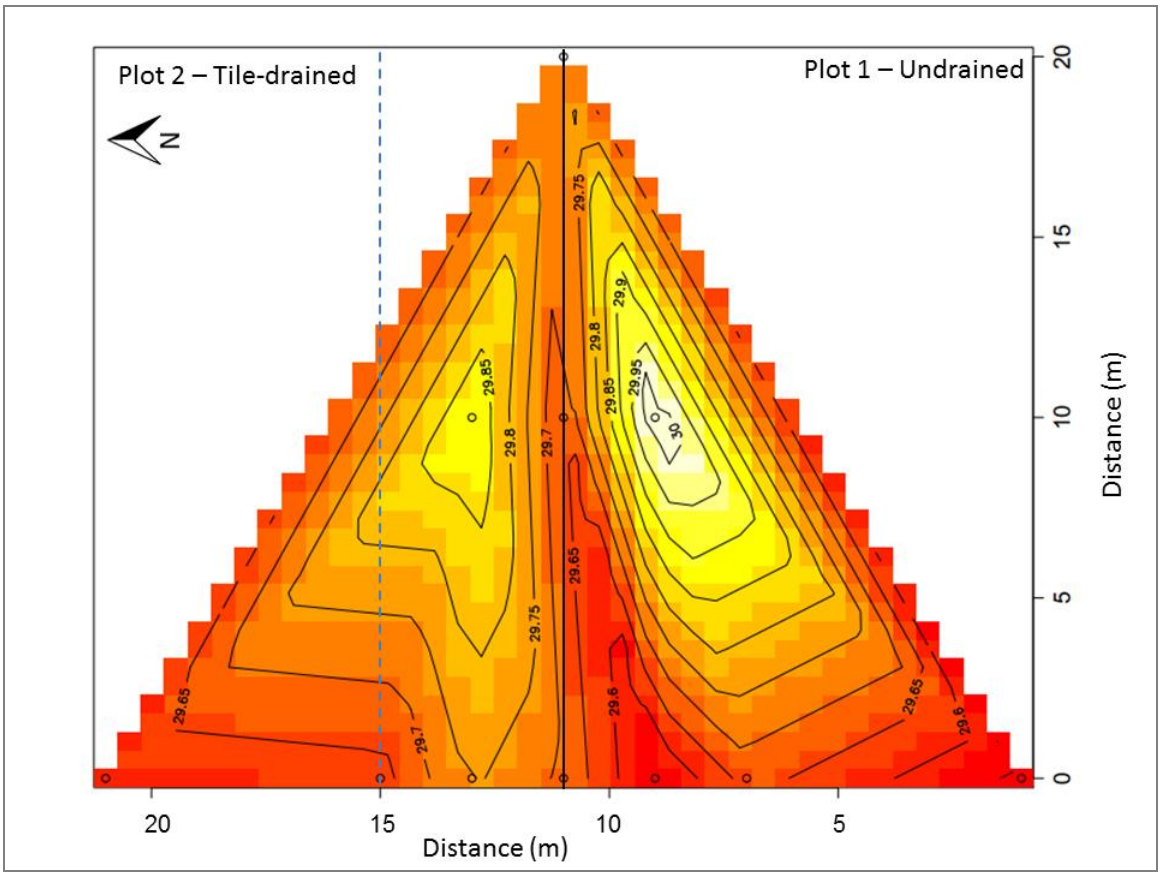

Figure 4.16: Water table contour map for plots 1 and 2 on 6/10/15 (07:45). X and Y axes represent distance (m), central vertical black line indicates the plot boundary, dotted blue vertical line indicates the outer tile line, and small circles indicate well locations.

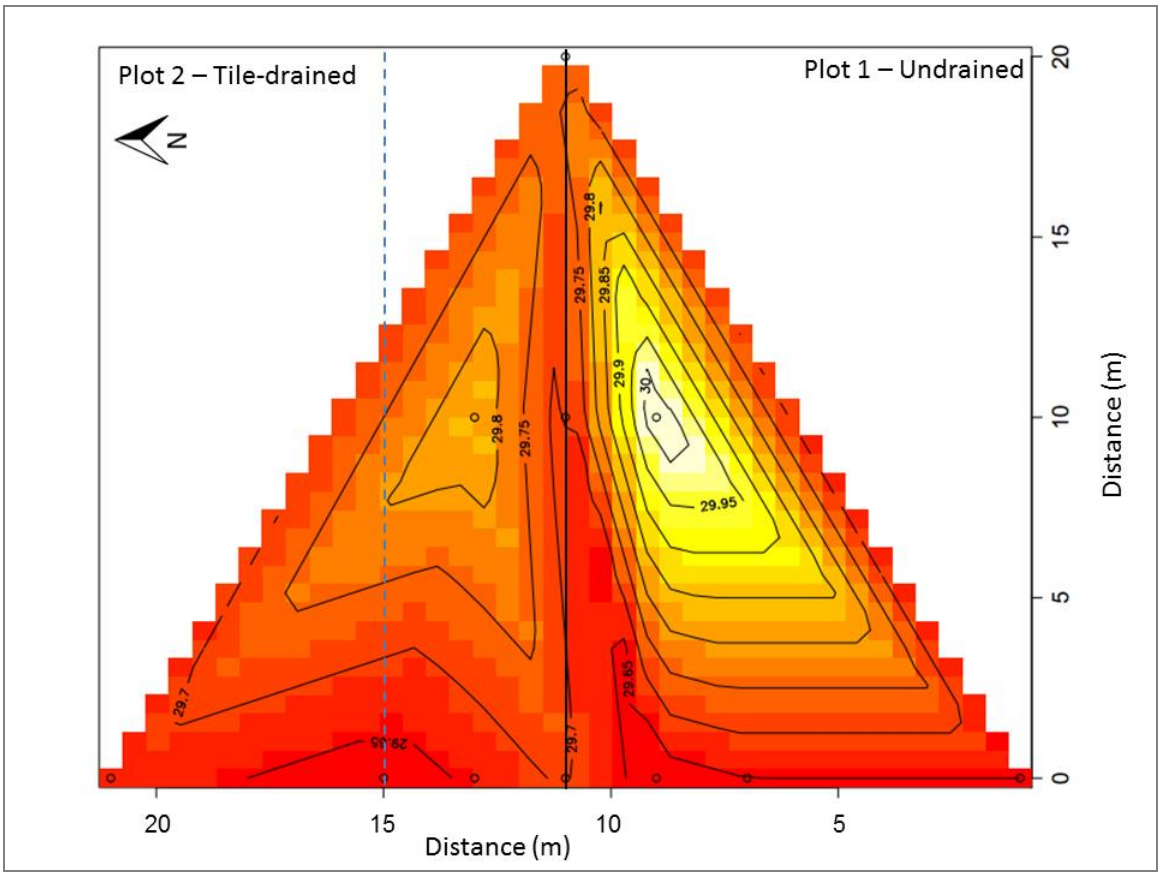

Figure 4.17: Water table contour map for plots 1 and 2 on 6/10/15 (16:00). X and Y axes represent distance (m), central vertical black line indicates the plot boundary, dotted blue vertical line indicates the outer tile line, and small circles indicate well locations.

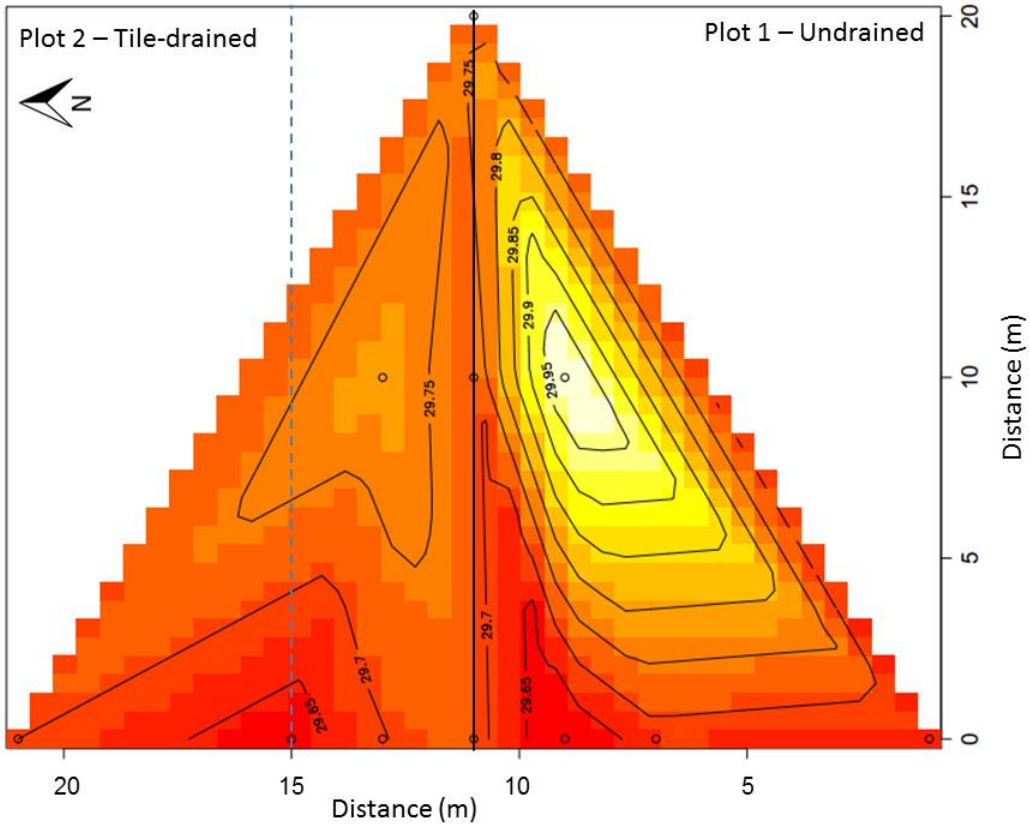

Figure 4.18: Water table contour map for plots 1 and 2 on 6/11/15. X and Y axes represent distance (m), central vertical black line indicates the plot boundary, dotted blue vertical line indicates the outer tile line, and small circles indicate well locations.

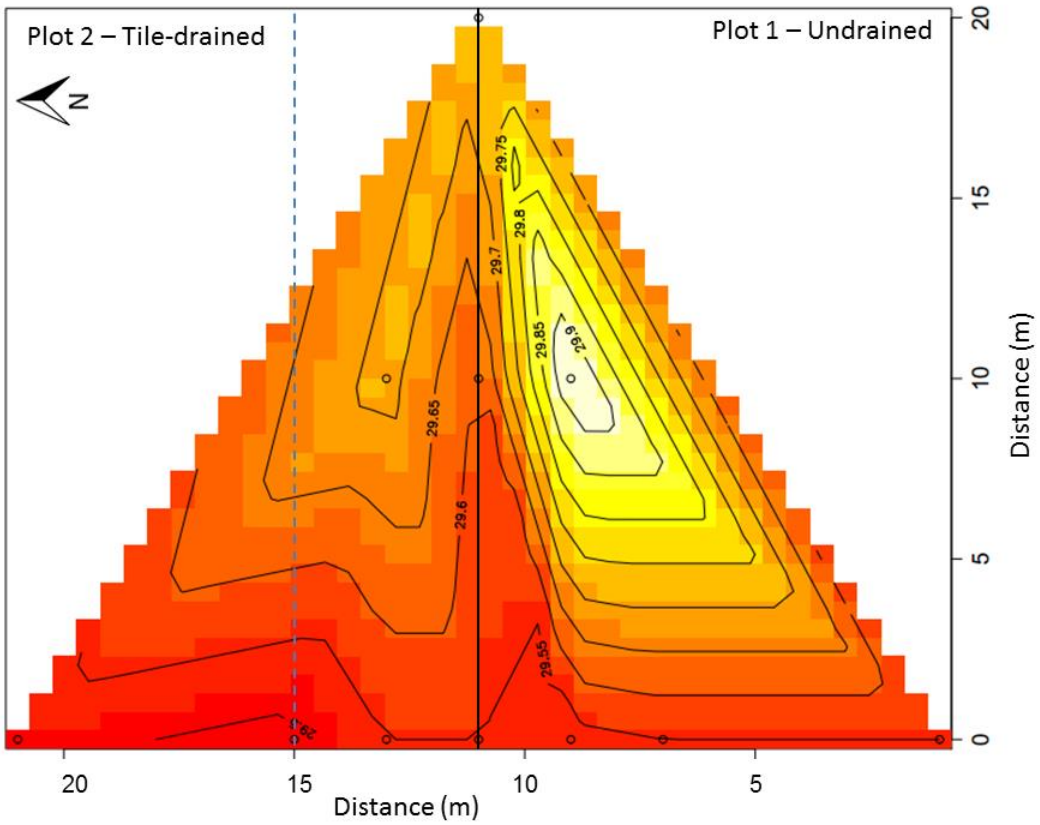

Figure 4.19: Water table contour map for plots 1 and 2 on 6/12/15. X and Y axes represent distance (m), central vertical black line indicates the plot boundary, dotted blue vertical line indicates the outer tile line, and small circles indicate well locations.

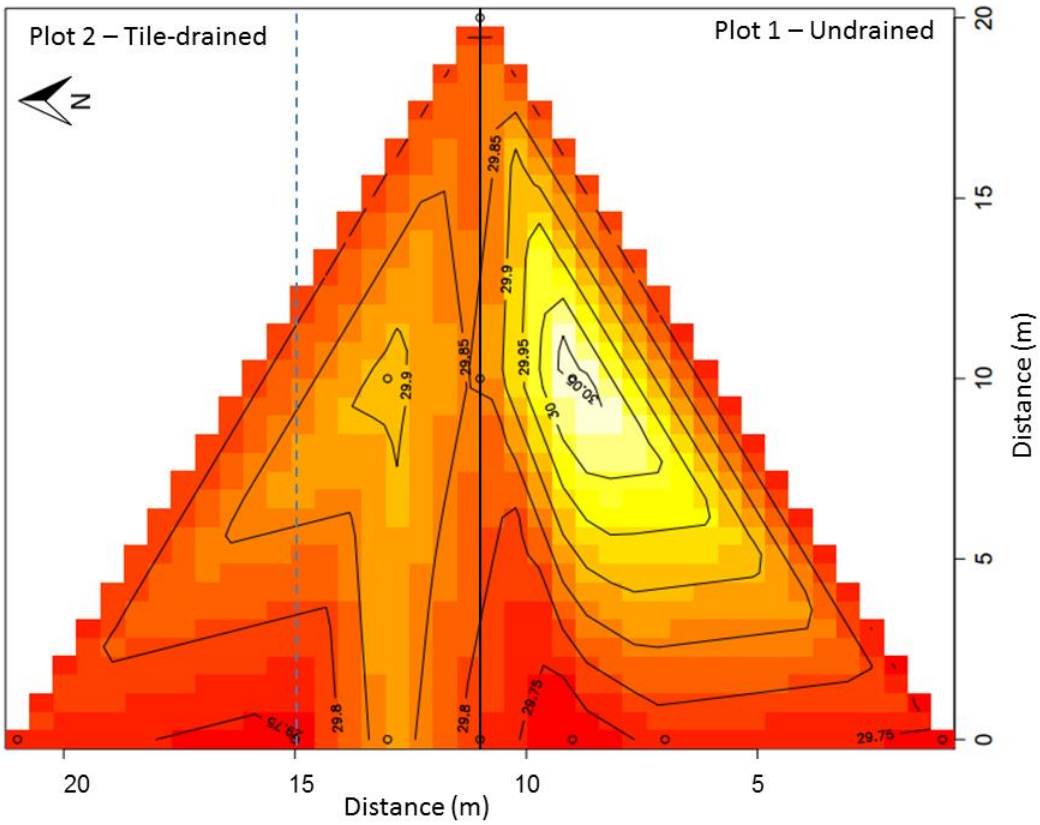

Figure 4.20: Water table contour map for plots 1 and 2 on 6/13/15. X and Y axes represent distance (m), central vertical black line indicates the plot boundary, dotted blue vertical line indicates the outer tile line, and small circles indicate well locations.

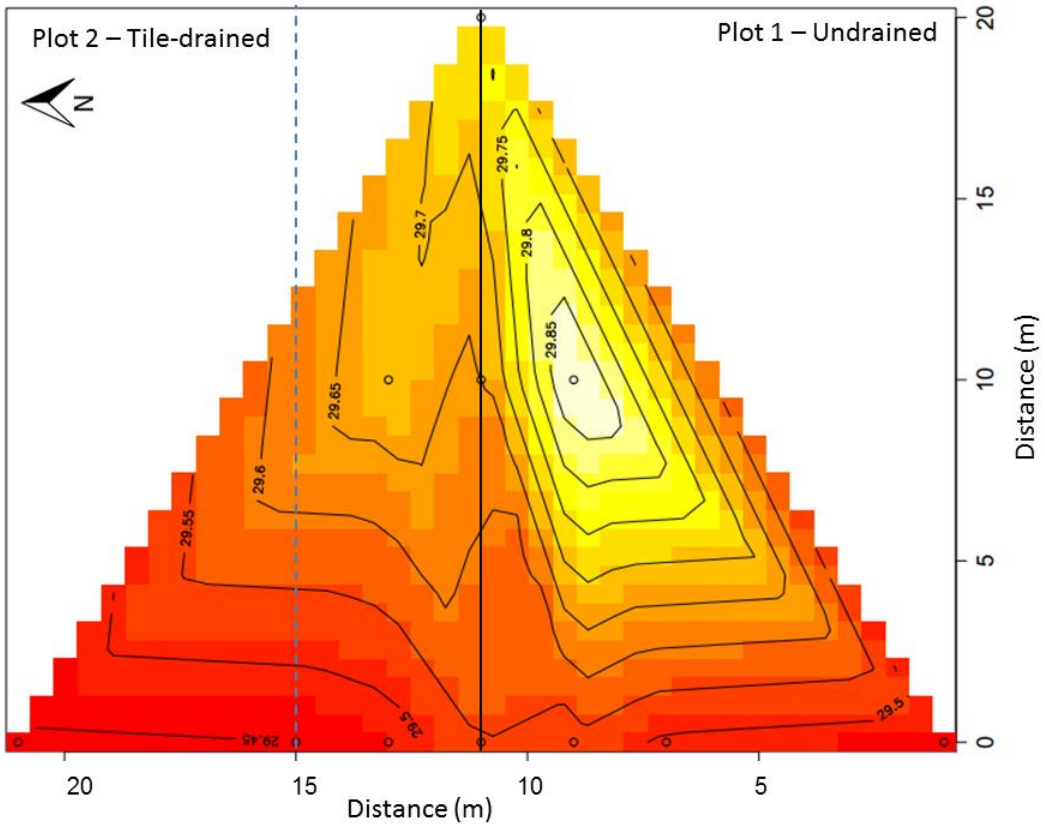

Figure 4.21: Water table contour map for plots 1 and 2 on 6/15/15. X and Y axes represent distance (m), central vertical black line indicates the plot boundary, dotted blue vertical line indicates the outer tile line, and small circles indicate well locations.

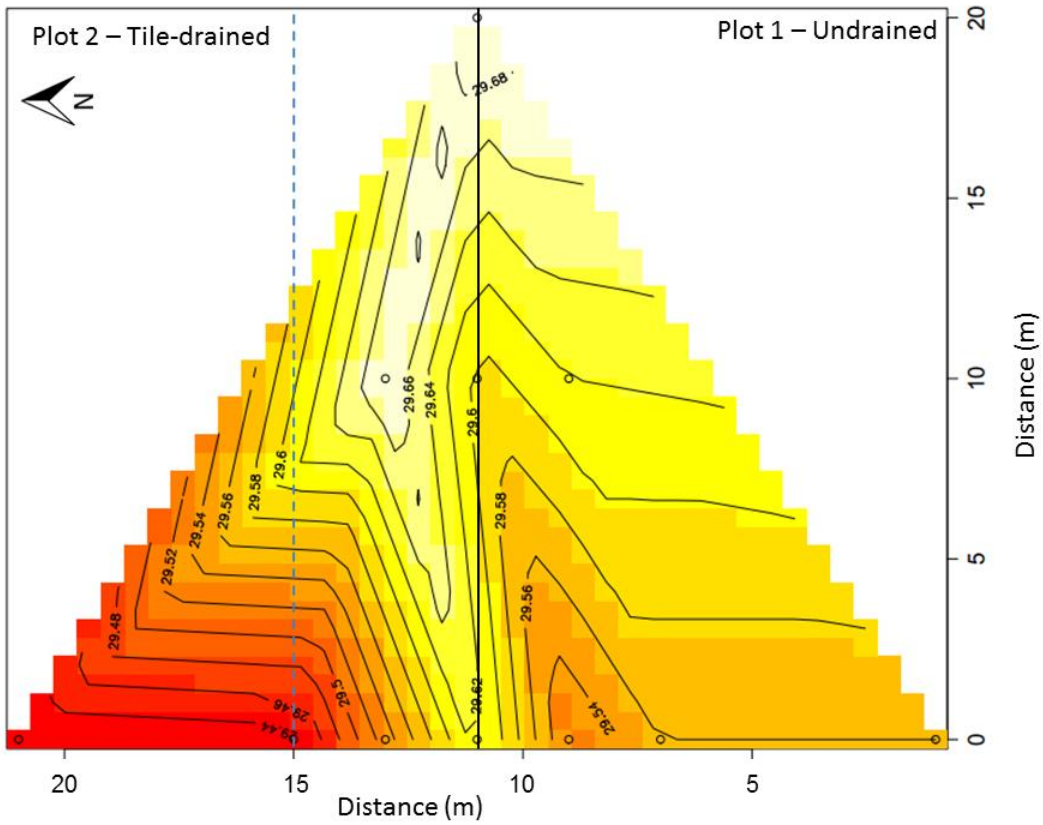

Figure 4.22: Water table contour map for plots 1 and 2 on 6/17/15. X and Y axes represent distance (m), central vertical black line indicates the plot boundary, dotted blue vertical line indicates the outer tile line, and small circles indicate well locations.

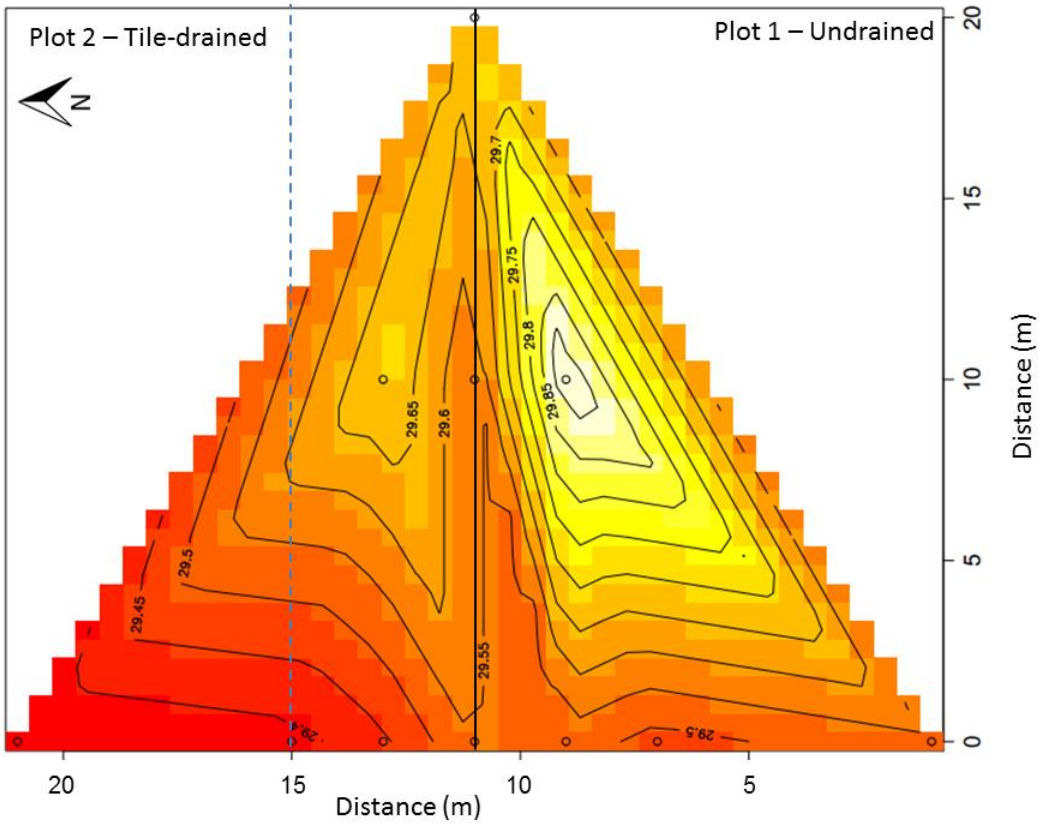

Figure 4.23: Water table contour map for plots 1 and 2 on 6/19/15. X and Y axes represent distance (m), central vertical black line indicates the plot boundary, dotted blue vertical line indicates the outer tile line, and small circles indicate well locations.

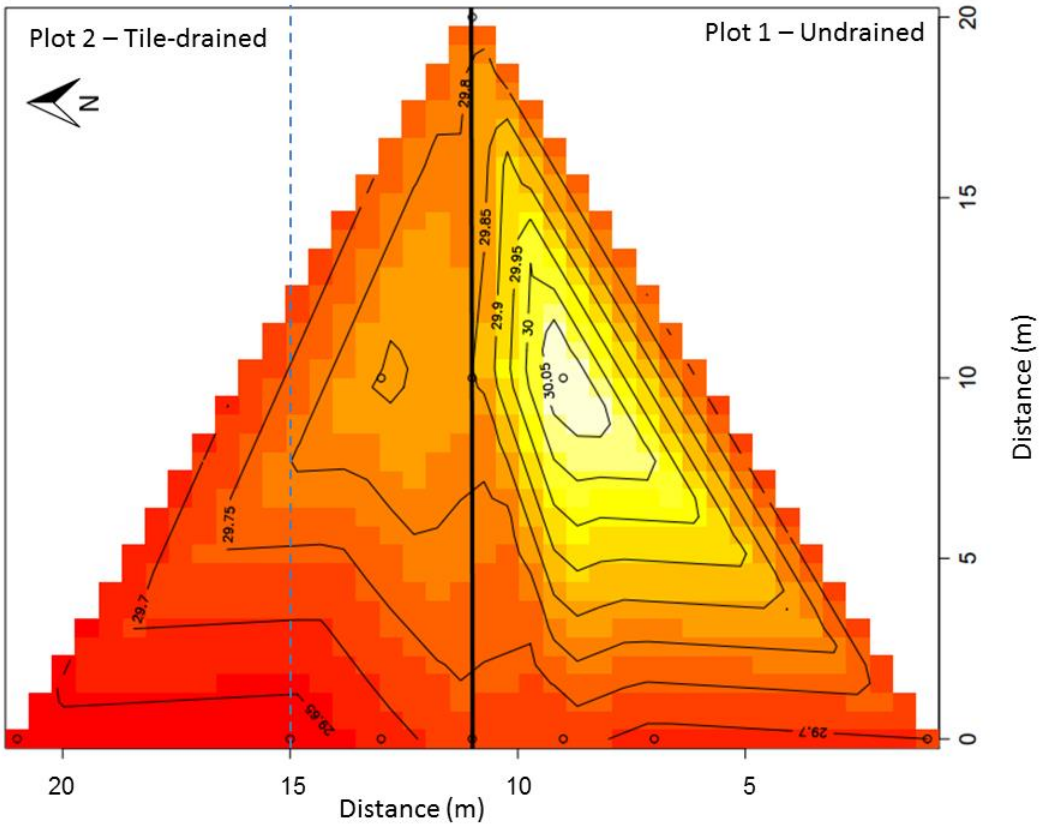

Figure 4.24: Water table contour map for plots 1 and 2 on 6/22/15 (17:00). X and Y axes represent distance (m), central vertical black line indicates the plot boundary, dotted blue vertical line indicates the outer tile line, and small circles indicate well locations.

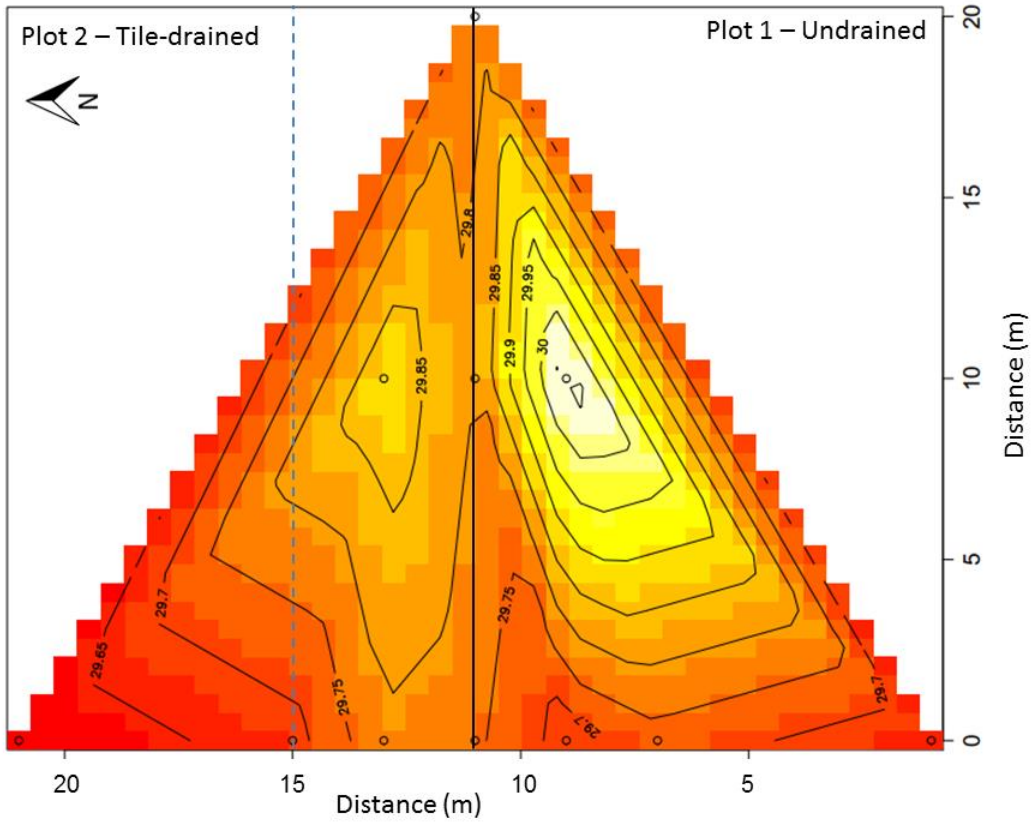

Figure 4.25: Water table contour map for plots 1 and 2 on 6/23/15. X and Y axes represent distance (m), central vertical black line indicates the plot boundary, dotted blue vertical line indicates the outer tile line, and small circles indicate well locations.

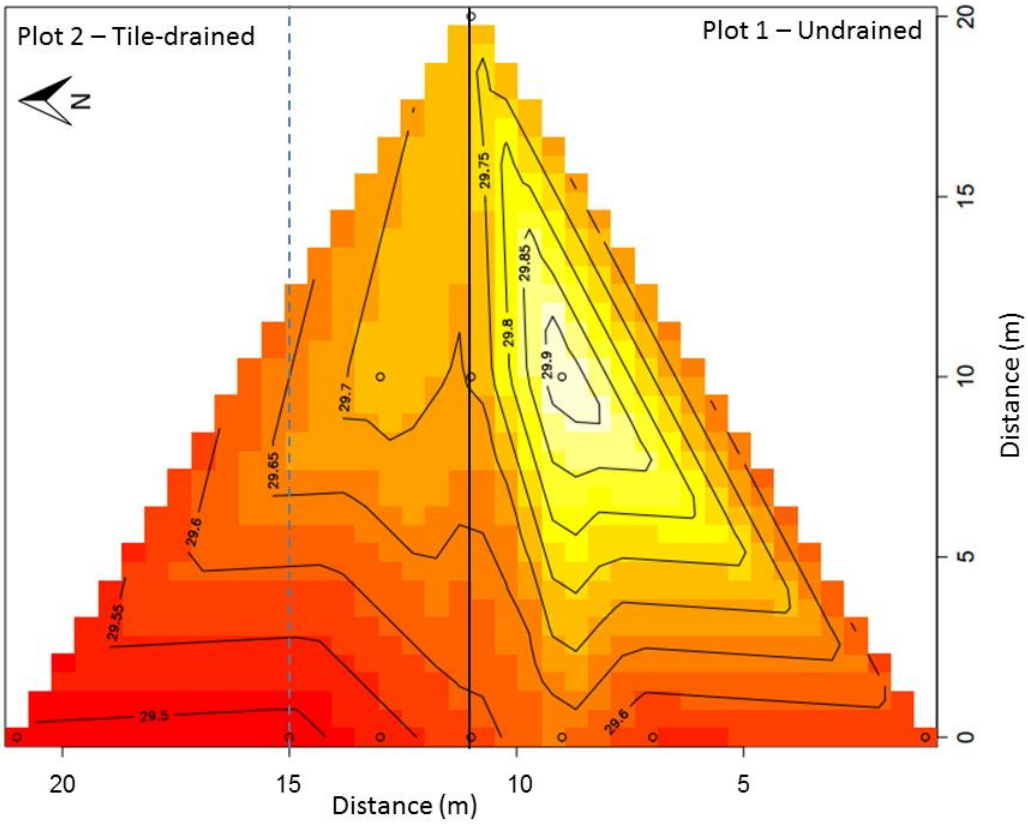

Figure 4.26: Water table contour map for plots 1 and 2 on 6/24/15. X and Y axes represent distance (m), central vertical black line indicates the plot boundary, dotted blue vertical line indicates the outer tile line, and small circles indicate well locations.

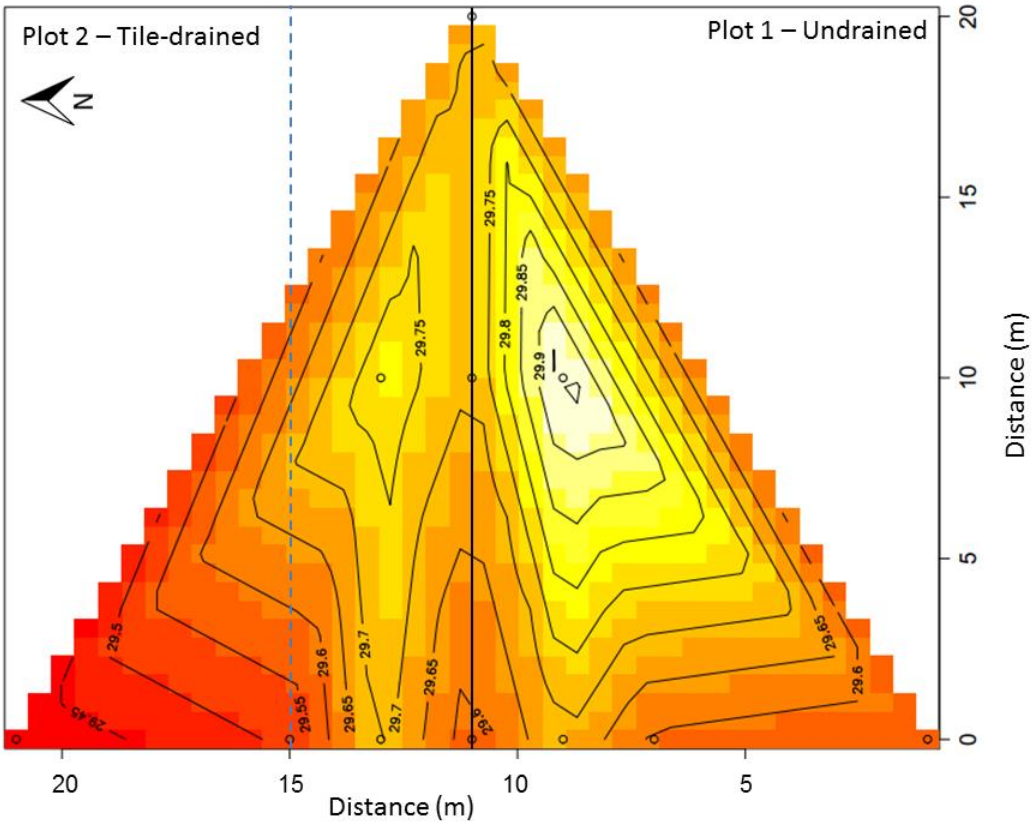

Figure 4.27: Water table contour map for plots 1 and 2 on 6/29/15. X and Y axes represent distance (m), central vertical black line indicates the plot boundary, dotted blue vertical line indicates the outer tile line, and small circles indicate well locations.

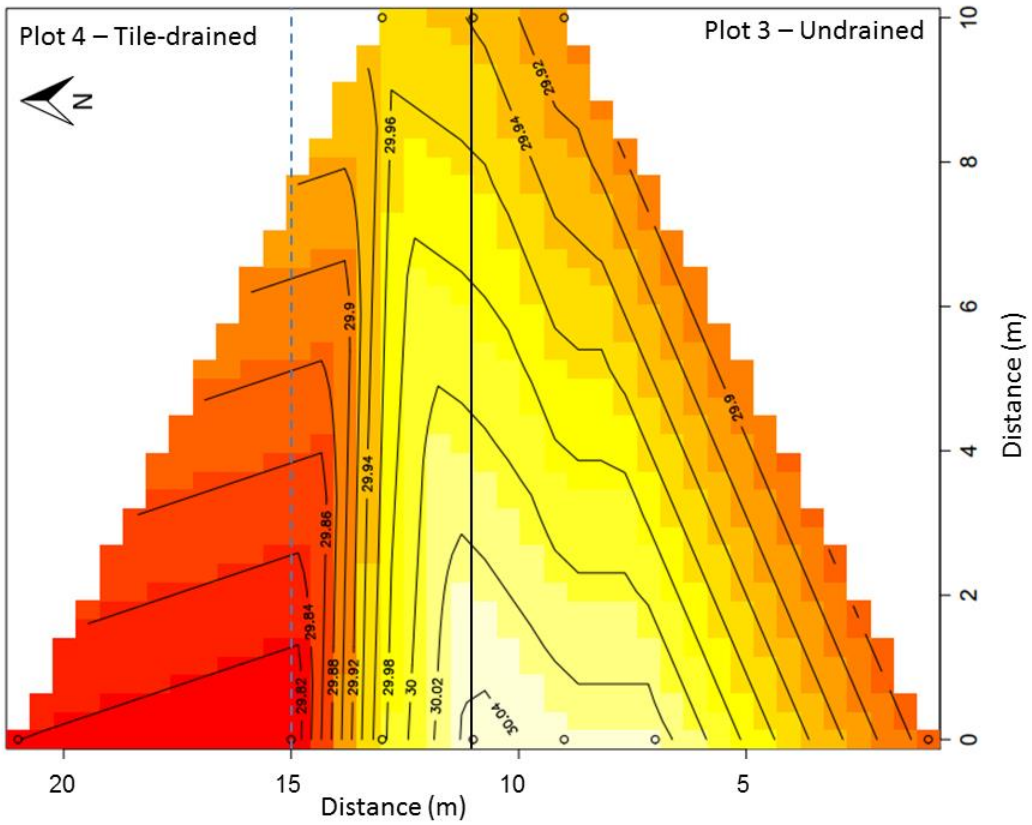

Figure 4.28: Water table contour map for plots 3 and 4 on 6/2/15 (09:00). X and Y axes represent distance (m), central vertical black line indicates the plot boundary, dotted blue vertical line indicates the outer tile line, and small circles indicate well locations.

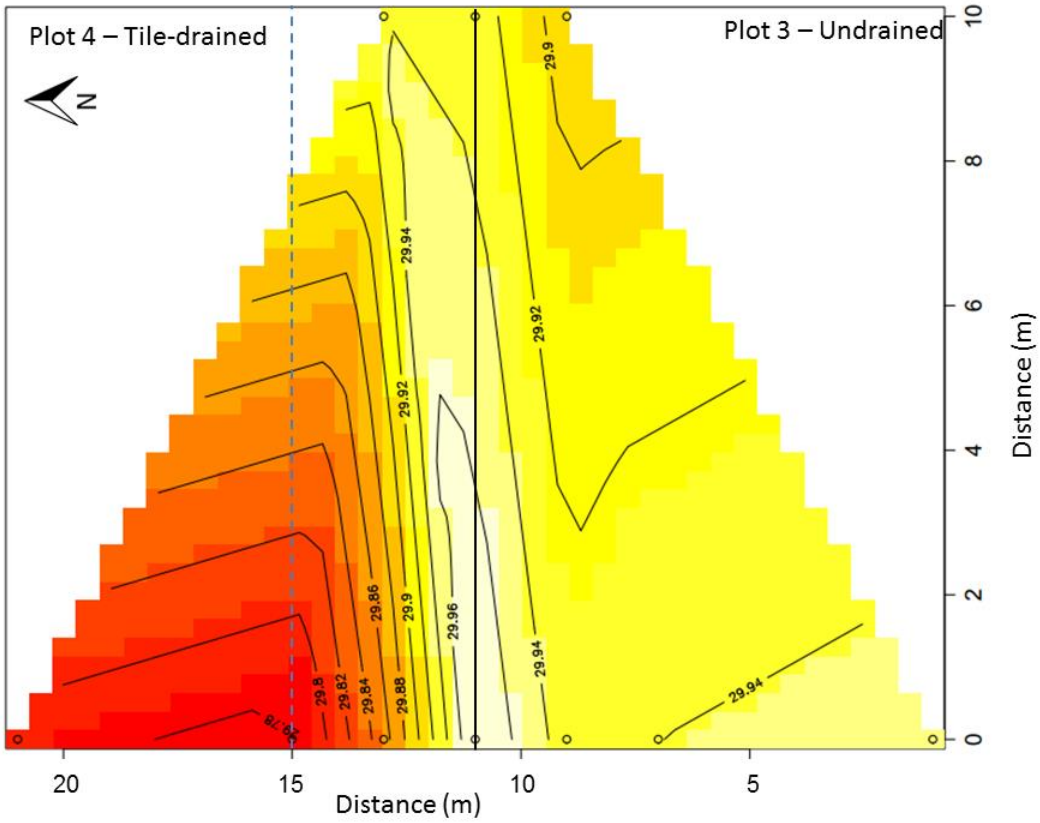

Figure 4.29: Water table contour map for plots 3 and 4 on 6/2/15 (17:00). X and Y axes represent distance (m), central vertical black line indicates the plot boundary, dotted blue vertical line indicates the outer tile line, and small circles indicate well locations.

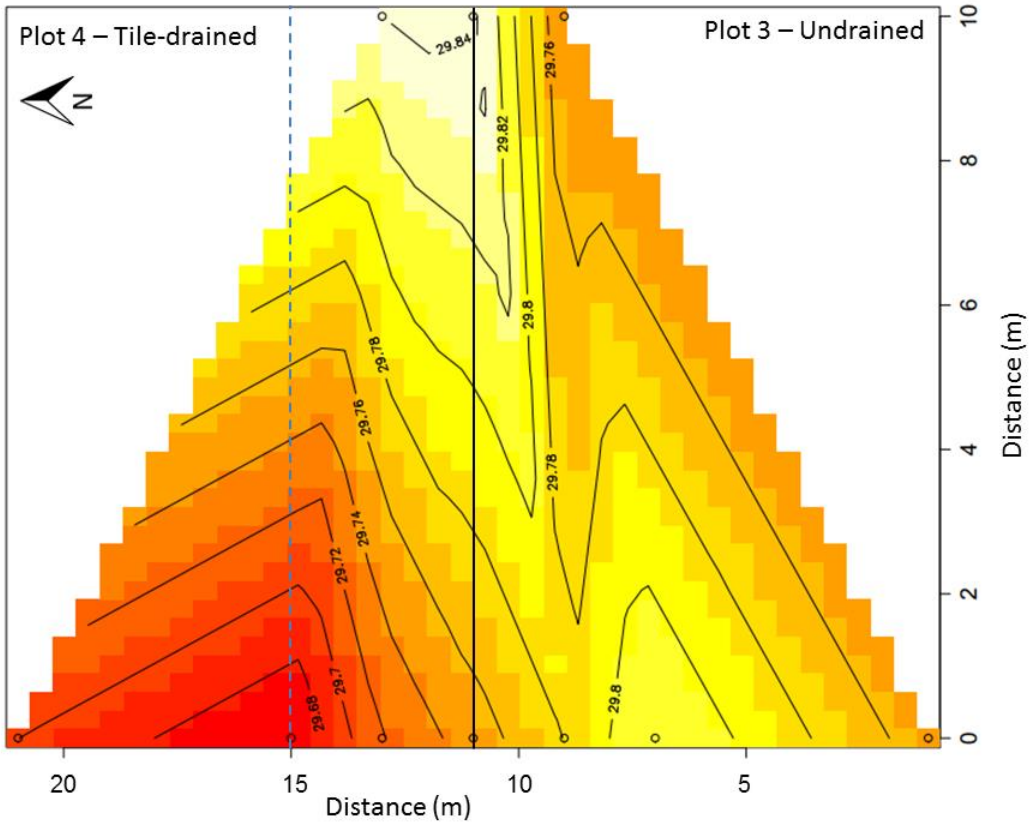

Figure 4.30: Water table contour map for plots 3 and 4 on 6/8/15. X and Y axes represent distance (m), central vertical black line indicates the plot boundary, dotted blue vertical line indicates the outer tile line, and small circles indicate well locations.

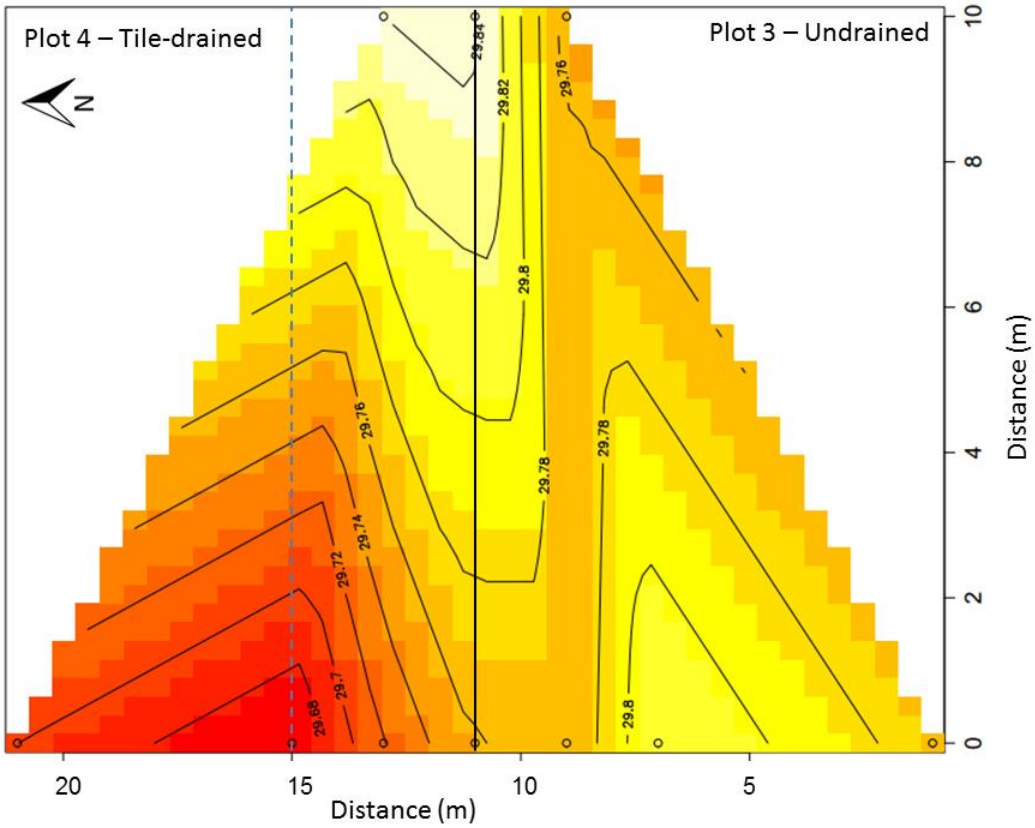

Figure 4.31: Water table contour map for plots 3 and 4 on 6/9/15. X and Y axes represent distance (m), central vertical black line indicates the plot boundary, dotted blue vertical line indicates the outer tile line, and small circles indicate well locations..

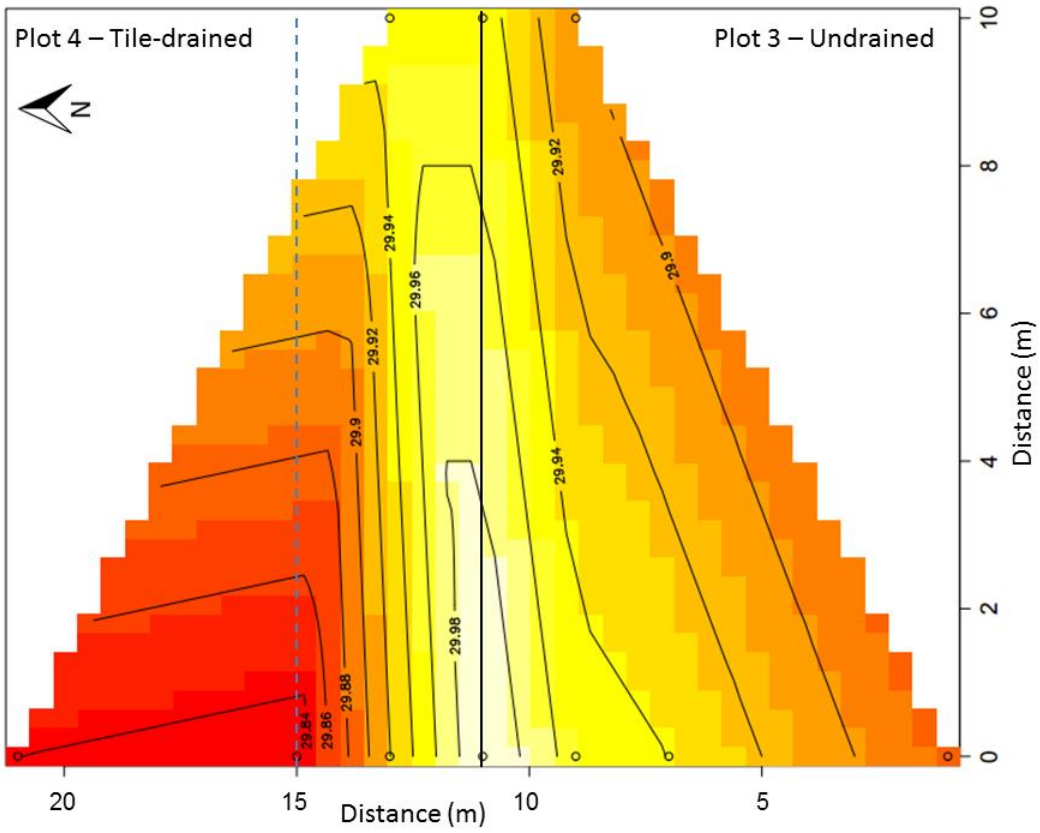

Figure 4.32 Water table contour map for plots 3 and 4 on 6/10/15 (07:45). X and Y axes represent distance (m), central vertical black line indicates the plot boundary, dotted blue vertical line indicates the outer tile line, and small circles indicate well locations.

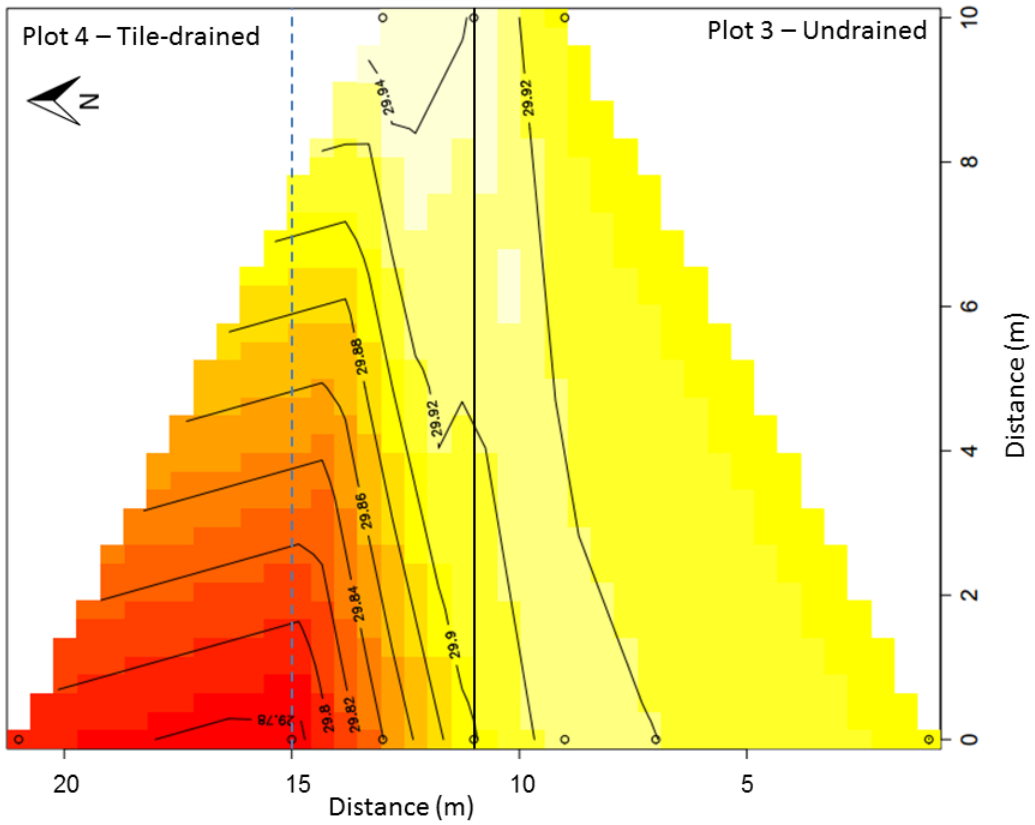

Figure 4.33 Water table contour map for plots 3 and 4 on 6/10/15 (16:00). X and Y axes represent distance (m), central vertical black line indicates the plot boundary, dotted blue vertical line indicates the outer tile line, and small circles indicate well locations.

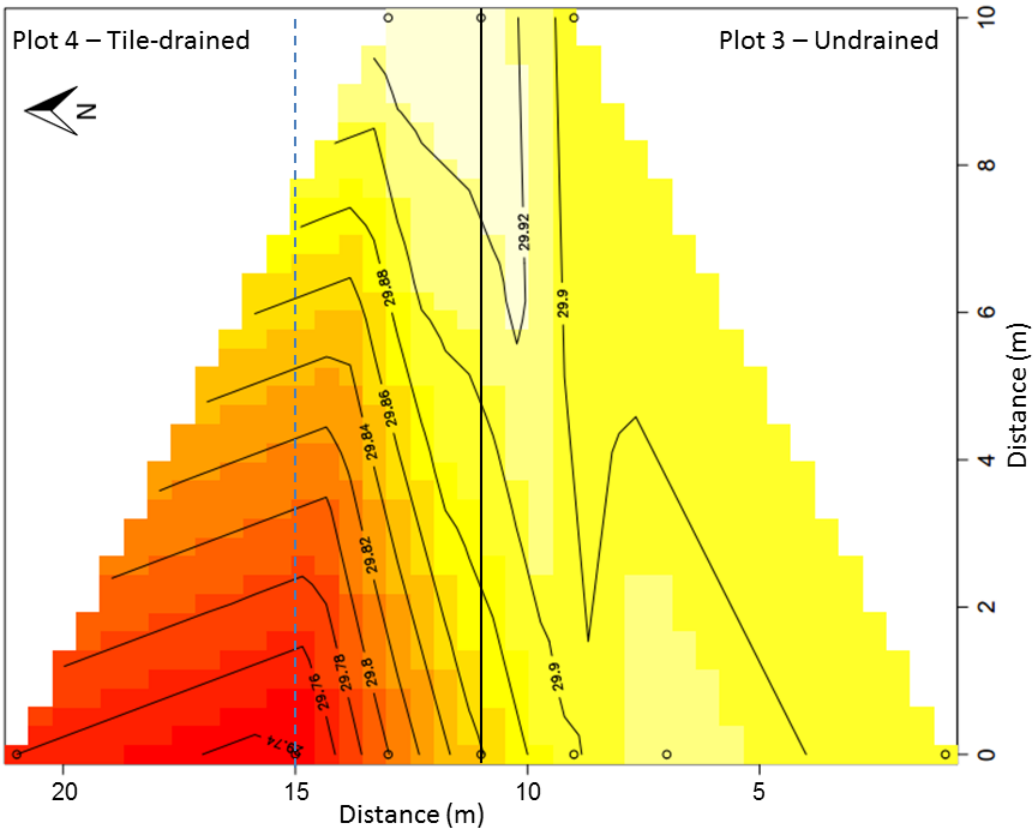

Figure 4.34: Water table contour map for plots 3 and 4 on 6/11/15. X and Y axes represent distance (m), central vertical black line indicates the plot boundary, dotted blue vertical line indicates the outer tile line, and small circles indicate well locations.

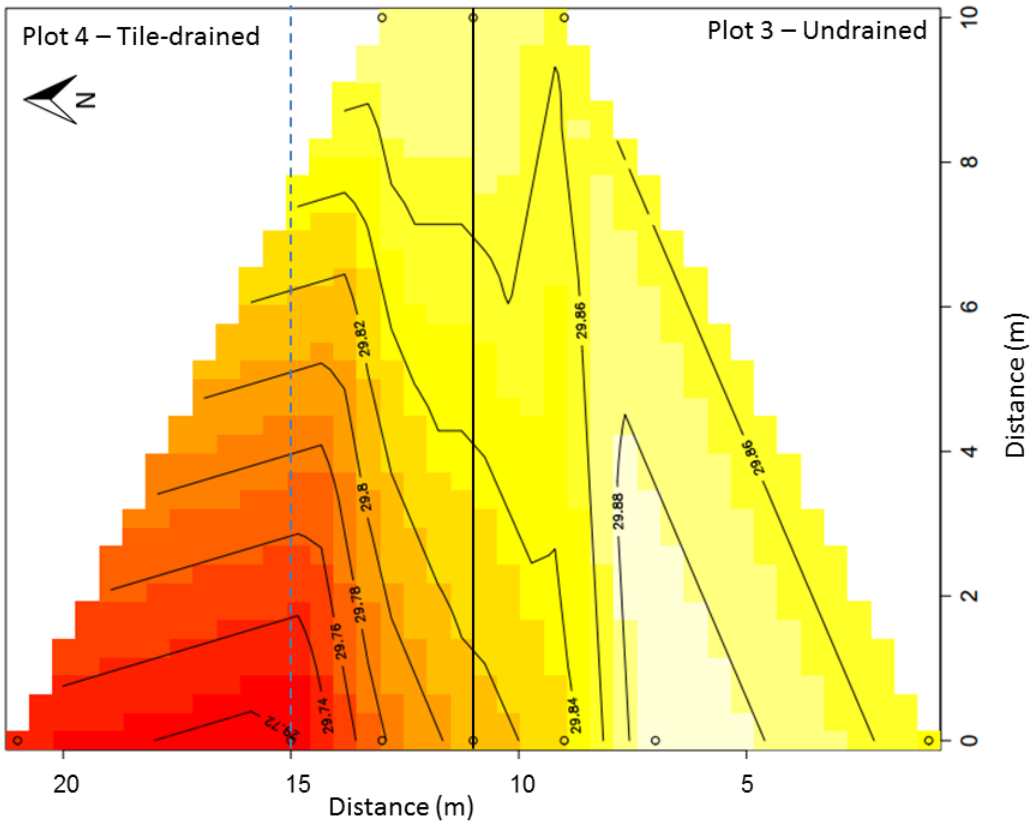

Figure 4.35: Water table contour map for plots 3 and 4 on 6/12/15. X and Y axes represent distance (m), central vertical black line indicates the plot boundary, dotted blue vertical line indicates the outer tile line, and small circles indicate well locations.

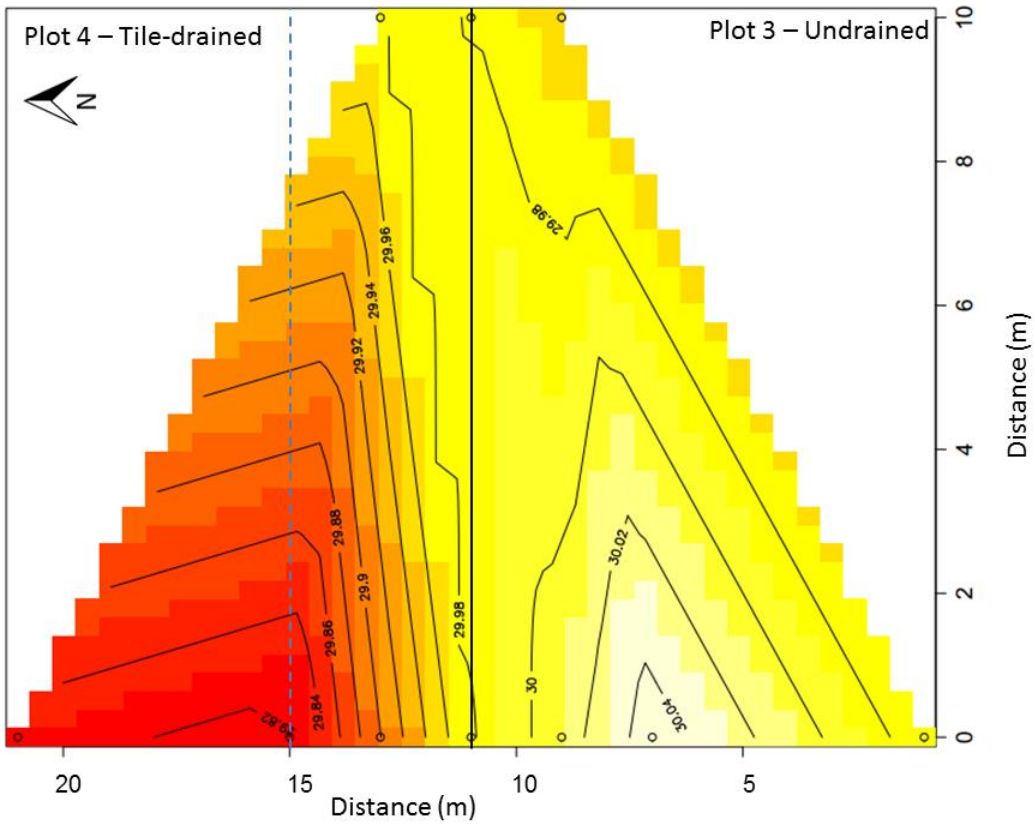

Figure 4.36: Water table contour map for plots 3 and 4 on 6/13/15. X and Y axes represent distance (m), central vertical black line indicates the plot boundary, dotted blue vertical line indicates the outer tile line, and small circles indicate well locations.

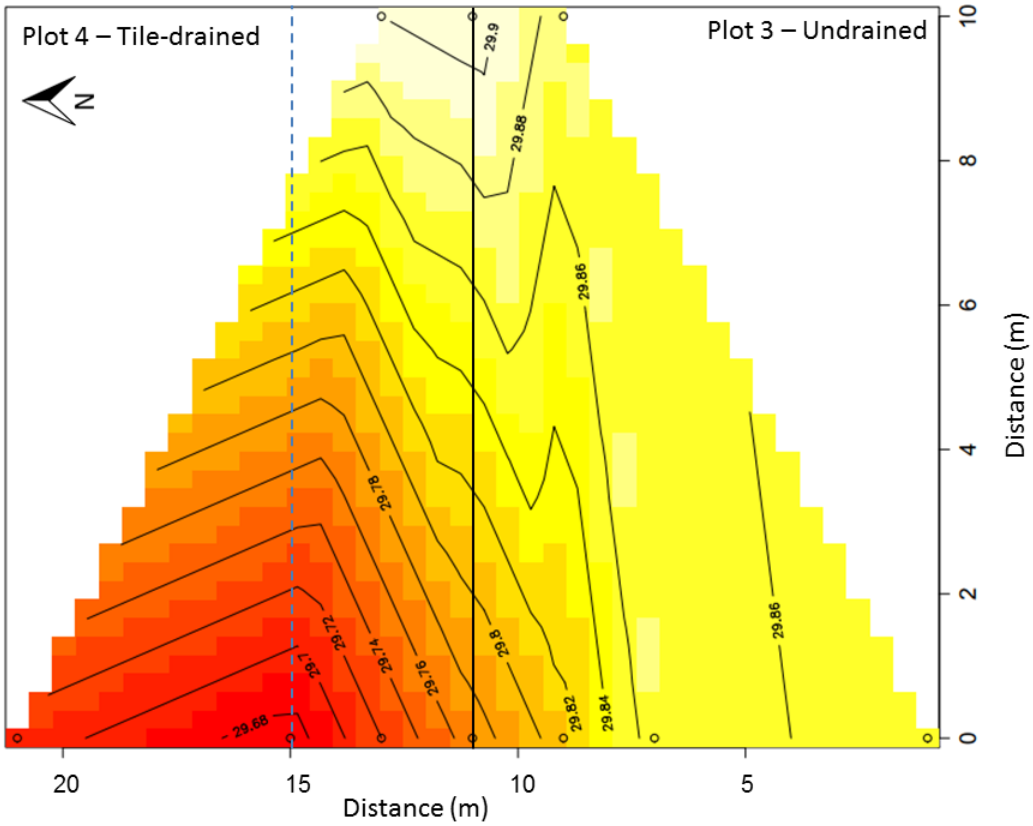

Figure 4.37: Water table contour map for plots 3 and 4 on 6/15/15. X and Y axes represent distance (m), central vertical black line indicates the plot boundary, dotted blue vertical line indicates the outer tile line, and small circles indicate well locations.

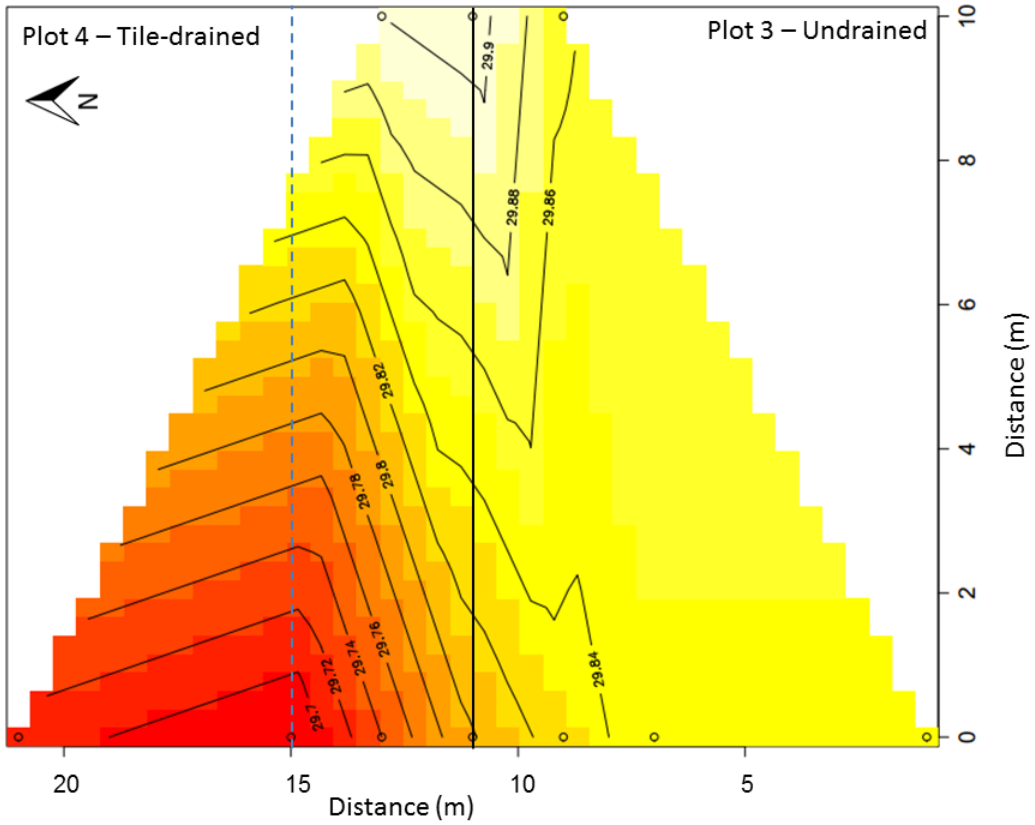

Figure 4.38: Water table contour map for plots 3 and 4 on 6/17/15. X and Y axes represent distance (m), central vertical black line indicates the plot boundary, dotted blue vertical line indicates the outer tile line, and small circles indicate well locations.

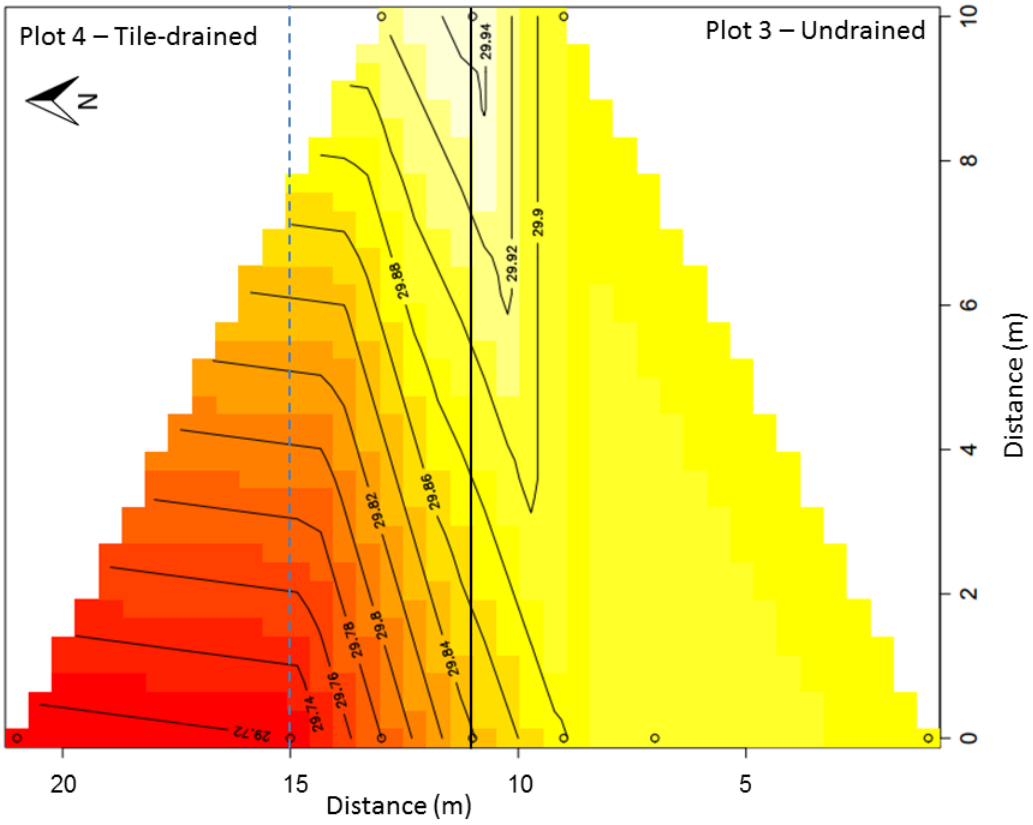

Figure 4.39: Water table contour map for plots 3 and 4 on 6/19/15. X and Y axes represent distance (m), central vertical black line indicates the plot boundary, dotted blue vertical line indicates the outer tile line, and small circles indicate well locations.

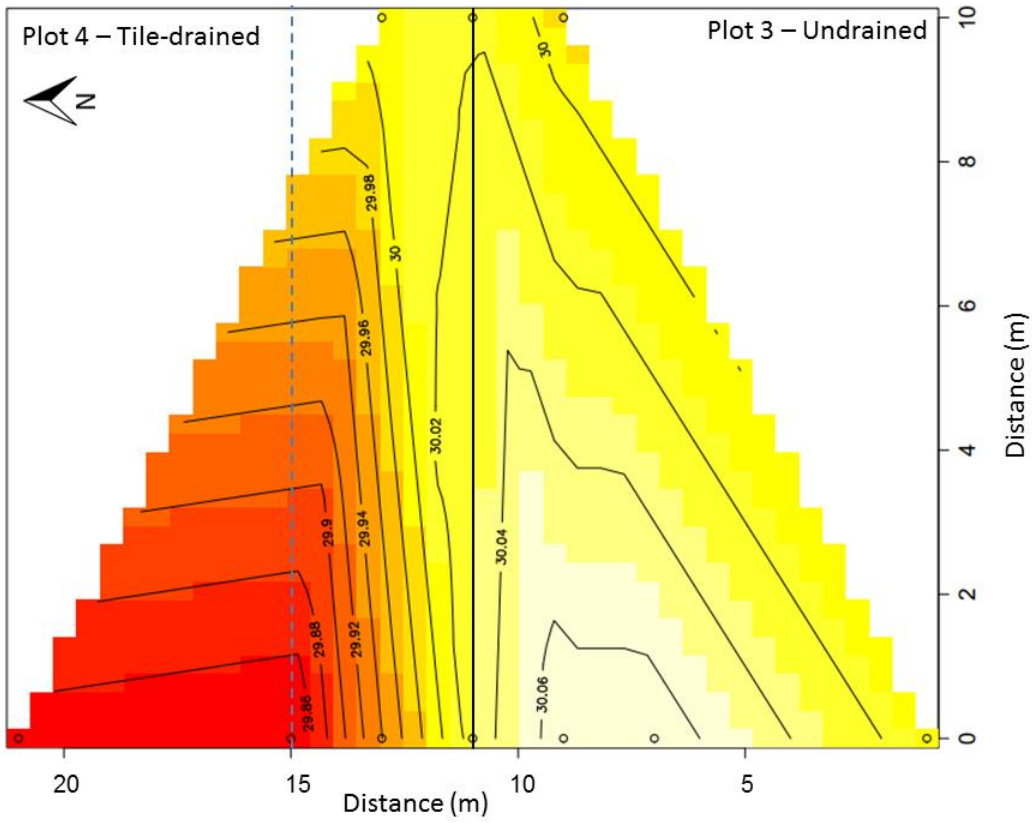

Figure 4.40: Water table contour map for plots 3 and 4 on 6/22/15 (10:00). X and Y axes represent distance (m), central vertical black line indicates the plot boundary, dotted blue vertical line indicates the outer tile line, and small circles indicate well locations.

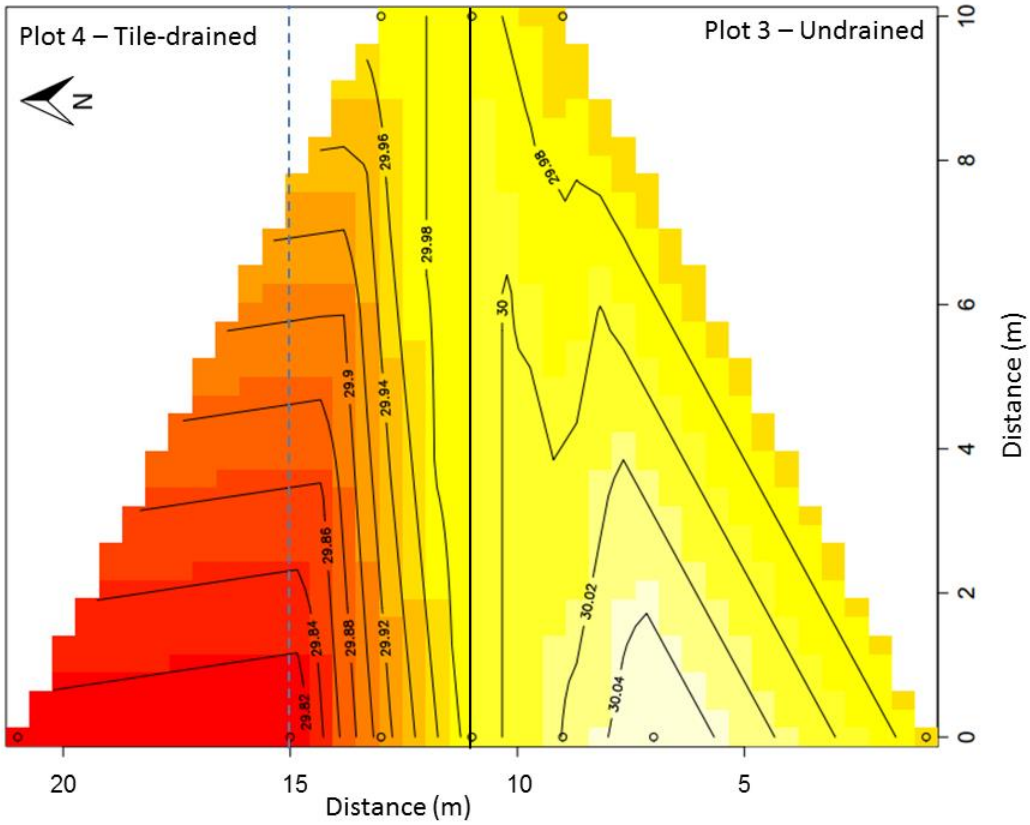

Figure 4.41: Water table contour map for plots 3 and 4 on 6/23/15. X and Y axes represent distance (m), central vertical black line indicates the plot boundary, dotted blue vertical line indicates the outer tile line, and small circles indicate well locations.

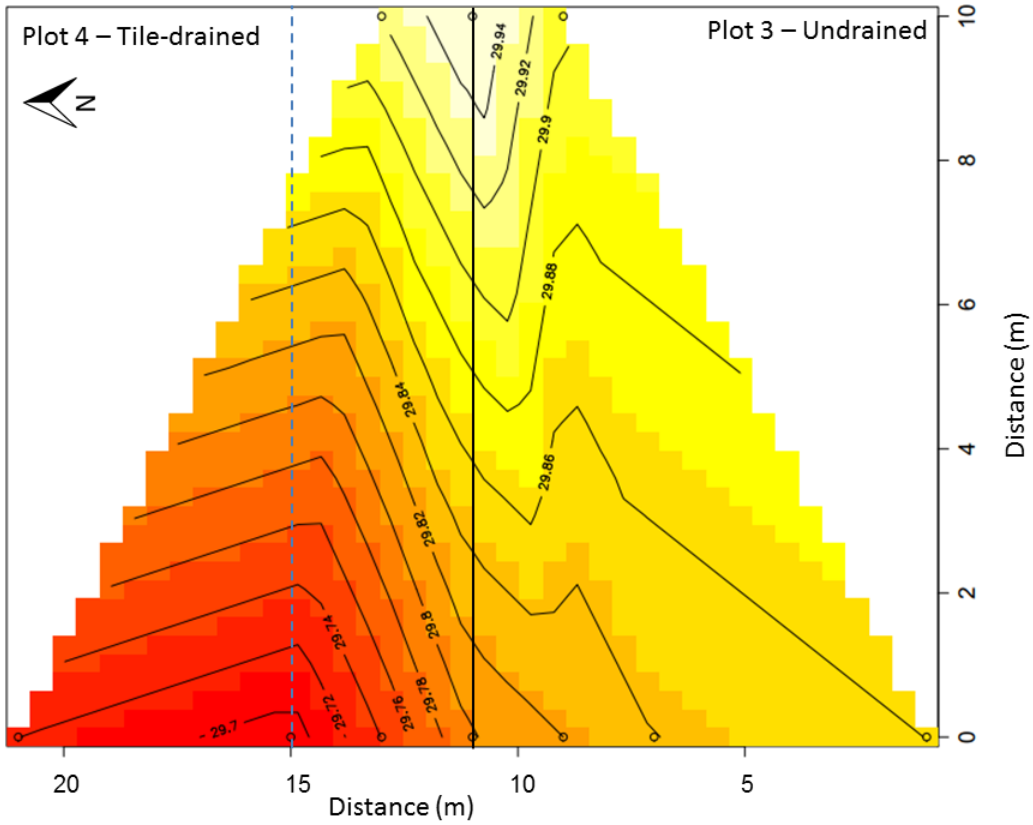

Figure 4.42: Water table contour map for plots 3 and 4 on 6/24/15. X and Y axes represent distance (m), central vertical black line indicates the plot boundary, dotted blue vertical line indicates the outer tile line, and small circles indicate well locations.

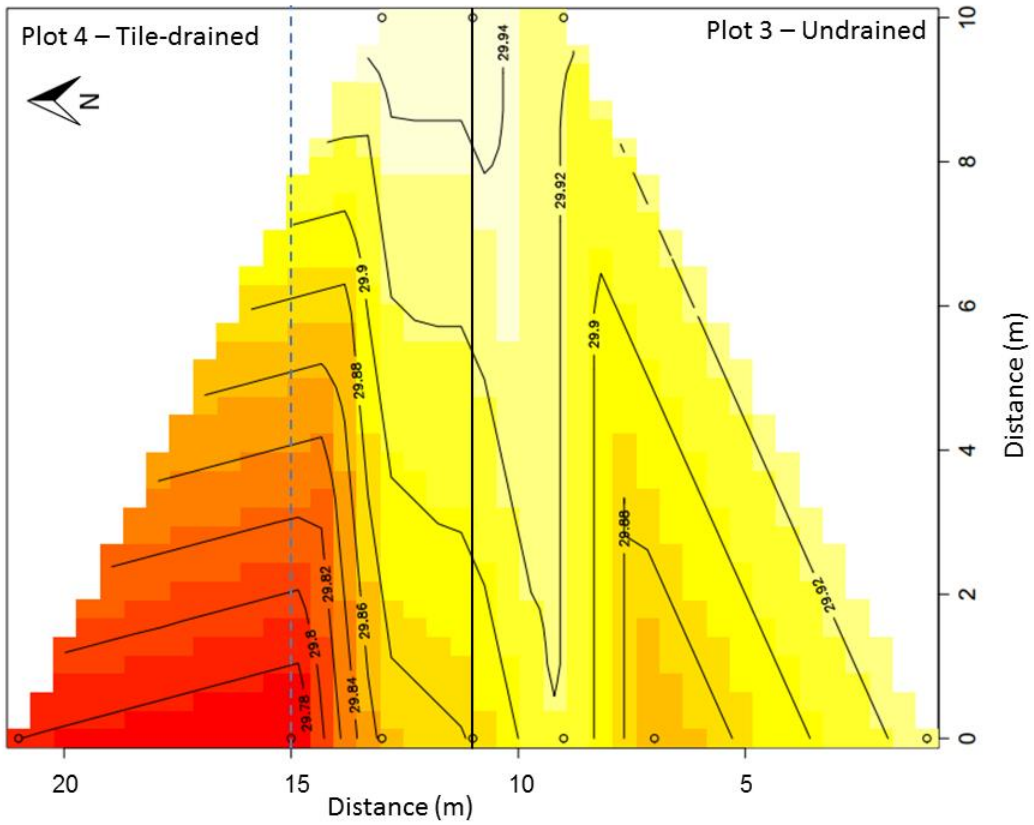

Figure 4.43: Water table contour map for plots 3 and 4 on 6/29/15. X and Y axes represent distance (m), central vertical black line indicates the plot boundary, dotted blue vertical line indicates the outer tile line, and small circles indicate well locations.

Figure 4.44: USDA-NRCS Web Soil Survey map of Lake Alice Experimental Site and surrounding area.